DYNAMICS AND CONTROL OF SATELLITE RELATIVE MOTION IN A CENTRAL GRAVITATIONAL FIELD

A Dissertation

by

PRASENJIT SENGUPTA

Submitted to the Office of Graduate Studies of
Texas A&M University
in partial fulfillment of the requirements for the degree of

DOCTOR OF PHILOSOPHY

December 2006

Major Subject: Aerospace Engineering

DYNAMICS AND CONTROL OF SATELLITE RELATIVE MOTION IN A CENTRAL GRAVITATIONAL FIELD

A Dissertation

by

PRASENJIT SENGUPTA

Submitted to the Office of Graduate Studies of
Texas A&M University
in partial fulfillment of the requirements for the degree of

DOCTOR OF PHILOSOPHY

Approved by:

Co-Chairs of Committee,	Srinivas R. Vadali
	Kyle T. Alfriend
Committee Members,	John L. Junkins
	John E. Hurtado
	Shankar P. Bhattacharyya
Head of Department,	Helen L. Reed

December 2006

Major Subject: Aerospace Engineering

ABSTRACT

Dynamics and Control of Satellite Relative Motion

in a Central Gravitational Field. (December 2006)

Prasenjit Sengupta, B.Tech., Indian Institute of Technology, Kharagpur;

M.S., Texas A&M University

Co–Chairs of Advisory Committee: Dr. Srinivas R. Vadali
Dr. Kyle T. Alfriend

The study of satellite relative motion has been of great historic interest, primarily due to its application to rendezvous, intercept, and docking maneuvers, between spacecraft in orbit about gravitational bodies, such as the Earth. Recent interest in the problem of satellite formation flight has also led to renewed effort in understanding the dynamics of relative motion. Satellite formations have been proposed for various tasks, such as deep-space interferometry, and terrestrial observation, among others. Oftentimes, the rich natural dynamics of the relative motion problem near a gravitational body are exploited to design formations of a specific geometry.

Traditional analysis models relative motion under the assumptions of a circular reference orbit, linearized differential gravity field (small relative distance), and without environmental perturbations such as oblateness effects of the attracting body, and atmospheric drag. In this dissertation, the dynamics of the relative motion problem are studied when these assumptions are relaxed collectively. Consequently, the combined effects of nonlinearity, eccentricity, and Earth oblateness effects on relative motion, are studied. To this end, coupling effects between the various

environmental perturbations are also accounted for. Five key problems are addressed - the development of a state transition matrix that accounts for eccentricity, nonlinearity, and oblateness effects; oblateness effects on averaged relative motion; eccentricity effects on formation design and planning; new analytical expressions for periodic relative motion that account for nonlinearity and eccentricity effects; and a solution to the optimal rendezvous problem near an eccentric orbit. The most notable feature of this dissertation, is that the solutions to the stated problems are completely analytical, and closed-form in nature. Use has been made of a generalized reversion of vector series, and several integral forms of Kepler's equations, without any assumptions on the magnitude of the eccentricity of the reference orbit.

চিত্ত জেথা ভয়শূন্য উচ্চ জেথা শির, জ্ঞান জেথা মুক্ত, জেথা গৃহের প্রাচীর
আপন প্রাঙ্গনতলে দিবস-শর্বরী বসুধারে রাখে নাই খণ্ড ক্ষুদ্র করি,

জেথা বাক্য হৃদয়ের উৎসমুখ হতে উচ্ছসিয়া উঠে, জেথা নির্বারিত স্রোতে,
দেশে দেশে দিশে দিশে কর্মধারা ধায় অজস্র সহস্রবিধ চরিতার্থতায়,

জেথা তুচ্ছ আচারের মরু-বালু-রাশি বিচারের স্রোতপথ ফেলে নাই গ্রাসি-
পৌরুষেরে করেনি শতধা, নিত্য জেথা তুমি সর্ব কর্ম-চিন্তা-আনন্দের নেতা,

নিজ হস্তে নির্দয় আঘাত করি পিতঃ, ভারতেরে সেই স্বর্গে করো জাগরিত॥

— রবীন্দ্রনাথ ঠাকুর (১৮৬১-১৯৪১), *গীতাঞ্জলি*

Where the mind is without fear and the head is held high;
Where knowledge is free;
Where the world has not been broken up into fragments by domestic walls;
Where words come out from the depth of truth;
Where tireless striving stretches its arms towards perfection;
Where the clear stream of reason has not lost its way into the dreary desert sand of dead habit;
Where the mind is led forward by Thee into ever-widening thought and action –
Into that heaven of freedom, my Father, let my country awake.

– Rabindranath Tagore (1861-1941), *Gitanjali*

ACKNOWLEDGMENTS

So long, and thanks for all the fish.[1]

The past five and a half years at Texas A&M have been rich in terms of of experience. I have had the opportunity and good fortune to work with some of the best and brightest minds in the world, and I can only hope, that after all this time, I will have absorbed some of the good qualities my mentors and colleagues have displayed. The debt of gratitude I owe is too large to express in words, and any attempt to repay this debt remains meaningless, as I thank,

Drs. Srinivas Vadali, and Terry Alfriend, my advisors, supervisors, beacons of knowledge, and source of inspiration;

Drs. John Junkins, Johnny Hurtado, Michael Pilant, and Shankar Bhattacharyya, for serving on my committee, evaluating my progress as a graduate student; and for being the finest teachers one could ask for;

the staff members of the Aerospace Engineering Department, who have looked after my professional and financial well-being;

Puneet, Kamesh, Sai, Hui, Raktim, Suman, and Tamás, for their insight and encouragement, through discussions, both technical and non-technical;

Dali, Waqar, Anuja, Rohit, Upali, Veera, and my roommate Bhoj, for all the good times;

the F&H gang, Sahoo, and Rajnish - my office (cell)mate, colleague, and friend -

[1]Douglas N. Adams (1952-2001)

for sharing with me some very interesting perspectives on life, research, and bicycle races;

the A1Top crew, for reminding me that I'm no better, nor worse, than they are;

the Texas A&M Kendo Kyokai, for showing me that good manners and fighting spirit are not mutually exclusive;

and my family, last in this list, always first in my thoughts, for, well, everything.

I thank you all, especially for the fish.

TABLE OF CONTENTS

CHAPTER Page

CHAPTER Page

LIST OF TABLES

LIST OF FIGURES

FIGURE Page

CHAPTER I

INTRODUCTION

The problem of relative motion between multiple satellites in orbit about an attracting body, such as a planet, has provoked great interest for many years. In the context of this dissertation, relative motion refers to the study of the dynamics of neighboring satellites, with respect to one satellite, real or fictitious, which is designated as the chief (also known as the leader, master or target, depending on the application). The satellite whose relative motion is of interest, is designated as the deputy (also known as the follower, slave or chaser). Though relative motion is not restricted to any particular environment, the problem is particularly interesting in a gravitational field associated with planets and their natural satellites. In this case, not only does the problem become more complicated, several features inherent to a gravitational field introduce rich dynamical behavior into the system. For example, it is possible in some cases, to use the differential gravity field between to satellites to generate periodic or quasi-periodic relative orbits.

An understanding of satellite relative motion is essential for two important applications of space flight: 1) The problem of rendezvous in space, and 2) The problem of formation flight. The first problem deals with the design of centralized and decentralized algorithms to successfully dock a satellite (for example, the space shuttle) with a structure (such as the International Space Station) in space. Such algorithms require the modeling of relative motion, without the need to constantly communicate with ground-based stations. The second problem is one in which

---

The journal model is Celestial Mechanics and Dynamical Astronomy.

the dynamics of the problem are exploited to place a number of satellites in a Distributed Space System (DSS). The purposes of DSS include, but are not limited to communication, space-based interferometry, and terrestrial observation. Some examples of proposed Earth-specific missions that use these concepts are the Laser Inteferometer Space Antenna (2006), Orion (How et al. 1998), and the TechSat 21 program (Martin and Stallard 1999). Examples of benchmark missions involving formation flight in low Earth orbits and highly elliptical orbits are present in Carpenter et al. (2003) and Curtis (1999).

The simplest model governing the dynamics of relative motion in a planetary gravitation field is given by the Hill-Clohessy-Wiltshire (HCW) equations (Hill 1878; Clohessy and Wiltshire 1960). These equations model relative motion between a chaser and target vehicle, in a frame attached to, and rotating with, the target vehicle (also known as Hill's frame). The HCW equations assume that the target's orbit is circular, and the differential gravity field is linear, in the absence of perturbations. Consequently, these equations constitute a constant-coefficient, sixth-order, linear model, and are extremely useful for preliminary analysis for rendezvous and formation flight. However, their scope is limited, in that large deviations are observed between the predicted solutions and real trajectory, when the target's orbit is non-circular and due to the assumption that the distance between the chaser and target is negligible when compared with the distance of the Target from the gravitational center.

The aim of the dissertation is to study the problem of relative motion by relaxing the assumptions of the HCW model. In particular, the effects of a nonlinear differential gravity field, eccentricity of the target's orbit, and an oblate Earth, on satellite rendezvous and formation flight, are studied. Th effects are studied in conjunction with each other, thus also accounting for the coupling between

phenomena. Furthermore, some interesting results pertaining to the use of Kepler's equation (Battin 1999, chap. 4) to the problem of rendezvous, are presented.

In the following text, the organization of this dissertation, as well as the specific topics that are dealt with, will be discussed.

Chapter II will introduce some preliminary concepts, terminology, and symbolic notation pertaining to the problem of rendezvous and formation flight. A survey of existing work on this subject will also be presented. The effects of Earth oblateness effects will also be discussed.

Chapter III will analyze relative motion near a non-circular orbit, under the assumptions of small relative distance (linearized differential gravity field), and a central gravity field, without perturbations. The deviation from the classical HCW solutions are will be analyzed and quantified, and this study will be shown useful, for the design of satellite formations. This chapter will also introduce a meaningful parameterization for relative motion.

Chapter IV will study the optimal rendezvous problem in the same context as Chapter III. By simple extension, the theory developed in this chapter can also be used for intercept maneuvers, or formation reconfiguration. The key result is an analytical expression for the optimal control, and consequently, a solution to a problem originally stated by Euler (1969).

Chapters V and VI study the problem of nonlinear formation flight, by analyzing the effects of second-order nonlinearities in the differential gravitational field. Results are obtained that are useful for relative motion where the satellites are seperated by large distances and are in non-circular orbits. In particular, the geometric aspects

of relative motion are used to develop state transition tensors that can accurately propagate the relative states. Furthermore, without additional computation, it is shown that the results in Chapter V can accommodate oblateness effects by using existing results in the literature. Chapter VI studies nonlinear formation flight in the context of periodic relative motion. An analytical formulation for suitable initial conditions will be presented, that accounts for nonlinearity effects, and are valid for any eccentricity. New expressions for periodic relative motion are also developed, that are useful for large formations in a central field.

In Chapter VII, the problem of average relative motion due to an oblate Earth, will be analyzed in greater detail. The short-periodic variations in position and velocity, induced by a oblate Earth are averaged, by the use of special integrals. This development results in a set of concise, expressions for position and velocity, that are useful for command generation where additional control effort for tracking short-periodic variations is not desired.

Finally, the dissertation is summarized in the last chapter, and a few concluding remarks on future work are presented.

CHAPTER II

PRELIMINARY CONCEPTS

2.1 Orbital Elements

2.1.1 Classical Orbital Elements

A comprehensive description of two-body motion is available in Battin (1999). In this dissertation, it is sufficient to note that the orbit of any satellite is completely determined by six elements, that arise as a consequence of integrals of motion associated with the two-body problem. The most common set used is the classical orbital element set, denoted by $\mathbf{oe} = \{a\ e\ i\ h\ g\ l\}^\top$, where a is the semimajor axis of the ellipse defining the satellite's orbit, e is the eccentricity, i is the inclination of the orbit, h is the right ascension of the ascending node (RAAN), g is the argument of periapsis, and l is the mean anomaly. In the two-body problem, the first five quantities are constants, and the mean anomaly is a linear function of time, given by $l = l_0 + n\,\Delta t$, where l_0 is the mean anomaly at epoch, Δt is the elapsed time since epoch, and $n = \sqrt{(\mu/a^3)}$ is the mean motion of the orbit. In the presence of perturbations or control acceleration, the orbital elements are no longer constant, and their rates can be obtained using Gauss' equations (Battin 1999, chap. 10).

Very often, the true anomaly, f, or eccentric anomaly E, are used as the independent variable element. The true and eccentric anomalies are related through geometry, by the following equation (Battin 1999, chap. 4):

$$\tan\frac{f}{2} = \sqrt{\frac{1+e}{1-e}}\tan\frac{E}{2} \tag{2.1}$$

The eccentric and mean anomalies are related by Kepler's equation:

$$l = E - e \sin E \tag{2.2}$$

Whereas solving for l, given e and E is straightforward, no closed-form solution to the inverse problem exists, due to the transcendental nature of the equation. Solutions using series expansions in eccentricity have been presented, as have algorithms to obtain E in terms of l numerically. Colwell (1993) provides a survey of existing techniques used to solve Kepler's equation.

2.1.2 Nonsingular Elements

Although the classical orbital elements are useful for describing satellite motion, their use often causes singularities when the orbit is circular or near-circular ($e \sim 0$), or the orbit is planar or near-planar ($i \sim 0$). For example, when the orbit is near-circular, g and f cannot be independently obtained, because the direction of the eccentricity vector is ill-defined. However, their sum, $g + f$ is still well-defined, since this is simply the angle between the radius vector of the satellite, and the line of nodal crossing. Consequently, a nonsingular element set is found useful, which is given by $\mathbf{ns} = \{a\ \lambda\ i\ q_1\ q_2\ h\}^\top$, where $\lambda = g + l$ is the mean argument of latitude. The variables q_1 and q_2 are the components of the eccentricity vector, such that $q_1 + \jmath\, q_2 = e \exp(\jmath g)$, where $\jmath = \sqrt{-1}$. Corresponding to the mean argument of latitude, also defined are the true argument of latitude, $\theta = g + f$, and the eccentric argument of latitude, $F = g + E$. The use of nonsingular elements is essential for solutions that are uniformly valid for $0 \leq e < 1$. However, as will be shown in the following chapters, their use also complicates analysis. It should also be noted that the use of nonsingular elements does not avoid singularities introduced by near-planar

orbits. For such cases, the equinoctial element set (Broucke and Cefola 1972), or the kinematic model (Junkins and Turner 1979; Sengupta and Vadali 2005; Gurfil 2005a), are useful. In the kinematic model, Euler parameters are used to describe the position of the satellite, instead of the orbital angles. The use of equinoctial elements, or the kinematic model, will not be discussed in this dissertation.

2.1.3 Canonical Elements

A part of this dissertation will also use the Delaunay element set (Goldstein 1965, chap. 9). The Delaunay elements are a set of canonical elements that are useful for analyzing the problem of satellite motion in a Hamiltonian framework. In this dissertation, it is more convenient to use the normalized Delaunay elements, with the generalized momenta defined as:

$$L = \sqrt{a}, \quad G = L\eta, \quad H = G\cos i \tag{2.3}$$

where $\eta = \sqrt{(1-e^2)}$. The generalized coordinates corresponding to L, G, and H, are l, g, and h, respectively, as defined earlier.

2.2 Frames of Reference for Relative Motion

Consider an Earth-centered inertial (ECI) frame, denoted by $\mathcal{N}$, with orthonormal basis $\mathcal{B}_N = \{\mathbf{i}_x \ \mathbf{i}_y \ \mathbf{i}_z\}$. The vectors $\mathbf{i}_x$ and $\mathbf{i}_y$ lie in the equatorial plane, with $\mathbf{i}_x$ coinciding with the line of the equinoxes, and $\mathbf{i}_z$ passing through the North Pole. Relative motion is conveniently described in a Local-Vertical-Local-Horizontal (LVLH) frame, as shown in Figure 2.1 and denoted by $\mathcal{L}$, that is attached to the chief satellite. This frame has basis $\mathcal{B}_L = \{\mathbf{i}_r \ \mathbf{i}_\theta \ \mathbf{i}_h\}$, with $\mathbf{i}_r$ lying along the radius vector

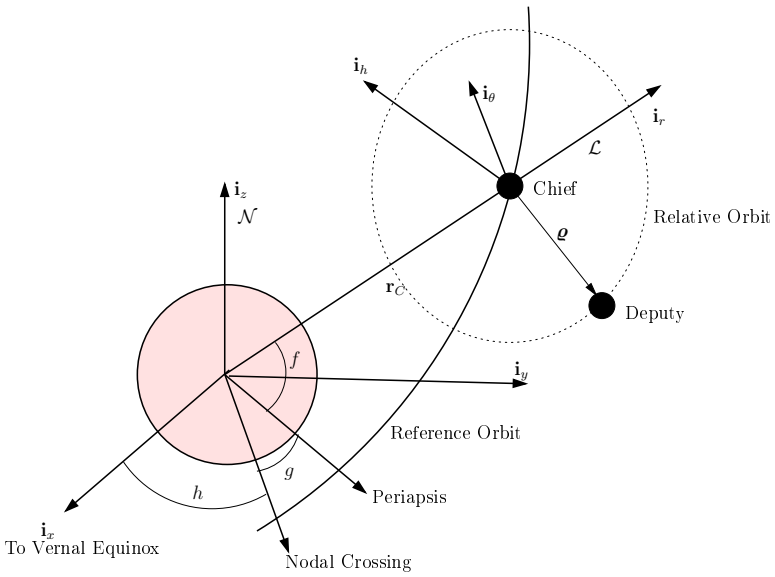

Fig. 2.1 Frames of Reference

from the Earth's center to the satellite, $\mathbf{i}_h$ coinciding with the normal to the plane defined by the position and velocity vectors of the satellite, and $\mathbf{i}_\theta = \mathbf{i}_h \times \mathbf{i}_r$. The LVLH frame rotates with angular velocity $\boldsymbol{\omega} = \omega_r \mathbf{i}_r + \omega_\theta \mathbf{i}_\theta + \omega_h \mathbf{i}_h$, and its current orientation with $\mathcal{N}$ is given by the 3-1-3 direction cosine matrix comprising RAAN, inclination, and true argument of latitude, respectively (Junkins and Turner 1986, chap. 2). The angular velocity can also be expressed in terms of orbital elements and their rates (Junkins and Turner 1979; Kechichian 1998).

Let the position of the deputy satellite in the chief's LVLH frame be denoted by $\boldsymbol{\varrho} = \xi \mathbf{i}_r + \vartheta \mathbf{i}_\theta + \zeta \mathbf{i}_h$, where ξ, ϑ and ζ denote the components of the position vector along the radial, along-track, and out-of-plane directions, respectively. Then, the most general equations modeling relative motion are given by the following:

$$\ddot{\boldsymbol{\varrho}} + 2\boldsymbol{\omega} \times \dot{\boldsymbol{\varrho}} + \dot{\boldsymbol{\omega}} \times \boldsymbol{\varrho} + \boldsymbol{\omega} \times \boldsymbol{\omega} \times \boldsymbol{\varrho} = \mathbf{f}_D - \mathbf{f} + \mathbf{u} \tag{2.4}$$

where $\mathbf{u} \in \mathbb{R}^3$ is the external control acceleration, and $\mathbf{f}_D$ and $\mathbf{f}$ are external forces

acting on the deputy and chief, respectively. In (2.4), $(\dot{})$ and $(\ddot{})$ denote the first and second derivative with respect to time. In this dissertation, it is assumed that quantities describing the motion of the chief satellite are written without subscripts, and those describing the motion of the deputy will either be written in terms of the chief's variables and relative position and velocity variables, or will have the subscript 'D'.

It is assumed in this dissertation that the external forces are potential forces, and that this potential function arises due to gravitational effects only. Due to the aspherical nature of the Earth (and many celestial bodies), the gravitational force is no longer simply of the inverse-square form. A full development of the theory is presented in Kaula (2000). For Earth operations, it is sufficient to extend the development to the first zonal harmonic term (due to the equatorial bulge), which has a coefficient $J_2 = 1.08269 \times 10^{-3}$, since the terms contributed by higher-order zonal, tesseral, and sectorial harmonics, are three magnitudes lower. Consequently, the gravitational potential including oblateness effects is of the following form:

$$\mathcal{V}(r,\phi) = -\frac{\mu}{r}\left[1 + J_2\left(\frac{R_\oplus}{r}\right)^2 P_2\left(\sin\phi\right)\right] \tag{2.5}$$

In this equation, $\mu = \mathcal{G}M_\oplus$, where $\mathcal{G}$ is the universal gravitation constant, and $M_\oplus$ is the mass of the Earth. The quantities r and ϕ denote the radial distance and latitude of the satellite, respectively; $R_\oplus$ is the radius of the Earth, and P_2 is the second Legendre polynomial. Representative values that are used in this dissertation are shown in Table 2.1.

The problem of relative motion is best studied by using simple models to begin with, and subsequently modifying these models to better reflect physical realities. Therefore, if it is first assumed that oblateness effects are absent and only a central

Table 2.1 Representative Values

Variable	Value
μ	$398600.4415\,\mathrm{km}^3/\mathrm{s}^2$
$R_\oplus$	$6378.1363\,\mathrm{km}$
J_2	1082.6269×10^{-6}
J_3	-2.44×10^{-6}
J_4	-1.70×10^{-6}
J_5	-0.18×10^{-6}

gravity field is active, then $\omega_r = \omega_\theta = 0$, and the frame $\mathcal{L}$ rotates with angular velocity $\dot{\theta}\mathbf{i}_h = \dot{f}\mathbf{i}_h$, since g is constant. The gravitational potential acting on the chief satellite is therefore simply $\mathcal{V} = -\mu/r$, and that acting on the deputy is given by:

$$\mathcal{V}_\mathcal{D} = -\frac{\mu}{|\mathbf{r}_D|} = -\frac{\mu}{r}\left(1 + \frac{\varrho^2}{r^2} + 2\frac{\xi}{r}\right)^{-\frac{1}{2}} \tag{2.6}$$

where $\mathbf{r}_D = (r+\xi)\mathbf{i}_r + \vartheta\mathbf{i}_\theta + \zeta\mathbf{i}_h$. Using $\mathcal{V}$ and $\mathcal{V}_D$ as the potential functions for gravitational forces, $\mathbf{f}$, and $\mathbf{f}_D$ acting on the chief and deputy, respectively, the nonlinear equations modeling relative motion in the two-body problem are then given by:

$$\ddot{\xi} - 2\dot{\theta}\dot{\vartheta} - \dot{\theta}^2\xi - \ddot{\theta}\vartheta = -\frac{\mu(r+\xi)}{\left[(r+\xi)^2 + \vartheta^2 + \zeta^2\right]^{\frac{3}{2}}} + \frac{\mu}{r^2} \tag{2.7a}$$

$$\ddot{\vartheta} + 2\dot{\theta}\dot{\xi} - \dot{\theta}^2\vartheta + \ddot{\theta}\xi = -\frac{\mu\vartheta}{\left[(r+\xi)^2 + \vartheta^2 + \zeta^2\right]^{\frac{3}{2}}} \tag{2.7b}$$

$$\ddot{\zeta} = -\frac{\mu\zeta}{\left[(r+\xi)^2 + \vartheta^2 + \zeta^2\right]^{\frac{3}{2}}} \tag{2.7c}$$

Also useful are the equations for the radius and the argument of latitude (Battin

1999, chap. 3):

$$\ddot{r} = \dot{\theta}^2 r - \frac{\mu}{r^2} \tag{2.8a}$$

$$\ddot{\theta} = -2\frac{\dot{r}}{r}\dot{\theta} \tag{2.8b}$$

although r and $\dot{\theta}$ (and by extension, $\ddot{\theta}$) can be obtained analytically from the true anomaly, using $r = p/(1 + e\cos f)$, and $\dot{\theta} = \hbar/r^2$, where $\hbar = \sqrt{(\mu p)}$ is the specific angular momentum of the orbit, and $p = a\eta^2$ is the semiparameter.

Observing that $\xi/r = (\xi/\varrho)\cdot(\varrho/r)$, the parenthesised term in (2.6) is the generating function for Legendre polynomials with argument $-\xi/\varrho$. Consequently,

$$\mathcal{V}_D = -\frac{\mu}{r}\sum_{k=0}^{\infty}(-1)^k\left(\frac{\varrho}{r}\right)^k P_k(\xi/\varrho) = -\frac{\mu}{r}\left[1 - \frac{\xi}{r} + \frac{1}{2}\frac{(2\xi^2 - \vartheta^2 - \zeta^2)}{r^2}\right] + \widetilde{\mathcal{V}} \tag{2.9}$$

$$\widetilde{\mathcal{V}} = -\frac{\mu}{r}\sum_{k=3}^{\infty}(-1)^k\left(\frac{\varrho}{r}\right)^k P_k(\xi/\varrho) \tag{2.10}$$

where P_k is the kth Legendre polynomial. Equations (2.7) thus can be rewritten as:

$$\ddot{\xi} - 2\dot{\theta}\dot{\vartheta} - \left(\dot{\theta}^2 + 2\frac{\mu}{r^3}\right)\xi - \ddot{\theta}\vartheta = -\frac{\partial\widetilde{\mathcal{V}}}{\partial\xi} \tag{2.11a}$$

$$\ddot{\vartheta} + 2\dot{\theta}\dot{\xi} - \left(\dot{\theta}^2 - \frac{\mu}{r^3}\right)\vartheta + \ddot{\theta}\xi = -\frac{\partial\widetilde{\mathcal{V}}}{\partial\vartheta} \tag{2.11b}$$

$$\ddot{\zeta} + \frac{\mu}{r^3}\zeta = -\frac{\partial\widetilde{\mathcal{V}}}{\partial\zeta} \tag{2.11c}$$

Higher-order Legendre polynomials in the perturbing potential can be generated from lower-order ones, by using the recursive relation $(k+1)P_{k+1}(z) = (2k+1)zP_k(z) - kP_{k-1}(z)$, with $P_0(z) = 1$ and $P_1(z) = z$. The perturbing gravitational acceleration $\partial\widetilde{\mathcal{V}}/\partial\boldsymbol{\varrho} = \{\partial\widetilde{\mathcal{V}}/\partial\xi \quad \partial\widetilde{\mathcal{V}}/\partial\vartheta \quad \partial\widetilde{\mathcal{V}}/\partial\zeta\}^\top$ contributes higher-order nonlinearities to the system, and if ignored, allows the treatment of (2.11) as a tenth-order linear system (additional equations are contributed by Keplerian motion).

2.3 Hill-Clohessy-Wiltshire Model

If it is assumed that the chief's orbit is circular, then r and $\dot{\theta}$ are constants given by a and n, respectively. A rotating frame with these properties is also referred to as Hill's frame (Hill 1878). The resulting equations are referred to as Hill's equations, or the Clohessy-Wiltshire (CW) equations (Clohessy and Wiltshire 1960), who used Hill's results for the rendezvous problem, or as the Hill-Clohessy-Wiltshire (HCW) equations. When the differential gravitation field is linearized ($\widetilde{\mathcal{V}} = 0$), the following sixth-order, linear system is obtained:

$$\ddot{\xi} - 2n\dot{\vartheta} - 3n^2\xi = 0 \tag{2.12a}$$

$$\ddot{\vartheta} + 2n\dot{\xi} = 0 \tag{2.12b}$$

$$\ddot{\zeta} + n^2\zeta = 0 \tag{2.12c}$$

This system can be easily solved, although their exact solution is not of particular interest at this point. It may be noted, however, that the out-of-plane equation (2.12c), is uncoupled with the in-plane equations, (2.12a) and (2.12b), and only has periodic solutions. The fundamental matrix corresponding to the in-plane equations has eigenvalues 0, 0, and $\pm\jmath\, n$, resulting in periodic terms and secular growth terms in the motion in the plane. Control inputs can also be included in (2.12), if necessary.

2.4 Tschauner-Hempel Model

If the objective is to study relative motion in the framework of an elliptic reference orbit, then (2.12) are no longer useful. If the nonlinear equations, as shown in (2.7) are analyzed, then it is observed that the coefficients of the states are periodic, but are

related implicitly to the independent variable, time. These equations become more amenable to analysis by performing two steps: 1) changing the independent variable to the true anomaly, and 2) scaling the relative position by the radius of the chief. The first step results in the following transformation:

$$
\begin{aligned}
(\dot{\ }) &= \dot{f}(\ ') = \sqrt{\frac{\mu}{p^3}}(1+e\cos f)^2(\ ') && (2.13a)\\
(\ddot{\ }) &= \dot{f}^2(\ '') + \ddot{f}(\ ') \\
&= \frac{\mu}{p^3}(1+e\cos f)^3\Big[(1+e\cos f)(\ '') - 2e\sin f(\ ')\Big] && (2.13b)
\end{aligned}
$$

where $(')$ and $('')$ denote derivatives with respect to f. The second step results in a scaled position vector, $\boldsymbol{\rho} = x\mathbf{i}_r + y\mathbf{i}_\theta + z\mathbf{i}_h = \boldsymbol{\varrho}/r$, with $x = \xi/r$, $y = \vartheta/r$, and $z = \zeta/r$, respectively. Consequently,

$$
\begin{aligned}
\boldsymbol{\rho}' &= (1+e\cos f)\frac{\boldsymbol{\varrho}'}{p} - e\sin f\frac{\boldsymbol{\varrho}}{p} && (2.14a)\\
\boldsymbol{\rho}'' &= (1+e\cos f)\frac{\boldsymbol{\varrho}''}{p} - 2e\sin f\frac{\boldsymbol{\varrho}'}{p} - e\cos f\frac{\boldsymbol{\varrho}}{p} && (2.14b)
\end{aligned}
$$

Using the scaled states and the new independent variable, it can be shown that (2.7) reduce to the following form:

$$
\begin{aligned}
x'' - 2y' &= \frac{1+x}{(1+e\cos f)}\left(1-\frac{1}{d^3}\right) && (2.15a)\\
y'' + 2x' &= \frac{y}{(1+e\cos f)}\left(1-\frac{1}{d^3}\right) && (2.15b)\\
z'' &= -\frac{z}{(1+e\cos f)}\left(e\cos f + \frac{1}{d^3}\right) && (2.15c)
\end{aligned}
$$

where $d = \sqrt{[(1+x)^2+y^2+z^2]}$. If $x, y, z \ll 1$, the term $1/d^3$ can be expanded as a series of Legendre polynomials, in the same manner as shown in (2.10), resulting in

the following equations:

$$\begin{Bmatrix} x'' \\ y'' \\ z'' \end{Bmatrix} + \begin{bmatrix} 0 & -2 & 0 \\ 2 & 0 & 0 \\ 0 & 0 & 0 \end{bmatrix} \begin{Bmatrix} x' \\ y' \\ z' \end{Bmatrix} + \begin{bmatrix} -3/(1+e\cos f) & 0 & 0 \\ 0 & 0 & 0 \\ 0 & 0 & 1 \end{bmatrix} \begin{Bmatrix} x \\ y \\ z \end{Bmatrix}$$

$$= \sum_{k=3}^{\infty} \frac{(-1)^k k}{(1+e\cos f)(y^2+z^2)} \left[\rho^k P_k(x/\rho) \begin{Bmatrix} 0 \\ y \\ z \end{Bmatrix} + \rho^{k-1} P_{k-1}(x/\rho) \begin{Bmatrix} y^2+z^2 \\ -xy \\ -xz \end{Bmatrix} \right]$$

$$= \frac{3}{2}(1+e\cos f)^{-1} \begin{Bmatrix} y^2+z^2-2x^2 \\ 2xy \\ 2xz \end{Bmatrix} + \mathcal{O}\left(|\boldsymbol{\rho}|^3\right) \tag{2.16}$$

If second- and higher-order terms are neglected in (2.16), then the resulting equations are known as the the Tschauner-Hempel (TH) equations (Tschauner and Hempel 1965). The TH model is thus concisely written as three, second-order, linear equations with periodic coefficients, and is valid for all eccentricities of the reference orbit. Although de Vries (1963) solved the TH equations treating e as a small parameter and only retained first-order terms in eccentricity, the TH equations admit analytical solutions that are valid for all eccentricities, in terms of a special integral (Carter and Humi 1987; Carter 1990), also known as Lawden's integral (Lawden 1963, chap. 5). The solutions to the TH equations, and their uses will be discussed in Chapter III.

2.5 The Geometric Method

Relative motion is completely analytically described by the use of orbital elements of each satellite. The geometric method (Alfriend et al. 2000) and the unit sphere model (Vadali 2002; Sengupta et al. 2004) are nonlinear models that require the orbital

elements of both satellites to be propagated individually. In the former approach, the relative position is given by the following equation:

$$\left\{ \begin{array}{c} \xi \\ \vartheta \\ \zeta \end{array} \right\} = \mathbf{C}\,\mathbf{C}_D^{\top} \left\{ \begin{array}{c} r_D \\ 0 \\ 0 \end{array} \right\} - \left\{ \begin{array}{c} r \\ 0 \\ 0 \end{array} \right\} \tag{2.17}$$

In the second approach, relative motion between satellites is studied by first projecting the position of the satellites onto a unit sphere, and subsequently extended to the physical space. Unlike the TH equations, where the relative position is scaled by the chief's radius, on the unit sphere, the position along the radial, along-track and out-of-plane directions, denoted by x_{us}, y_{us}, and z_{us}, respectively, are given by:

$$\left\{ \begin{array}{c} x_{\mathrm{us}} \\ y_{\mathrm{us}} \\ z_{\mathrm{us}} \end{array} \right\} = \mathbf{C}\,\mathbf{C}_D^{\top} \left\{ \begin{array}{c} 1 \\ 0 \\ 0 \end{array} \right\} - \left\{ \begin{array}{c} 1 \\ 0 \\ 0 \end{array} \right\} \tag{2.18}$$

Sengupta et al. (2004) have shown that some reduction of computation labor can be achieved, if the true anomaly of the chief is used as independent variable. The same objective was achieved by Sabol et al. (2003), but in a time-explicit manner. In this case, a Fourier-Bessel expansion of the true anomaly in terms of the mean anomaly was used. However, for eccentricities of 0.7, terms up to the tenth order in eccentricity are required in the series. Ketema (2005) also used an approach similar to Sengupta et al. (2004), but employed a nesting function to solve Kepler's equation iteratively. Furthermore, a numerical procedure to obtain periodic relative motion was presented.

It is clear that given the orbital elements of the reference satellite, once the initial orbital elements of the chief and deputy corresponding to the respective initial states

are known, the relative trajectory can be completely determined. As a consequence, given the initial orbital elements of the chief, and the differential orbital elements corresponding to the relative states, the relative trajectory can be determined without the requirement of position and velocity data of the deputy in the ECI frame. However, the relationship between orbital element differences and relative states is nonlinear, and in general the former cannot be obtained from the latter in a straightforward manner. Relative motion can also be characterized in a linear setting, by the use of differential orbital elements (Garrison et al. 1995; Alfriend et al. 2000; Vadali et al. 2001; Schaub 2004). Due to the nonlinear mapping between local frame Cartesian coordinates and orbital elements, errors in the Cartesian frame are translated into very small errors in the orbital angles. Although the geometric method uses a non-Cartesian, curvilinear coordinate frame, in the linear case, under the assumption of small elemental differences, this is the same as the rotating Cartesian frame. Alfriend et al. (2000); Vadali et al. (2001); Schaub (2004) approached the problem by linearizing the direction cosine matrix of the orientation of the Deputy with respect to the Chief. Garrison et al. (1995) used true anomaly as the independent variable to obtain analytical expressions for relative motion near high-eccentricity orbits.

In this dissertation, two definitions of the differential orbital element set used to characterize a relative orbit are used. The first uses classical orbital elements, and is defined as:

$$\boldsymbol{\delta\mathfrak{oe}} \triangleq \{\delta a/a \ \delta e \ \delta i \ \delta h \ \delta g \ \delta l_0\}^\top \tag{2.19}$$

The second set is defined as:

$$\boldsymbol{\delta\mathfrak{ns}} \triangleq \{\delta a/a \ \delta\theta \ \delta i \ \delta q_1 \ \delta q_2 \ \delta h\}^\top \tag{2.20}$$

It should be noted that both definitions scale the differential semimajor axis by the semimajor axis of the chief's orbit, to make it dimensionally equivalent to the other differential elements. The use of the classical orbital element differences, as given by (2.19), will be restricted to the analysis of eccentricity effects on relative motion geometry (Chapter III), since they very easily relate to the physics of the problem. The latter definition, as given by (2.20) will be used everywhere else because the results in this dissertation are intended to be uniformly valid even for circular orbits. Finally, when analyzing the problem of relative orbit design and parameterization (Chapter III), and averaged relative motion (Chapter VII), δl will be used instead of $\delta\theta$.

2.6 Effects of the J_2 Perturbation

The presence of Earth oblateness effects complicates the study of satellite motion, as well as relative motion, by causing the orbital elements of a satellite to change with time. The effects on the orbital elements, to the first order in J_2, have been studied by Brouwer (1959) and Kozai (1959), and are classified as secular growth, short-periodic, and long-periodic perturbations. If the study of the change of orbital elements is limited to that due to the first-order secular component, it can be shown that orbital elements a, e, and i can be considered constant and the elements l, g, and h show secular growth. These elements are known as mean elements, and will henceforth be denoted by an overbar (for example, $\overline{a}$ denotes the mean semimajor axis). If the short-periodic and long-periodic perturbations are also included then the instantaneous elements, also known as osculating elements, describe the true orbit.

While Brouwer (1959) posed the problem of orbital element variation as a solution

to a Hamiltonian system perturbed by J_2, Kozai (1959) obtained the secular, short- and long-periodic behavior by a process of averaging. Furthermore, Brouwer (1959) derived generating functions for the short- and long-periodic variations, to the second-order in J_2, by the use of Delaunay elements. Consequently, the osculating elements can be obtained from the mean elements by the addition of periodic variations that are also dependent on mean elements.

It should be noted from (2.3) that the Delaunay elements L and G are identical when the orbit is circular, and the Brouwer transformation loses validity for $e < 0.05$. This problem has been dealt with using a variety of techniques. Smith (1961) reformulated the problem in terms of ECI coordinates without the singular terms, and analytically determined the required correction to these coordinates. Lyddane (1963) modified Brouwer's theory in terms of Poincaré variables, instead of Delaunay elements. The Poincaré variables are a set of canonical variables that are nonsingular for zero eccentricity or inclination, and are written in terms of Delaunay elements as shown below:

$$\begin{array}{cccc} L, & \sqrt{2(L-G)}\cos(g+h), & \sqrt{2(G-H)}\cos h \\ l+g+h, & -\sqrt{2(L-G)}\sin(g+h), & -\sqrt{2(G-H)}\sin h \end{array} \tag{2.21}$$

Similarly, Aksnes (1972) modified Brouwer's theory by using Hill's variables, that use $\dot{r}$, r, and θ, instead of L, l, and g; while Hoots (1981a) used a set of 'position elements', that are valid for the circular and/or equatorial case. However, the exact formulation used is not important. As shown by Gim and Alfriend (2003, 2005), the short- and long-periodic variations in nonsingular or equinoctial elements can also be obtained by using the generating functions in Brouwer (1959), if the partials of these variables with respect to the Delaunay elements are known. Consequently, this dissertation will only refer to the transformation from mean to osculating elements

as Brouwer theory, irrespective of the element set used.

This dissertation (and many other works) limit results to the first order in J_2 only, since an inclusion of second order terms is meaningless without the inclusion of tesseral and sectorial harmonics and higher order zonal harmonics in the potential. However, other works in the literature do extend analysis to $\mathcal{O}(J_2^2)$ and higher. For example, Déprit and Rom (1970) obtained analytical expressions for short- and long-periodic variations through $\mathcal{O}(J_2^3)$, and for secular variations through $\mathcal{O}(J_2^4)$. In their work, eccentricity expansions were made, limiting usage to near-circular orbits. Coffey and Déprit (1982) devised a computational procedure using symbolic algebra to extend the theory for $0 \leq e < 1$.

The effects of J_2 on formation flight manifest themselves by the introduction of differential relative acceleration terms, and by a precession of the rotating frame. the short-periodic variations in a, e, and i also have an effect on relative motion. The complete nonlinear description in the presence of J_2 perturbations has been developed by Kechichian (1998), although the system of equations presented therein cannot be solved in closed form. Simplified, linear relative motion models that include J_2 effects were developed by Vadali et al. (2002) and Schweigart and Sedwick (2002), but their use is limited to circular reference orbits and small relative orbits only. The STM formulated by Gim and Alfriend (2003), using the geometric method in nonsingular orbital elements, also accounts for first-order J_2 effects. This STM can completely characterize linear relative motion in eccentric orbits. A similar result was obtained by Yan et al. (2004), but by utilizing the unit sphere formulation for relative motion.

2.7 Summary

In this chapter, several useful concepts have been introduced, with the relevant background. The equations presented here will be periodically revisited in future chapters that use these preliminary concepts as a starting point for several interesting results. The discussion of the rendezvous problem is reserved until Chapter IV, to place it in proper context.

CHAPTER III

THE GEOMETRY OF FORMATIONS IN KEPLERIAN ELLIPTIC ORBITS WITH ARBITRARY ECCENTRICITY

3.1 Introduction

A formation refers to the special case of relative motion, where initial conditions on the relative states obtained such that the resulting relative motion is bounded and periodic. General two-body motion between two satellites, expressed in the rotating frame is always bounded, though not necessarily periodic. For formation flight, boundedness refers to *local* boundedness, or 1:1 resonance, where the periods of all the satellites in the formation are equal to each other. In Chapter II, the HCW equations were presented, and it can be shown that these equations admit a special class of solutions that are periodic in nature, given by:

$$\xi_h = k_1 \sin(nt + \overline{\psi}_0) \tag{3.1a}$$

$$\vartheta_h = 2k_1 \cos(nt + \overline{\psi}_0) + k_2 \tag{3.1b}$$

$$\zeta_h = k_3 \sin(nt + \overline{\phi}_0) \tag{3.1c}$$

where $k_{1...3}$, $\overline{\psi}_0$ and $\overline{\phi}_0$, are arbitrary constants, and the subscript 'h' is used to denote periodic solutions to the HCW equations. These solutions are obtained when the following condition is satisfied:

$$\dot{\vartheta}_0 + 2n\xi_0 = 0 \tag{3.2}$$

where the subscript '0' is used to denote initial conditions. However, (3.1) are not useful, and (3.2) is no longer a valid condition, when the chief's orbit is eccentric, since

the HCW equations do not account for eccentricity effects. The use of these equations for formation flight, is therefore limited. Inalhan et al. (2002) obtained a boundedness condition for the linear problem for arbitrary eccentricities, by providing an explicit equation relating the initial conditions at perigee. For all other cases of epoch, the initial conditions can be obtained by matrix operations. Gurfil (2005b) posed the bounded-motion problem in terms of an energy-matching condition and presented an algorithm for optimal single-impulse formation-keeping. The boundedness condition in Gurfil (2005b) is presented as the solution to a sixth-order polynomial equation in one variable, and is valid for general two-body motion.

State transition matrices that reflect the effect of eccentricity, have also been derived, and are presented in Melton (2000); Broucke (2003); Wolfsberger et al. (1983); Yamanaka and Ankersen (2002). Melton (2000) used a series expansion for radial distance and true anomaly, in terms of time. However, for moderate eccentricities, the convergence of such series requires the inclusion of higher-order terms. Other state transition matrices are obtained from the TH equations, and use the true anomaly f as the independent variable, and are therefore implicit in time.

The linear relationship between relative motion in the rotating frame, and differential orbital elements, as shown by the geometric method (Alfriend et al. 2000), allows the characterization of small orbital element differences in terms of the constants of the HCW solutions, viz. relative orbit size and phase. This feature has also been used by Vadali et al. (2001) to design formations in near-circular orbits. The basic zero-secular drift condition is satisfied by setting the semi-major axes of the deputy and chief to be equal. The characterization of relative orbit geometry is achieved by relating the rest of the orbital element differences to its shape, size, and the initial phase angle.

Even though relative motion near an arbitrary Keplerian elliptic orbit is well-represented in the literature, the characterization of formations in such orbits has still not been addressed completely. Schaub (2004) related the differential orbital elements to the constants of the HCW solution for near-circular references orbits. Lane and Axelrad (2006) parameterized relative motion in terms of integration constants and differential orbital elements, but their use in the design of formations remains unexplored.

This chapter presents a meaningful parameterization for formation geometry near arbitrarily eccentric orbits. These parameters are directly related to orbit shape and size, in the sense that changing these parameters provides useful and direct insight into the relative orbit geometry, for arbitrarily eccentric orbits. These parameters are derived using the TH model as a basis. This model is useful in deriving a simple linear relationship between the initial conditions that lead to bounded motion, for arbitrary eccentricity and epoch. By simple manipulation, the similarity between the TH model and the geometric method as proposed by Alfriend et al. (2000) is revealed, and the linear relationships between the new parameterization, constants of integration of the TH model, and differential orbital elements, are developed. Furthermore, by the use of Fourier-Bessel expansions, the effects of eccentricity on formation geometry are characterized. The use of the new parameterization intuitively reveals these effects, and schemes for formation design are suggested that accomodate eccentricity effects.

3.2 General Solution to TH Relative Motion Equations

The TH equations are re-stated below:

$$x'' - 2y' - \frac{3x}{(1 + e\cos f)} = 0 \tag{3.3a}$$

$$y'' + 2x' = 0 \tag{3.3b}$$

$$z'' + z = 0 \tag{3.3c}$$

Equations (3.3) have the following general solution (Lawden 1963; Carter and Humi 1987):

$$\begin{aligned} x(f) &= \frac{d_1}{e}\cos f\,(1 + e\cos f) + d_2 \sin f\,(1 + e\cos f) \\ &\quad + d_3 \sin f\,(1 + e\cos f) I(f) \end{aligned} \tag{3.4a}$$

$$\begin{aligned} y(f) &= -\frac{d_1}{e}\sin f\,(2 + e\cos f) + \frac{d_2}{e}\,(1 + e\cos f)^2 \\ &\quad + \frac{d_3}{e}\left[(1 + e\cos f)^2 I(f) + \cot f\right] + d_4 \end{aligned} \tag{3.4b}$$

$$z(f) = d_5 \cos f + d_6 \sin f \tag{3.4c}$$

where

$$I(f) = \int_{f_0}^{f} \frac{1}{\sin^2 f\,(1 + e\cos f)^2}\, df \tag{3.5}$$

As shown in Carter and Humi (1987), (3.5) is easily evaluated in terms of the eccentric anomaly, E, which is related to the true anomaly by (2.1). However, $I(f)$ has a singularity for $f = k\pi$, $k \in \mathbb{Z}$, which can be removed, as shown by Carter (1990), by integrating (3.5) by parts:

$$\begin{aligned} I(f) &= 2e \int_{f_0}^{f} \frac{\cos f}{(1 + e\cos f)^3}\, df - \frac{\cot f}{(1 + e\cos f)^2} + c_J \\ &= 2e\, J(f) - \frac{\cot f}{(1 + e\cos f)^2} + c_J \end{aligned} \tag{3.6}$$

where c_J is an arbitrary constant. Carter (1998) has shown that the state transition matrix formulated utilizing $J(f)$ also has singularities when $e = 0$, which can be removed if $J(f)$ too, is integrated by parts. Yamanaka and Ankersen (2002) have shown that $J(f)$ may also be conveniently rewritten in terms of Kepler's equation, to be uniformly valid for $0 \leq e < 1$. As will be shown later, this step also demonstrates the unity between the TH solutions and the differential orbital element approach (Alfriend et al. 2000), by revealing a linear relationship between the constants of integration of the former approach, and differential orbital elements of the latter approach. The integral $J(f)$ is rewritten as:

$$J(f) = -\frac{3e}{2\eta^5}K(f) + \frac{1}{2\eta^2}\frac{\sin f\,(2 + e\cos f)}{(1 + e\cos f)^2} \tag{3.7}$$

where, $K(f)$, as defined by Yamanaka and Ankersen (2002), is Kepler's equation:

$$K(f) = \int_{f_0}^{f} \frac{\eta^3}{(1 + e\cos f)^2}\,df = (E - e\sin E) - (E_0 - e\sin E_0) = n\,\Delta t \tag{3.8}$$

The constants are rearranged for convenience in the following fashion: $c_1 = d_1/e - d_3/\eta^2$, $c_2 = d_2 + d_3 c_J$, $c_3 = e d_3$, $c_4 = d_2/e + d_3 c_J/e + d_4$, and $c_{5,6} = d_{5,6}$. Then, the solutions to the TH equations are:

$$\begin{aligned} x(f) &= c_1 \cos f\,(1 + e\cos f) + c_2 \sin f\,(1 + e\cos f) \\ &\quad + \frac{2c_3}{\eta^2}\left[1 - \frac{3e}{2\eta^3}\sin f\,(1 + e\cos f)K(f)\right] \qquad (3.9a) \\ y(f) &= -c_1 \sin f\,(2 + e\cos f) + c_2 \cos f\,(2 + e\cos f) \\ &\quad - \frac{3c_3}{\eta^5}(1 + e\cos f)^2 K(f) + c_4 \qquad (3.9b) \\ z(f) &= c_5 \cos f + c_6 \sin f \qquad (3.9c) \end{aligned}$$

The relative velocity components are as follows:

$$x'(f) \;=\; -c_1(\sin f + e\sin 2f) + c_2(\cos f + e\cos 2f)$$

$$-\frac{3ec_3}{\eta^2}\left[\frac{\sin f}{(1+e\cos f)}+\frac{1}{\eta^3}(\cos f+e\cos 2f)K(f)\right] \tag{3.10a}$$

$$y'(f) = -c_1(2\cos f+e\cos 2f)-c_2(2\sin f+e\sin 2f)$$
$$-\frac{3c_3}{\eta^2}\left[1-\frac{e}{\eta^3}(2\sin f+e\sin 2f)K(f)\right] \tag{3.10b}$$

$$z'(f) = -c_5\sin f+c_6\cos f \tag{3.10c}$$

It is clear that the states at any value of true anomaly can be written in the form $\mathbf{x}=\mathbf{L}(f)\mathbf{c}$ where $\mathbf{c}=\{c_1\cdots c_6\}^\top$, and the (j,k)th entry of $\mathbf{L}$ is the term with c_k as a coefficient, in the expression for the jth component of the state vector. In particular, let the initial conditions be denoted by $\mathbf{x}_0=\{x_0\ y_0\ z_0\ x_0'\ y_0'\ z_0'\}^\top$, specified at arbitrary initial true anomaly f_0. It can be shown that $\det\mathbf{L}=1$, and if $\mathbf{M}$ denotes the inverse of $\mathbf{L}$, then $\mathbf{M}=\text{adjoint}\,\mathbf{L}$. It follows that $\mathbf{c}=\mathbf{M}(f_0)\mathbf{x}_0$, where:

$$c_1 = -\frac{3}{\eta^2}(e+\cos f_0)x_0-\frac{1}{\eta^2}\sin f_0\,(1+e\cos f_0)x_0'$$
$$-\frac{1}{\eta^2}(2\cos f_0+e+e\cos^2 f_0)y_0' \tag{3.11a}$$

$$c_2 = -\frac{3}{\eta^2}\frac{\sin f_0(1+e\cos f_0+e^2)}{(1+e\cos f_0)}x_0+\frac{1}{\eta^2}(\cos f_0-2e+e\cos^2 f_0)x_0'$$
$$-\frac{1}{\eta^2}\sin f_0(2+e\cos f_0)y_0' \tag{3.11b}$$

$$c_3 = (2+3e\cos f_0+e^2)\,x_0+e\sin f_0\,(1+e\cos f_0)\,x_0'+(1+e\cos f_0)^2\,y_0' \tag{3.11c}$$

$$c_4 = -\frac{1}{\eta^2}(2+e\cos f_0)\left[\frac{3e\sin f_0}{(1+e\cos f_0)}x_0+(1-e\cos f_0)x_0'+e\sin f_0 y_0'\right]$$
$$+y_0 \tag{3.11d}$$

$$c_5 = \cos f_0\,z_0-\sin f_0\,z_0' \tag{3.11e}$$

$$c_6 = \sin f_0\,z_0+\cos f_0\,z_0' \tag{3.11f}$$

As shown by Yamanaka and Ankersen (2002), the state transition matrix for the TH equations is easily formulated by noting that $\mathbf{x}(f)=\mathbf{L}(f)\,\mathbf{M}(f_0)\,\mathbf{x}_0$.

3.3 Mapping Between States and Differential Orbital Elements

In the geometric description for relative motion, the position in the LVLH frame is written in terms of differential orbital elements by linearizing the direction cosine matrix that orients the deputy LVLH frame with respect to the chief LVLH frame. Alfriend et al. (2000) have shown that:

$$\xi = \delta r \tag{3.12a}$$

$$\vartheta = r(\delta\theta + \delta h \cos i) \tag{3.12b}$$

$$\zeta = r(\delta i \sin\theta - \delta h \sin i \cos\theta) \tag{3.12c}$$

Dividing by r to get the corresponding normalized states, the following equations are obtained:

$$x = \delta r / r \tag{3.13a}$$

$$y = \delta\theta + \delta h \cos i \tag{3.13b}$$

$$z = \delta i \sin\theta - \delta h \sin i \cos\theta \tag{3.13c}$$

Following the development in Schaub (2004), it can be shown that:

$$\begin{aligned} \frac{\delta r}{r} &= \frac{e}{\eta^3}\sin f(1+e\cos f)\delta l_0 - \frac{1}{\eta^2}\cos f(1+e\cos f)\delta e \\ &\quad + \left[1 - \frac{3e}{2\eta^3}\sin f\,(1+e\cos f)\,n\,\Delta t\right]\frac{\delta a}{a} \end{aligned} \tag{3.14}$$

wherein the fact that the mean anomaly difference, δl is the sum of its initial value, δl_0, and the difference in mean motion propagated over the elapsed time since epoch, has been used:

$$\delta l = \delta l_0 + \delta n\,\Delta t = \delta l_0 - \frac{3}{2} n\,\Delta t\,\frac{\delta a}{a} \tag{3.15}$$

Using (3.8), $n\,\Delta t = K(f)$, a direct correspondence between (3.14) and (3.9a) is observed:

$$\delta a = \frac{2a}{\eta^2} c_3 \tag{3.16}$$

$$\delta l_0 = \frac{\eta^3}{e} c_2 \tag{3.17}$$

$$\delta e = -\eta^2 c_1 \tag{3.18}$$

Comparing the expression for z from (3.13) with (3.9c), the following are obtained:

$$\delta i \sin g - \delta h \sin i \cos g = c_5 \tag{3.19a}$$

$$\delta i \cos g + \delta h \sin i \sin g = c_6 \tag{3.19b}$$

Consequently,

$$\delta i = \sin g\, c_5 + \cos g\, c_6 = \sin\theta_0\, z_0 + \cos\theta_0\, z_0' \tag{3.20}$$

$$\delta h \sin i = -\cos g\, c_5 + \sin g\, c_6 = -(\cos\theta_0\, z_0 - \sin\theta_0\, z_0') \tag{3.21}$$

where $\theta_0 = g + f_0$. Finally, comparing the expression for y from (3.13) with (3.9b), the following result is obtained:

$$\delta g = c_4 - \frac{\delta l_0}{\eta^3} - \delta h \cos i \tag{3.22}$$

Thus, the orbital element differences (to the first order) can be obtained by substituting $c_{1\ldots6}$ in the above equations. Let $\boldsymbol{\delta oe} = \{\delta a\ \delta e\ \delta i\ \delta h\ \delta g\ \delta l_0\}^\top$ denote the vector of differential orbital elements. Let $\mathbf{oe}_C$ denote the orbital elements of the chief. Then the equations relating differential orbital elements to the constants of integration as shown above, may be summarized by $\boldsymbol{\delta oe} = \mathbf{N}(\mathbf{oe}_C)\mathbf{c}$, where the matrix $\mathbf{N}$ has as its entries, the coefficients of the integration constants comprising the differential orbital elements. Consequently, the relation $\boldsymbol{\delta oe} = \mathbf{N}(\mathbf{oe}_C)\mathbf{M}(f_0)\mathbf{x}_0$

yields the differential orbital elements in terms of the initial conditions. It can be shown that $\det \mathbf{N} = 2\eta^3 a/(e \sin i)$ and $\det \mathbf{M} = 1$; this means the mapping from relative Cartesian coordinates to differential orbital elements is singular when the reference orbit is circular or equatorial ($e = 0$ or $i = 0$, respectively). In particular, if e is a small number (or zero), then calculations for δl_0 and δg from (3.17) and (3.22), respectively, yield large numbers (or are undefined) due to e appearing in the denominator. However, their sum is a small number, consistent with assumption of small orbital element differences. This problem may be solved by using nonsingular orbital elements. The solutions to the TH equations, and the development of differential nonsingular orbital elements in terms of the initial conditions are presented in a later section. The singularity due to $e = 0$ also ceases to be a problem if the parameterization developed in this chapter, is used. However, for the following sections, results are shown using the classical orbital element set since they are more concisely expressed in terms of these elements.

3.4 Drift per Orbit due to Mismatched Semimajor Axes

If δa (and consequently, c_3) is not zero, then from (3.9) it is evident that x and y will grow in an unbounded fashion, due to the presence of $K(f)$, which is an increasing function. After one orbit of the chief, the drift in x and y directions are thus:

$$x_{\text{drift}} = x(f_0 + 2\pi) - x(f_0) = -\frac{6\pi c_3}{\eta^5} e \sin f_0 \,(1 + e \cos f_0) \tag{3.23a}$$

$$y_{\text{drift}} = y(f_0 + 2\pi) - y(f_0) = -\frac{6\pi c_3}{\eta^5} (1 + e \cos f_0)^2 \tag{3.23b}$$

The drift in the unscaled coordinates, in terms of differential semimajor axis, can be calculated to yield the following:

$$\xi_{\text{drift}} = -\frac{3\pi}{\eta}\, e \sin f_0\, \delta a \tag{3.24a}$$

$$\vartheta_{\text{drift}} = -\frac{3\pi}{\eta}\, (1 + e\cos f_0)\, \delta a \tag{3.24b}$$

It should be noted that ζ remains bounded. Thus the total drift in position, denoted by ϱ_{drift} is:

$$\varrho_{\text{drift}} = \left(\xi^2_{\text{drift}} + \vartheta^2_{\text{drift}}\right)^{\frac{1}{2}} = \frac{3\pi}{\eta}\, \delta a\, (1 + e^2 + 2e\cos f_0)^{\frac{1}{2}} \tag{3.25}$$

This drift is maximum at $f_0 = 0$, and minimum at $f_0 = \pi$, and is bounded as shown below (Carpenter and Alfriend 2005):

$$3\pi\, \delta a \sqrt{\frac{1-e}{1+e}} \leq \varrho_{\text{drift}} \leq 3\pi\, \delta a \sqrt{\frac{1+e}{1-e}} \tag{3.26}$$

3.5 Periodic Orbits

Periodic solutions may be obtained by choosing initial conditions such that $c_3 = 0$, since the rest of the terms in the solution are sinusoids, and therefore, periodic. Consequently, (3.11c) results in the following relation for bounded relative motion:

$$(2 + 3e\cos f_0 + e^2)\, x_0 + e\sin f_0\, (1 + e\cos f_0)\, x_0' + (1 + e\cos f_0)^2\, y_0' = 0 \tag{3.27}$$

In unscaled coordinates, this is transformed into the following linear condition for bounded relative motion, for arbitrary eccentricity and epoch:

$$\begin{aligned}&(2 + e\cos f_0)\, (1 + e\cos f_0)^2 \left(\frac{\xi}{p}\right) + (1 + e\cos f_0) \left(\dot{\xi}\sqrt{\frac{p}{\mu}}\right) \\ &-e\sin f_0\, (1 + e\cos f_0)^2 \left(\frac{\vartheta}{p}\right) + e\sin f_0 \left(\dot{\vartheta}\sqrt{\frac{p}{\mu}}\right) = 0\end{aligned} \tag{3.28}$$

Equation (3.27) is satisfied for an infinite combination of initial conditions, except when $f_0 = 0$ or $f_0 = \pi$. Furthermore, when $e = 0$, this reduces to the well-known Hill's condition for periodicity. Without loss of generality, one may choose:

$$y_0' = -\frac{(2 + 3e\cos f_0 + e^2)}{(1 + e\cos f_0)^2} x_0 - \frac{e\sin f_0}{(1 + e\cos f_0)} x_0' \tag{3.29}$$

With $c_3 = 0$, the expressions for the trajectory are considerably simplified. Upon substituting (3.29) in (3.11), the constants may be rewritten in terms of dimensional position and velocity with f as the independent variable,

$$\begin{aligned}
c_1 &= \frac{(\cos f_0 + e\cos 2f_0)}{(1 + e\cos f_0)^2} x_0 - \frac{\sin f_0}{(1 + e\cos f_0)} x_0' = \frac{\xi_0}{p}\cos f_0 - \frac{\xi_0'}{p}\sin f_0 && (3.30a)\\
c_2 &= \frac{(\sin f_0 + e\sin 2f_0)}{(1 + e\cos f_0)^2} x_0 + \frac{\cos f_0}{(1 + e\cos f_0)} x_0' = \frac{\xi_0}{p}\sin f_0 + \frac{\xi_0'}{p}\cos f_0 && (3.30b)\\
c_4 &= y_0 - \frac{(2 + e\cos f_0)}{(1 + e\cos f_0)} \left(\frac{e\sin f_0}{1 + e\cos f_0} x_0 + x_0' \right) \\
&= \frac{\vartheta_0}{p}(1 + e\cos f_0) - \frac{\xi_0'}{p}(2 + e\cos f_0) && (3.30c)\\
c_5 &= z_0\cos f_0 - z_0'\sin f_0 = \frac{\zeta_0}{p}(\cos f_0 + e) - \frac{\zeta_0'}{p}\sin f_0(1 + e\cos f_0) && (3.30d)\\
c_6 &= z_0\sin f_0 + z_0'\cos f_0 = \frac{\zeta_0}{p}\sin f_0 + \frac{\zeta_0'}{p}\cos f_0(1 + e\cos f_0) && (3.30e)
\end{aligned}$$

Using (3.30), new relative orbit parameters, $\varrho_{1\ldots3}$, ψ_0, and ϕ_0 may be defined:

$$\begin{aligned}
\varrho_1 &= \left(\xi_0^2 + \xi_0'^2\right)^{\frac{1}{2}} = \frac{a}{\eta}\left(\eta^2\delta e^2 + e^2\delta l_0^2\right)^{\frac{1}{2}} && (3.31a)\\
\varrho_2 &= \vartheta_0(1 + e\cos f_0) - \xi_0'(2 + e\cos f_0) = p\left(\delta g + \delta h\cos i + \frac{1}{\eta^3}\delta l_0\right) && (3.31b)\\
\varrho_3 &= \left[(1 + 2e\cos f_0 + e^2)\zeta_0^2 + (1 + e\cos f_0)^2\zeta_0'^2 - 2e\sin f\,(1 + e\cos f)\zeta_0\zeta_0'\right]^{\frac{1}{2}} \\
&= p\left(\delta i^2 + \delta h^2\sin^2 i\right)^{\frac{1}{2}} && (3.31c)\\
\psi_0 &= \tan^{-1}\left(\frac{\xi_0}{\xi_0'}\right) - f_0 = \tan^{-1}\left(-\frac{\eta}{e}\frac{\delta e}{\delta l_0}\right) && (3.31d)\\
\phi_0 &= \tan^{-1}\left(\frac{(1 + e\cos f_0)\zeta_0}{(1 + e\cos f_0)\zeta_0' - e\sin f_0\zeta_0}\right) - f_0
\end{aligned}$$

$$= \tan^{-1}\left(-\frac{\delta h \sin i}{\delta i}\right) + g \tag{3.31e}$$

Using these relative orbit parameters, the most general solution for periodic motion near a Keplerian elliptic orbit with linearized differential gravity, denoted by the subscript '$\wp$', is given by:

$$x_\wp(f) = \frac{\varrho_1}{p}\sin(f+\psi_0)\,(1+e\cos f) \tag{3.32a}$$

$$y_\wp(f) = \frac{\varrho_1}{p}\cos(f+\psi_0)\,(2+e\cos f) + \frac{\varrho_2}{p} \tag{3.32b}$$

$$z_\wp(f) = \frac{\varrho_3}{p}\sin(f+\phi_0) \tag{3.32c}$$

The constants $c_{1\ldots6}$ may be expressed using the design parameters, as shown:

$$c_1 = \frac{\varrho_1}{p}\sin\psi_0, \quad c_2 = \frac{\varrho_1}{p}\cos\psi_0, \quad c_4 = \frac{\varrho_2}{p}, \quad c_5 = \frac{\varrho_3}{p}\sin\phi_0, \quad c_6 = \frac{\varrho_3}{p}\cos\phi_0 \tag{3.33}$$

Obviously, the most general form of periodic solutions to the HCW equations are a special case of (3.32).

Two advantages of using the new parameterization have been mentioned earlier, viz. their uniform validity for $0 \leq e < 1$, and the fact that ϱ_1 and ϱ_3 are obviously size parameters, ϱ_2 is a bias parameter, and ψ_0 and ϕ_0 are phase angle parameters. The differential orbital elements may also be rewritten in terms of the parameter set. These relations are useful, for example, if Gauss' variational equations are used to initiate a numerical procedure for formation establishment or reconfiguration. Such an approach was used by Vaddi et al. (2005), to establish and reconfigure formations near circular orbits, using impulsive thrust. Upon substituting (3.33) into (3.16)-(3.22), and setting $c_3 = 0$, the following are obtained:

$$\delta a = 0 \tag{3.34a}$$

$$\delta e = -\eta^2 c_1 = -\frac{\varrho_1}{a}\sin\psi_0 \tag{3.34b}$$

$$\delta i = \sin g\, c_5 + \cos g\, c_6 = \frac{\varrho_3}{p}\cos(\phi_0 - g) \tag{3.34c}$$

$$\delta h = \frac{1}{\sin i}\left(-\cos g\, c_5 + \sin g\, c_6\right) = -\frac{\varrho_3}{p}\frac{\sin(\phi_0 - g)}{\sin i} \tag{3.34d}$$

$$\delta l_0 = \frac{\eta^3}{e}c_2 = \frac{\varrho_1}{a}\frac{\eta}{e}\cos\psi_0 \tag{3.34e}$$

$$\delta g = \frac{\varrho_2}{p} - \frac{\delta l_0}{\eta^3} - \delta h\cos i \tag{3.34f}$$

Corresponding expressions for nonsingular orbital elements are presented in a later section.

3.6 Eccentricity-Induced Effects on Relative Orbit Geometry

The most general form of periodic motion in the setting of the HCW equations is given (3.1), written in a slightly modified form:

$$\xi_h = k_1 \sin(\tau + \overline{\psi}_0) \tag{3.35a}$$

$$\vartheta_h = 2k_1 \cos(\tau + \overline{\psi}_0) + k_2 \tag{3.35b}$$

$$\zeta_h = k_3 \sin(\tau + \overline{\phi}_0) \tag{3.35c}$$

where $\tau = nt$ is the normalized time or mean anomaly, though in the case of the HCW equations, this is equivalent to true anomaly since eccentricity is assumed zero. The relative orbit obtained from the solution to the TH equations has a trajectory in

the local frame whose components are given by the following expressions:

$$\xi_\wp = r x_\wp = \varrho_1 \sin(f + \psi_0) \tag{3.36a}$$

$$\vartheta_\wp = r y_\wp = 2\varrho_1 \cos(f + \psi_0) \frac{(1 + (e/2)\cos f)}{(1 + e\cos f)} + \frac{\varrho_2}{(1 + e\cos f)} \tag{3.36b}$$

$$\zeta_\wp = r z_\wp = \varrho_3 \frac{\sin(f + \phi_0)}{(1 + e\cos f)} \tag{3.36c}$$

Eccentricity effects may be studied by expanding $\vartheta_\wp$ and $\zeta_\wp$ as Fourier series. In this section, the effects of eccentricity are analyzed by using both true anomaly, and time as the independent variable.

3.6.1 True Anomaly as the Independent Variable

The Cauchy residue theorem is now used to resolve the periodic terms in the denominator of (3.36), into a Fourier series of terms composed of $\cos kf$ and $\sin kf$, $k = 1 \ldots \infty$. This is similar to the approach used in Battin (1999, chap. 5) to obtain a series expansion of eccentric anomaly in terms of mean anomaly. As an example, an expansion of $1/(1 + e\cos f)$, of the following form is desired:

$$\frac{1}{(1 + e\cos f)} = \gamma_0 + \sum_{k=1}^{\infty} \gamma_k \cos kf \tag{3.37}$$

The coefficient γ_0 is obtained in a straightforward manner, as follows:

$$\gamma_0 = \frac{1}{2\pi} \int_0^{2\pi} \frac{df}{(1 + e\cos f)} = \frac{1}{2\pi} \frac{1}{\eta} \int_0^{2\pi} dE = \frac{1}{\eta} \tag{3.38}$$

The procedure to obtain γ_k, $k = 1 \ldots \infty$ is slightly more involved. The following integral is considered:

$$I_{\gamma k} = \frac{1}{\pi} \int_0^{2\pi} \frac{\exp(\jmath k f)\, df}{(1 + e\cos f)} \tag{3.39}$$

The integral $I_{\gamma k}$ can be solved by the change of variable, $\exp(\jmath f) = \chi$. Furthermore, a new, eccentricity-dependent term is introduced, as shown:

$$\varepsilon = \sqrt{\frac{1-\eta}{1+\eta}} = \frac{e}{2}\left(1 + \frac{1}{4}e^2 + \frac{1}{8}e^4 + \frac{5}{64}e^6 + \cdots\right) = \mathcal{O}(e) \tag{3.40}$$

The change of variable to χ results in the following equations:

$$\exp(\jmath k f) = \chi^k \tag{3.41a}$$

$$df = -\frac{\jmath}{\chi}\, d\chi \tag{3.41b}$$

$$1 + e\cos f = 1 + \frac{e}{2}\left(\chi + \frac{1}{\chi}\right) = \frac{e}{2\chi}(\chi+\varepsilon)(\chi+1/\varepsilon) \tag{3.41c}$$

Using (3.41), $I_{\gamma k}$ reduces to the following form:

$$\begin{aligned} I_{\gamma k} &= -\frac{2\jmath}{\pi e}\oint_C \frac{\chi^k\, d\chi}{(\chi+\varepsilon)(\chi+1/\varepsilon)} \\ &= -\frac{\jmath}{\pi\eta}\left[\oint_C \frac{\chi^k\, d\chi}{(\chi+\varepsilon)} - \oint_C \frac{\chi^k\, d\chi}{(\chi+1/\varepsilon)}\right] \end{aligned} \tag{3.42}$$

where subscript 'C' denotes integration over the unit imaginary circle centered at zero. Observing that $\varepsilon < 1$ and $1/\varepsilon > 1$, Cauchy's residue theorem is made use of, to show that:

$$\oint_C \frac{\chi^k\, d\chi}{(\chi+1/\varepsilon)} = 0 \tag{3.43a}$$

$$\oint_C \frac{\chi^k\, d\chi}{(\chi+\varepsilon)} = 2\pi\jmath(-\varepsilon)^k \tag{3.43b}$$

Upon substituting (3.43) in (3.42), the following is obtained:

$$I_{\gamma k} = \frac{2}{\eta}(-\varepsilon)^k \tag{3.44}$$

Since γ_k is simply the real part of $I_{\gamma k}$, and $I_{\gamma k}$ is real, the following series is obtained:

$$\frac{1}{(1+e\cos f)} = \frac{1}{\eta}+\frac{2}{\eta}\sum_{k=1}^{\infty}(-\varepsilon)^k\cos kf \tag{3.45}$$

Similarly, it can be shown that:

$$\begin{aligned}\cos f\,\frac{(2+e\cos f)}{(1+e\cos f)} &= -\frac{\varepsilon}{\eta}+\frac{(2+\eta+\eta^2)}{\eta(1+\eta)}\cos f \\ &\quad +\frac{2}{\eta(1+\eta)}\sum_{k=2}^{\infty}(-\varepsilon)^{k-1}\cos kf \qquad (3.46a)\\ \sin f\,\frac{(2+e\cos f)}{(1+e\cos f)} &= \frac{(3+\eta)}{(1+\eta)}\sin f+\frac{2}{(1+\eta)}\sum_{k=2}^{\infty}(-\varepsilon)^{k-1}\sin kf \qquad (3.46b)\end{aligned}$$

Using these series, the periodic solutions are resolved as the following:

$$\begin{aligned}\vartheta_{\wp}(f) &= \left[-\frac{\varepsilon}{\eta}\varrho_1\cos\psi_0+\frac{1}{\eta}\varrho_2\right] \qquad (3.47a)\\ &\quad +\left[\frac{(2+\eta+\eta^2)}{\eta(1+\eta)}\varrho_1\cos\psi_0-2\frac{\varepsilon}{\eta}\varrho_2\right]\cos f-\frac{(3+\eta)}{(1+\eta)}\varrho_1\sin\psi_0\sin f \\ &\quad +\frac{2}{\eta(1+\eta)}\sum_{k=2}^{\infty}(-\varepsilon)^{k-1}\Big[\,\{\varrho_1\cos\psi_0-\varepsilon(1+\eta)\varrho_2\}\cos kf-\eta\varrho_1\sin\psi_0\,\sin kf\Big] \\ \zeta_{\wp}(f) &= -\frac{\varepsilon}{\eta}\varrho_3\sin\phi_0+\frac{2}{\eta(1+\eta)}\varrho_3\left(\eta\cos\phi_0\,\sin f+\sin\phi_0\,\cos f\right) \qquad (3.47b)\\ &\quad +\frac{2}{\eta(1+\eta)}\varrho_3\sum_{k=2}^{\infty}(-\varepsilon)^{k-1}\left(\eta\cos\phi_0\,\sin kf+\sin\phi_0\,\cos kf\right)\end{aligned}$$

It is observed that both the ϑ and ζ components of motion have constant terms, a primary harmonic, associated with relative orbit size parameters, and higher-order harmonics. Thus the five effects of eccentricity are immediately recognized. The first effect is obviously the presence of higher-order harmonics, whose amplitudes decrease by a factor of ε successively. For non-zero eccentricities, this causes deviation from the well-known circular shape of the HCW solutions.

The second effect is that of amplitude scaling, as may be observed by the presence of

terms dependent on η in the amplitudes of the primary harmonics in both ϑ and ζ. Consequently, as eccentricity increases, for the same choice of $\varrho_{1...3}$, the orbit tends to shrink in the along-track direction and expand in the out-of-plane direction.

Third, a phase shift is introduced. This is readily observed by recasting (3.47*b*) as:

$$\begin{aligned}\zeta_{\wp}(f) &= -\frac{\varepsilon}{\eta}\varrho_3 \sin\phi_0 + \frac{2}{\eta(1+\eta)}\left(\sin^2\phi_0 + \eta^2\cos^2\phi_0\right)^{\frac{1}{2}}\varrho_3 \sin\left(f+\widetilde{\phi}_0\right) \\ &\quad + \frac{2}{\eta(1+\eta)}\left(\sin^2\phi_0 + \eta^2\cos^2\phi_0\right)^{\frac{1}{2}}\varrho_3 \sum_{k=2}^{\infty}(-\varepsilon)^{k-1}\sin\left(kf+\widetilde{\phi}_0\right)\end{aligned} \tag{3.48}$$

where

$$\widetilde{\phi}_0 = \tan^{-1}\left(\frac{1}{\eta}\tan\phi_0\right) = \phi_0 + \frac{e^2}{4}\sin 2\phi_0 + \frac{e^4}{8}\left(\sin 2\phi_0 + \frac{1}{4}\sin 4\phi_0\right) + \mathcal{O}(e^6) \tag{3.49}$$

Furthermore, the phase angle of the deputy also affects its amplitude.

Fourth, the formation is rendered off-center, due to the presence of constant terms in the $\vartheta_{\wp}$ and $\zeta_{\wp}$ components of motion. The bias depends on the phase angles ψ_0 and ϕ_0 of the deputy. While the bias in $\zeta_{\wp}$ cannot be controlled since ϱ_3 is specified by relative orbit design requirements, the bias in $\vartheta_{\wp}$ can be removed by an appropriate choice of ϱ_2.

The appearance of higher-order harmonics in $\vartheta_{\wp}$ and $\zeta_{\wp}$, but not in $\xi_{\wp}$, causes the fifth effect - that of skewness of the relative orbit plane. When formations require the phase angles in the along-track and out-of-plane to be equal, the radial motion is in-phase with the along-track, and consequently, out-of-plane motion. Consequently, a plot of the out-of-plane motion vs. the radial motion would result in a straight line. However, due to eccentricity effects, higher-order harmonics appear in $\zeta_{\wp}$, but not in $\xi_{\wp}$. This causes deviations in the plane normal to the along-track direction. This will be demonstrated in the context of Projected Circular Orbit solutions.

3.6.2 Time as the Independent Variable

In this section, time is treated as the independent variable, since this is what is directly observable with time-tagged data. Use is made of the normalized time τ, which is the same as the mean anomaly. In this case, the relative motion expressions are qualitatively the same, i.e., they exhibit the same properties as in the previous section. However, in the quantitative sense, the equations are different. In this section use is made of the following relations (Battin 1999, chap. 5):

$$\cos kl = \sum_{m=-\infty}^{\infty} J_m(-ke)\cos(m+k)E \tag{3.50a}$$

$$\sin kl = \sum_{m=-\infty}^{\infty} J_m(-ke)\sin(m+k)E \tag{3.50b}$$

where J_m are Bessel functions of the first kind of order m (not to be confused with the zonal harmonic J_2), and

$$J_m(\nu) = \sum_{p=0}^{\infty} \frac{(-1)^p}{2^{2p+m}\, p!\, (m+p)!}\nu^{2p+m} \tag{3.51}$$

It can then be shown that:

$$\begin{aligned} \vartheta_{\wp}(\tau) &= (A_0\varrho_1\cos\psi_0 + B_0\varrho_2) + \sum_{k=1}^{\infty}\Big[(A_k\varrho_1\cos\psi_0 + B_k\varrho_2)\cos k\tau \\ &\quad -C_k\sin\psi_0\sin k\tau\Big] \end{aligned} \tag{3.52a}$$

$$\zeta_{\wp}(\tau) = S_0\varrho_3\sin\phi_0 + \varrho_3\sum_{k=1}^{\infty}(S_k\sin\phi_0\cos k\tau + T_k\cos\phi_0\sin k\tau) \tag{3.52b}$$

where,

$$A_0 = -\frac{e}{2\eta^2}(3+2\eta^2) \tag{3.53a}$$

$$A_k = -\frac{(1-k\eta^4)}{k\eta^2}J_{k+1}(ke) + \frac{(1+k\eta^4)}{k\eta^2}J_{k-1}(ke) \tag{3.53b}$$

$$B_0 = \frac{3-\eta^2}{2\eta^2} \tag{3.53c}$$

$$B_k = \frac{e}{k\eta^2}\left[J_{k+1}(ke) - J_{k-1}(ke)\right] \tag{3.53d}$$

$$C_k = \frac{2}{\eta}\frac{J_k(ke)}{ke} - \eta\left[J_{k+1}(ke) - J_{k-1}(ke)\right] \tag{3.53e}$$

$$S_0 = -\frac{3e}{2\eta^2} \tag{3.53f}$$

$$S_k = -\frac{1}{k\eta^2}\left[J_{k+1}(ke) - J_{k-1}(ke)\right] \tag{3.53g}$$

$$T_k = \frac{2}{\eta}\frac{J_k(ke)}{ke} \tag{3.53h}$$

Even though C_k and T_k have e in the denominator, the computation of these expressions do not cause problems as $e \to 0$, because of the following expansion:

$$\frac{J_k(ke)}{ke} = \sum_{m=0}^{\infty} \frac{(-1)^m}{2^{2m+k}\, l!\,(k+m)!}\,(ke)^{2m+k-1}, \quad k \geq 1 \tag{3.54}$$

The expansion of $\xi_\wp$ in terms of harmonics of the mean anomaly is straightforward since the equations relating $\cos f$ and $\sin f$ to $\cos kl$ and $\sin kl$ are provided in Battin (1999):

$$\begin{aligned}
\xi_\wp(\tau) &= \varrho_1 \sin\psi_0 \cos f + \varrho_1 \cos\psi_0 \sin f \\
&= -e\varrho_1 \sin\psi_0 + \frac{2\eta^2}{e}\varrho_1 \sin\psi_0 \sum_{k=1}^{\infty} J_k(ke)\cos kl \\
&\quad -\eta\varrho_1 \cos\psi_0 \sum_{k=1}^{\infty}\left[J_{k+1}(ke) - J_{k-1}(ke)\right]\sin kl
\end{aligned} \tag{3.55}$$

Consequently, using a numerical procedure, table lookup, or truncation of the series to the desired order of eccentricity, (3.52a), (3.52b), and (3.55) provide time-explicit expressions for bounded relative motion, which can perform as excellent reference trajectories for formation-keeping.

3.6.3 Correcting for Bias

The problem of bias correction is now studied in detail, for the two choices of the independent variable. Although a bias correction is not strictly necessary, it is useful to study eccentricity effects on bias, because this may cause a close approach between the deputy and chief. Since the bias in $\zeta_\wp$ cannot be controlled, only the bias in $\vartheta_\wp$ is examined. An examination of $(3.47a)$ suggests the following choice of ϱ_2, to correct for bias:

$$\varrho_2 = \varepsilon \varrho_1 \cos\psi_0 \tag{3.56}$$

Equation $(3.52a)$ suggests the following condition:

$$\varrho_2 = [e(3+2\eta^2)/(3-\eta^2)]\varrho_1 \cos\psi_0 \tag{3.57}$$

However, the bias corrections suggested by (3.56), and (3.57) have different interpretations. Equation (3.56) does not offer meaningful physical interpretation, in the sense that it is the average of a quantity of a variable that is a nonlinear function of time. In this sense, Equation (3.57) is physically more significant, since this correction will imply that the deputy spends equal amounts of time on either side of the chief in the along-track direction. It is obvious that both interpretations converge as the chief's orbit eccentricity decreases, and have vastly different intepretations for high eccentricities.

This point is illustrated by Figure 3.1, for a chief's eccentricity of 0.6. Let $\varrho_1 = 1/2$, $\varrho_3 = 1$ and $\psi_0 = \phi_0 = 0$. For a circular reference orbit, these correspond to the HCW initial conditions for a projected circular orbit. If $\varrho_2 = \varepsilon\varrho_1 \cos\psi_0$, then the variation of $\vartheta_\wp$ with respect to τ is shown by the dashed, green line. It is therefore

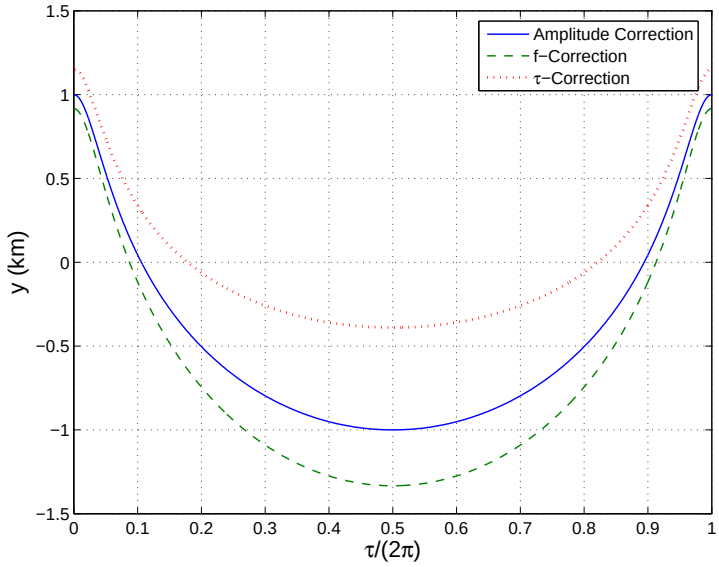

Fig. 3.1 Effect of Bias Corrections on Along-Track lotion, $e = 0.6$

not immediately apparent that this implies the deputy is on either side of the chief in the along track direction, for equal portions of the true anomaly. Moreover, the motion is not symmetric with respect to the $\mathbf{i}_h$ vector since $|\vartheta_\wp(-\psi_0)/\varrho_1| < 2\varrho_1$ and $|\vartheta_\wp(\pi - \psi_0)/\varrho_1| > 2\varrho_1$. If $\varrho_2 = [e(3+2\eta^2)/(3-\eta^2)]\varrho_1 \cos\psi_0$, then, the variation of $\vartheta_\wp$ is depicted by the dotted, red line. This shows values that are greater than $2\varrho_1$ for regions near the chief's perigee, and less than $2\varrho_1$ for regions near the chief's apogee. However, the *time-averaged* value is zero. Thus if the mission requires the deputy to be near the chief in the along track direction for large periods of time, this bias correction is suitable.

The following condition is now examined:

$$\varrho_2 = e\varrho_1 \cos\psi_0 \tag{3.58}$$

This condition ensures that equality $|\vartheta_\wp(-\psi_0)| = |\vartheta_\wp(\pi - \psi_0)|$. This may be

demonstrated by direct substitution in (3.36), which leads to $\vartheta_{\wp}(-\psi_0) = 2\varrho_1$ and $\vartheta_{\wp}(\pi - \psi_0) = -2\varrho_1$. The use of this correction results in the solid, blue line in Figure 3.1. It should be noted that motion subsequent to this correction is also bounded between $\pm 2\varrho_1$.

Other versions of bias correction exist in the literature. Vaddi et al. (2003) and Melton (2000) employ a correction that is valid for low eccentricities. Inalhan et al. (2002) describe a process for obtaining initial relative velocity for symmetric motion, by posing the problem as a linear program. However, any of the corrections derived in this section, are valid for arbitrary eccentricity. For example, using (3.31) and (3.58), results in the following:

$$\vartheta_0 - 2\xi_0' = \frac{e \sin f_0}{(1 + e \cos f_0)} \xi_0 \tag{3.59}$$

3.7 Corrections to HCW Initial Conditions

It is of interest to study the deviation induced from the classical HCW solutions due to eccentricity. The different cases are analyzed individually.

3.7.1 Leader-Follower Formation Modified by an Eccentric Reference Orbit

In the Leader-Follower Formation, the deputy is at a fixed distance from the chief, along the reference orbit. In the classical HCW environment, this is obtained by setting $k_1 = k_3 = 0$, and $k_2 = d$ in (3.35), where d is the desired separation of the deputy from the chief. However, if $\varrho_1 = \varrho_3 = 0$ and $\varrho_2 = d$ in (3.36), then the deputy-chief separation varies from $d/(1+e)$ to $d/(1-e)$, with a time-averaged value of $c_0 d$. Consequently, the correct choice for ϱ_2 should be $\varrho_2 = d/B_0 = 2\eta^2 d/(3-\eta^2)$.

Irrespective of whether or not the distance is corrected for, care must be taken that a value of ϱ_2 is chosen to ensure that the minimum separation meets design requirements, because as eccentricity increases, the minimum separation decreases.

3.7.2 Projected Circular Orbit Modified by an Eccentric Reference Orbit

Projected Circular Orbits (PCO) are obtained in the HCW equations by setting $2k_1 = k_3 = \varrho$, and $\psi_0 = \varphi_0$ in (3.35). Consequently, $\vartheta_h^2 + \zeta_h^2 = \varrho^2$. However, PCOs can never be obtained near an eccentric reference, as is evident from (3.36). It is possible, however, to choose initial conditions such that the relative orbit is as circular as possible, at least to the first harmonic. Assuming that $\varrho_2 = e\varrho_1 \cos\psi_0$ is chosen as the zero-bias condition, then $\varrho_1 = \varrho/2$ is sufficient to ensure that maximum and minimum values of $\vartheta_{\wp}(\tau)$ are consistent with HCW conditions. However, the new phase angle for the first harmonic of $\vartheta_{\wp}(\tau)$ is now $\widetilde{\psi}_0$, where:

$$\tan\widetilde{\psi}_0 = \frac{C_1}{A_1 + e}\tan\psi_0 \tag{3.60}$$

For consistency, it is desired that the first harmonic of $\zeta_{\wp}(\tau)$ also have the same phase angle as $\vartheta_{\wp}(\tau)$, so that to the first harmonic, a corrected-PCO is obtained. The phase angle of the first harmonic of $\zeta_{\wp}(\tau)$ is denoted by $\widetilde{\phi}_0$, where:

$$\tan\widetilde{\phi}_0 = \frac{S_1}{T_1}\tan\phi_0 \tag{3.61}$$

Consequently,

$$\tan\phi_0 = \frac{T_1}{S_1}\tan\widetilde{\phi}_0 = \frac{T_1}{S_1}\tan\widetilde{\psi}_0 = \frac{T_1 C_1}{S_1(A_1 + e)}\tan\psi_0 \tag{3.62}$$

Finally, though out-of-plane bias cannot be controlled, its amplitude can be corrected so that the time average of $\zeta_{\wp}(\tau)$ is equal to ϱ. Consequently,

$$\varrho_3 = \frac{\varrho}{\left(S_1^2 \sin^2 \phi_0 + T_1^2 \cos^2 \phi_0\right)^{\frac{1}{2}}} \tag{3.63}$$

It is also possible to ensure that maximum $\zeta_{\wp}(\tau)$ does not exceed ϱ. From (3.36), the extrema of $\zeta_{\wp}(f)$ occur when $\cos(f + \phi_0) + e\cos\phi_0 = 0$, or when $f = -\phi_0 \pm \cos^{-1}(-e\cos\phi_0)$. Of these, the negative sign corresponds to minimum $\zeta_{\wp}(f)$ and positive sign to maximum $\zeta_{\wp}(f)$. Thus if

$$\varrho_3 = \left(-e\sin\phi_0 + \sqrt{1 - e^2\cos^2\phi_0}\right)\varrho \tag{3.64}$$

then the maximum deviation in the out-of-plane motion will be bounded by $\pm\varrho$. An issue with this approach is that by placing bounds on the maximum out-of-plane motion, its minimum is also naturally reduced, which may bring the deputy very close to the chief.

Figure 3.2 shows examples of a formation initiated with the corrected and uncorrected initial conditions, for a reference orbit with $e = 0.2$ and $e = 0.7$, with $\psi_0 = 0°$. In these figures, the ideal PCO is shown as a dashed-dotted, black line. If the (3.35) are used to generate initial conditions for a PCO, then these will result in unbounded motion since (3.29) is not satisfied. However, if (3.35) are used to generate initial conditions for all the states excluding ϑ_0', and (3.29) is used to generate an initial condition for ϑ_0', the result will be a relative orbit that is bounded, but without a circular projection. The extent of this deviation is depicted by the dashed, red line. The solid, blue line depicts the result of applying the amplitude correction developed in this section, and the bias correction from (3.58). In both cases, bias in the out-of-plane direction is absent, but as shown in Figure 3.2b, bias in the along-track direction

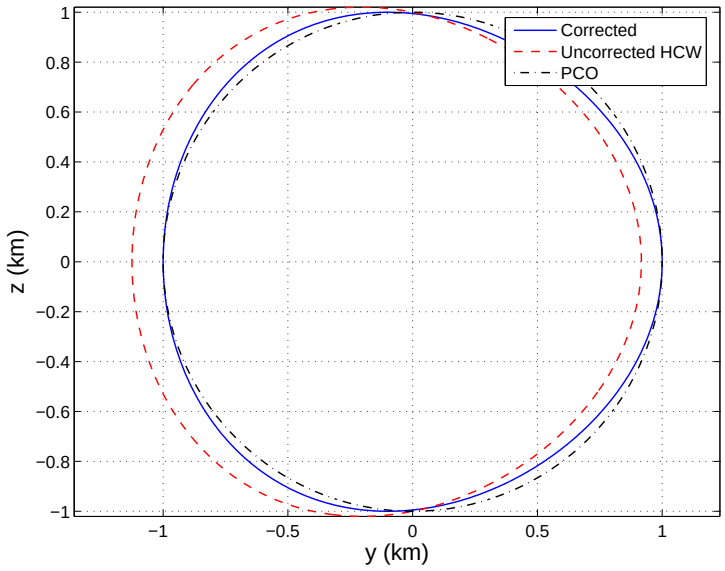

(a) $e = 0.2$

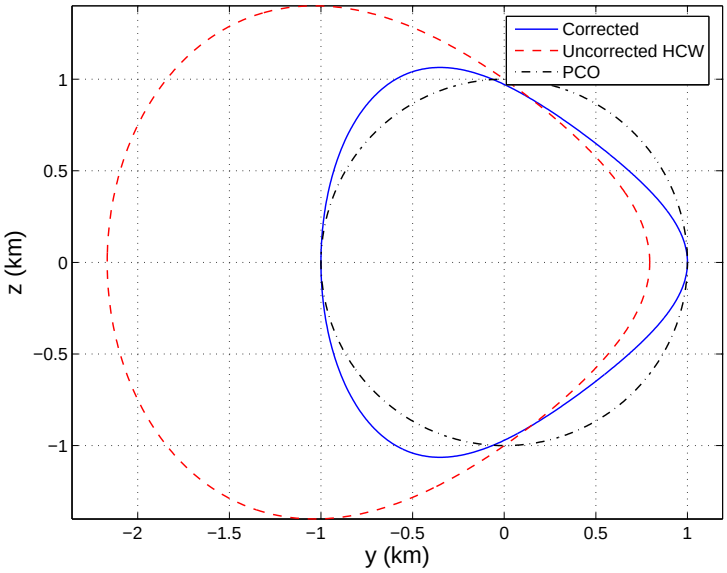

(b) $e = 0.7$

Fig. 3.2 Near-PCO Relative Motion with HCW and Corrected Initial Conditions, $\varrho = 1\,\text{km}$, $\psi_0 = 0°$

is significant. The corrections developed in this chapter successfully keep along-track motion bounded to the desired value of 1 km. It should also be observed that for high eccentricities, as shown in in Figure 3.2b, projected motion resembles a triangle; this may be exploited for mission design. The bias in the y direction, which is a function of $\cos\psi_0$, and consequently is maximum when $\psi_0 = 0°$, is removed entirely, as is shown in Figure 3.2a.

Figure 3.3 shows the effects of eccentricity, if $\psi_0 = 90°$. In this case, bias in the along-track direction is absent, but out-of-plane bias, which is a function of ϕ_0, is maximum. While there is no significant difference upon application of the corrections in Figure 3.3a, the amplitude correction is evident in Figure 3.3b. As eccentricity increases, the deputy's maximum displacement out of the plane increases to several kilometers. The amplitude correction limits this excursion.

The effect of eccentricity on the three-dimensional character of the relative orbit is shown in Figure 3.4. This figure corresponds to initial conditions consistent with Figure 3.2, for three values of eccentricity. The solid, blue line shows the out-of-plane vs. radial motion for a circular reference, which will be a straight line, since the phase angles have been chosen to be equal. However, the dashed, red line, and the dashed-dotted black line, which correspond to $e = 0.3$ and $e = 0.8$, respectively, show that the effect of higher-order harmonics causes increasing deviation from the relative orbit plane.

3.7.3 General Circular Orbit Modified by an Eccentric Reference Orbit

The General Circular Orbit (GCO) is obtained in the HCW sense by requiring that $\xi_h^2 + \vartheta_h^2 + \zeta_h^2 = \varrho^2$. Consequently, $k_1 = \varrho/2$, $k_3 = \sqrt{3}\varrho/2$, $k_2 = 0$, and $\overline{\psi}_0 = \overline{\phi}_0$. These

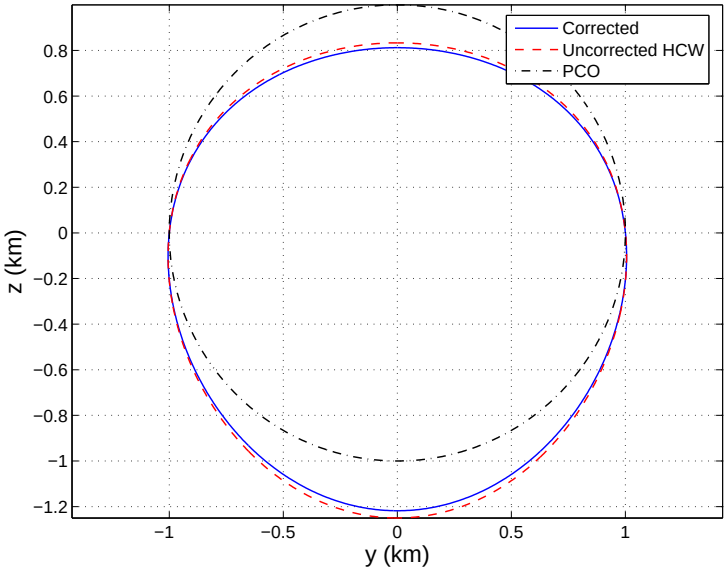

(a) $e = 0.2$

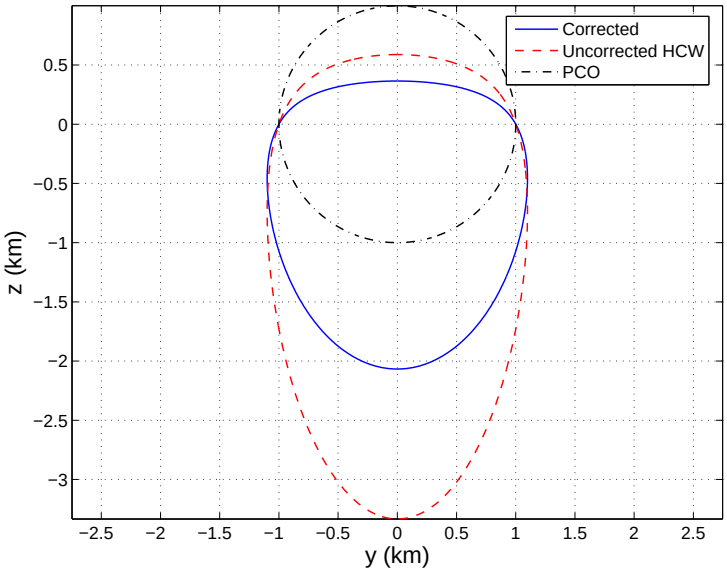

(b) $e = 0.7$

Fig. 3.3 Near-PCO Relative Motion with HCW and Corrected Initial Conditions, $\varrho = 1\,\text{km}$, $\psi_0 = 90°$

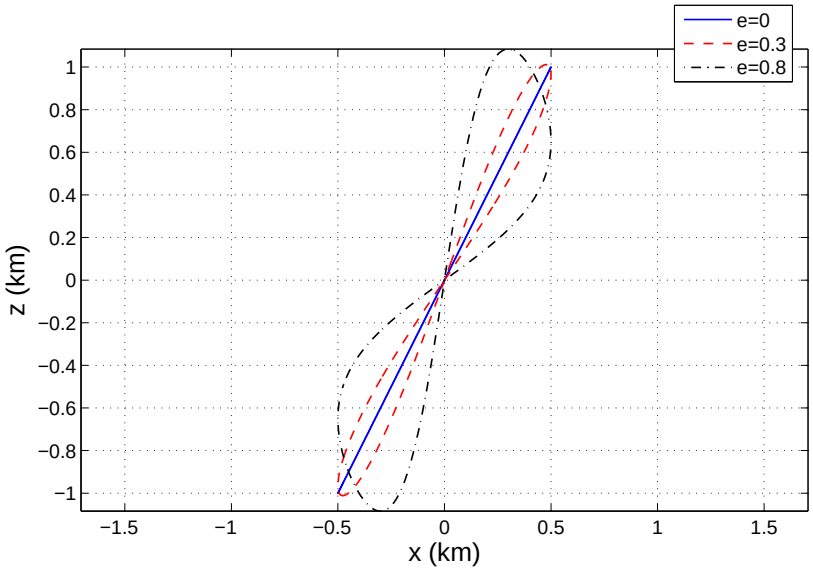

Fig. 3.4 Effect of Eccentricity on Relative Orbit Plane

conditions lead to a relative orbit that is circular on a plane (local in the rotating frame). For an eccentric reference, the initial conditions need to be modified, since using the HCW initial conditions do not lead to GCOs. The modifications derived in this section only account for the first harmonic in the Fourier-Bessel expansions of (3.36).

Upon choosing $\varrho_3 = (\sqrt{3}/2)\,\varrho/\sqrt{(S_1^2 \sin^2\phi_0 + T_1^2 \cos^2\phi_0)}$, it is evident that $\zeta_\varrho^2(\tau) = (3/4)\,\varrho^2 \sin^2(f + \widetilde{\phi}_0)$. Thus, $\varrho_1 = \varrho/2$ remains a valid choice to obtain a GCO-like relative orbit. The phase angles are chosen in the same fashion as those for the PCO. Figures 3.5a and 3.5b show near-GCO formations for a reference orbit with $e = 0.2$, for $\psi_0 = 0°$ (maximum y-bias), and $\psi_0 = 90°$ (maximum z-bias), respectively. The legend in the figures is consistent with the previous section, as is the choice of boundedness condition. Furthermore, similar to the previous section, the corrections are able to eliminate bias in the y direction, but not in the z direction.

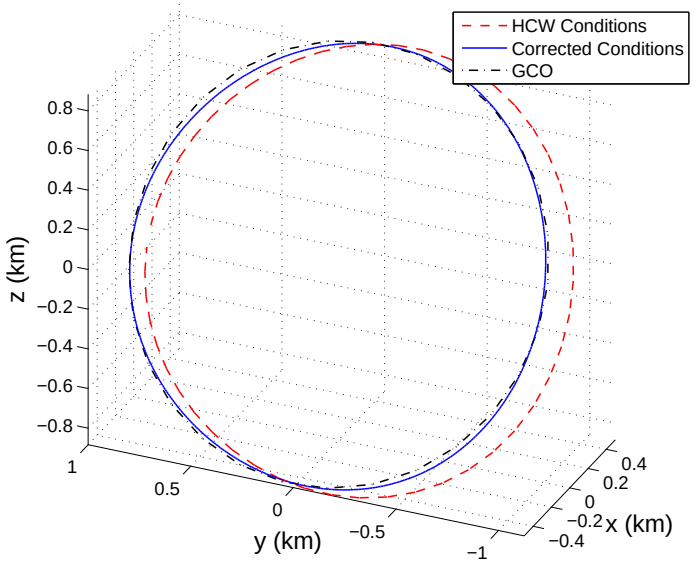

(a) $\psi_0 = 0°$

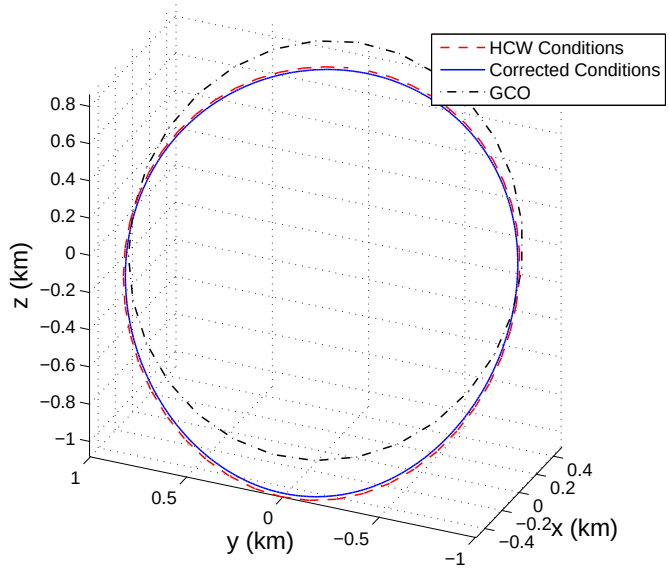

(b) $\psi_0 = 90°$

Fig. 3.5 Near-GCO Relative Motion with HCW and Modified Initial Conditions, $e = 0.2$, $\varrho = 1\,\mathrm{km}$

3.8 Relative Orbit Design Using Nonsingular Elements

The theory in this chapter is now extended by the use of the nonsingular element set $\boldsymbol{\delta\mathfrak{n}\mathfrak{s}} = \{a\ \lambda_0\ i\ q_1\ q_2\ h\}^\top$, as given by (2.20). A solution to the TH equations using θ as the independent variable is easily obtained, by observing that (3.9) may be rewritten as:

$$x(\theta) = (\widetilde{c}_1 \cos\theta + \widetilde{c}_2 \sin\theta)\,\alpha + \frac{2c_3}{\eta^2}\left[1 - \frac{3}{2\eta^3}\alpha\beta\,K(\theta)\right] \tag{3.65a}$$

$$y(\theta) = (-\widetilde{c}_1 \sin\theta + \widetilde{c}_2 \cos\theta)\,(1+\alpha) - \frac{3c_3}{\eta^5}\,\alpha^2\,K(\theta) + c_4 \tag{3.65b}$$

$$z(\theta) = c_5 \cos\theta + c_6 \sin\theta \tag{3.65c}$$

where,

$$\alpha = 1 + q_1 \cos\theta + q_2 \sin\theta = 1 + e\cos f \tag{3.66a}$$

$$\beta = q_1 \sin\theta - q_2 \cos\theta = e \sin f \tag{3.66b}$$

The arbitrary constants $\widetilde{c}_1$ and $\widetilde{c}_2$ are evaluated as follows:

$$\begin{aligned}
\widetilde{c}_1 &= c_1 \cos g - c_2 \sin g \\
&= -\frac{3}{\eta^2\alpha_0}\left[q_1(1+\cos^2\theta_0) + q_2 \sin\theta_0 \cos\theta_0 + (2-\eta^2)\cos\theta_0\right] x_0 \\
&\quad -\frac{1}{\eta^2}\left[q_1 \sin\theta_0 \cos\theta_0 - q_2(1+\cos^2\theta_0) + \sin\theta_0\right] x_0' \\
&\quad -\frac{1}{\eta^2}\left[q_1(1+\cos^2\theta_0) + q_2 \sin\theta_0 \cos\theta_0 + 2\cos\theta_0\right] y_0'
\end{aligned} \tag{3.67a}$$

$$\begin{aligned}
\widetilde{c}_2 &= c_1 \sin g + c_2 \cos g \\
&= -\frac{3}{\eta^2\alpha_0}\left[q_1 \sin\theta_0 \cos\theta_0 + q_2(1+\sin^2\theta_0) + (2-\eta^2)\sin\theta_0\right] x_0 \\
&\quad -\frac{1}{\eta^2}\left[q_1(1+\sin^2\theta_0) - q_2 \sin\theta_0 \cos\theta_0 - \cos\theta_0\right] x_0' \\
&\quad -\frac{1}{\eta^2}\left[q_1 \sin\theta_0 \cos\theta_0 + q_2(1+\sin^2\theta_0) + 2\sin\theta_0\right] y_0'
\end{aligned} \tag{3.67b}$$

where α_0 and β_0 are (3.66) evaluated at $\theta = \theta_0$. The constants c_5 and c_6 are already nonsingular, and c_4 is rewritten as:

$$c_4 = -\frac{1}{\eta^2}\left[1+\alpha_0\right]\left[\frac{3\beta_0}{\alpha_0}x_0 + (2-\alpha_0)x_0' + \beta_0 y_0'\right] + y_0 \tag{3.68}$$

Furthermore, $K(\theta)$ is Kepler's equation rewritten in nonsingular variables:

$$K(\theta) = (F - q_1 \sin F + q_2 \cos F) - (F_0 - q_1 \sin F_0 + q_2 \cos F_0) = \lambda - \lambda_0 \tag{3.69}$$

The differential nonsingular orbital elements, δq_1, δq_2, and $\delta\lambda_0$ can be written in terms of the initial conditions as shown:

$$\begin{aligned}
\delta q_1 &= \cos g\,\delta e - e\sin g\,\delta g \\
&= (3q_1 + 3\cos\theta_0)x_0 - q_2 y_0 - q_2\cot i\cos\theta_0\, z_0 + \sin\theta_0(1 + q_1\cos\theta_0 + q_2\sin\theta_0)x_0' \\
&\quad + \{q_1 + \cos\theta_0(2 + q_1\cos\theta_0 + q_2\sin\theta_0)\}\, y_0' + q_2\cot i\sin\theta_0\, z_0' \qquad (3.70a) \\
\delta q_2 &= \sin g\,\delta e + e\cos g\,\delta g \\
&= (3q_2 + 3\cos\theta_0)x_0 + q_1 y_0 + q_1\cot i\cos\theta_0\, z_0 - \cos\theta_0(1 + q_1\cos\theta_0 + q_2\sin\theta_0)x_0' \\
&\quad + \{q_2 + \sin\theta_0(2 + q_1\cos\theta_0 + q_2\sin\theta_0)\}\, y_0' - q_1\cot i\sin\theta_0\, z_0' \qquad (3.70b) \\
\delta\lambda_0 &= \delta g + \delta l_0 \\
&= \cot i\ (\cos\theta_0\, z_0 - \sin\theta_0\, z_0') + \frac{1}{1+\eta}(2 - \eta - \eta^2 + q_1\cos\theta_0 + q_2\sin\theta_0)x_0 + y_0 \\
&\quad - \frac{1}{1+\eta}\left\{2\eta + 2\eta^2 + (q_1\cos\theta_0 + q_2\sin\theta_0)(1 + q_1\cos\theta_0 + q_2\sin\theta_0)\right\} x_0' \\
&\quad + \frac{1}{1+\eta}(q_1\sin\theta_0 - q_2\cos\theta_0)(2 + q_1\cos\theta_0 + q_2\sin\theta_0)y_0 \qquad (3.70c)
\end{aligned}$$

Equations (3.70) are free from singularities when $e = 0$, but are more complicated than the corresponding expressions for the classical orbital elements.

The most general form for periodic relative motion is also modified, since f cannot

be uniquely determined. Therefore, (3.32) are rewritten as:

$$x_{\wp}(f) = \frac{\varrho_1}{p}\sin(\theta+\psi_0)\,(1+q_1\cos\theta+q_2\sin\theta) \tag{3.71a}$$

$$y_{\wp}(f) = \frac{\varrho_1}{p}\cos(\theta+\psi_0)\,(2+q_1\cos\theta+q_2\sin\theta)+\frac{\varrho_2}{p} \tag{3.71b}$$

$$z_{\wp}(f) = \frac{\varrho_3}{p}\sin(\theta+\phi_0) \tag{3.71c}$$

where,

$$\begin{aligned}\varrho_1 &= \left(\xi_0^2+\xi_0'^2\right)^{\frac{1}{2}}\\ &= \frac{a}{\eta}\Big[\left(1-\eta^2\right)\delta\lambda_0^2+2\left(q_2\delta q_1-q_1\delta q_2\right)\delta\lambda_0-\left(q_1\delta q_1+q_2\delta q_2\right)^2\\ &\quad +\delta q_1^2+\delta q_2^2\Big]^{\frac{1}{2}}\end{aligned} \tag{3.72a}$$

$$\begin{aligned}\varrho_2 &= \vartheta_0(1+q_1\cos\theta_0+q_2\sin\theta_0)-\xi_0'(2+q_1\cos\theta_0+q_2\sin\theta_0)\\ &= p\left[\delta h\cos i+\frac{(1+\eta+\eta^2)}{\eta^3(1+\eta)}\left(q_2\delta q_1-q_1\delta q_2\right)+\frac{1}{\eta^3}\delta\lambda_0\right]\end{aligned} \tag{3.72b}$$

$$\begin{aligned}\varrho_3 &= \big[(1+2q_1\cos\theta_0+2q_2\sin\theta_0+q_1^2+q_2^2)\zeta_0^2+(1+q_1\cos\theta_0+q_2\sin\theta_0)^2\zeta_0'^2\\ &\quad -2\left(q_1\sin\theta-q_2\cos\theta\right)(1+q_1\cos\theta_0+q_2\sin\theta_0)\zeta_0\zeta_0'\big]^{\frac{1}{2}}\\ &= p\left(\delta i^2+\delta h^2\sin^2 i\right)^{\frac{1}{2}}\end{aligned} \tag{3.72c}$$

$$\begin{aligned}\psi_0 &= \tan^{-1}\left(\frac{\xi_0}{\xi_0'}\right)-\theta_0\\ &= \tan^{-1}\left[\frac{(1+\eta)\left(\delta q_1+q_2\delta\lambda_0\right)-q_1\left(q_1\delta q_1+q_2\delta q_2\right)}{(1+\eta)\left(\delta q_2-q_1\delta\lambda_0\right)-q_2\left(q_1\delta q_1+q_2\delta q_2\right)}\right]\end{aligned} \tag{3.72d}$$

$$\begin{aligned}\phi_0 &= \tan^{-1}\left(\frac{(1+q_1\cos\theta_0+q_2\sin\theta_0)\zeta_0}{(1+q_1\cos\theta_0+q_2\sin\theta_0)\zeta_0'-\left(q_1\sin\theta_0-q_2\cos\theta_0\right)\zeta_0}\right)-\theta_0\\ &= \tan^{-1}\left(-\frac{\delta h\sin i}{\delta i}\right)\end{aligned} \tag{3.72e}$$

Conversely, the orbital element differences δq_1, δq_2, and $\delta\lambda_0$ may be written in terms of the design parameters $\varrho_{1\ldots3}$, ψ_0, and ϕ_0, as shown:

$$\delta q_1 = q_1q_2\frac{\varrho_1}{p}\cos\psi_0-(1-q_1^2)\frac{\varrho_1}{p}\sin\psi_0-q_2\left(\frac{\varrho_2}{p}-\delta h\cos i\right) \tag{3.73a}$$

$$\delta q_2 = q_1 q_2 \frac{\varrho_1}{p} \sin\psi_0 - (1 - q_2^2)\frac{\varrho_1}{p}\cos\psi_0 + q_2\left(\frac{\varrho_2}{p} - \delta h \cos i\right) \qquad (3.73b)$$

$$\delta\lambda_0 = \frac{\varrho_2}{p} - \delta h\cos i - \frac{(1+\eta+\eta^2)}{(1+\eta)}\frac{\varrho_1}{p}\Big[q_1\cos\psi_0 - q_2\sin\psi_0\Big] \qquad (3.73c)$$

It should be noted that though the use of nonsingular orbital elements eliminates problems with $e \to 0$, they are still not suitable for use when $i \to 0$. For example, $\cot i$ appears in (3.70).

Even though the Fourier-Bessel expansions with respect to f and τ as independent variables, as given by (3.47a), (3.47b), (3.52a), and (3.52b) are only meaningful for $e \neq 0$, the fact that they are written in terms of variables that cannot be determined independently of g for very low eccentricities also requires some attention. It can be shown that by using θ or λ as independent variables, uniformly valid expansions can be written. This is demonstrated by the expansion of $1/(1 + e\cos f)$. With θ as the independent variable,

$$\begin{aligned}
\frac{1}{1 + q_1\cos\theta + q_2\sin\theta} &= \frac{1}{1+e\cos f} = \frac{1}{\eta} + \frac{2}{\eta}\sum_{k=1}^{\infty}(-\varepsilon)^k\cos kf \\
&= \frac{1}{\eta} + \frac{2}{\eta}\sum_{k=1}^{\infty}(-\varepsilon)^k\left(\cos kg\,\cos k\theta + \sin kg\,\sin k\theta\right) \\
&= \frac{1}{\eta} + \frac{2}{\eta}\sum_{k=1}^{\infty}\left(-\frac{1}{1+\eta}\right)^k\left(q_{1k}\cos k\theta + q_{2k}\sin k\theta\right)
\end{aligned}$$

where,

$$q_{1k} + \jmath\, q_{2k} \triangleq (q_1 + \jmath\, q_2)^k \qquad (3.74)$$

When λ is to be used as the independent variable, the approach is similar. In this

case,

$$\frac{1}{1+q_1\cos\theta+q_2\sin\theta} = \frac{3-\eta^2}{2\eta^2}+\sum_{k=1}^{\infty}\frac{B_k}{e^k}\left(q_{1k}\cos k\lambda+q_{2k}\sin k\lambda\right) \tag{3.75}$$

where,

$$\frac{B_k}{e^k}=\frac{1}{k\eta^2e^{k-1}}\left[J_{k+1}(ke)-J_{k-1}(ke)\right] \tag{3.76}$$

From (3.51), the lowest power of e in $J_k(ke)$ is e^k. Therefore, e is not present in the denominator of the above expression, as can be shown by the following expansion:

$$\frac{J_{k+1}(ke)}{e^{k-1}}=\sum_{m=0}^{\infty}\frac{(-1)^m\,k^{k+2m+1}}{2^{k+2m+1}\,m!\,(k+m+1)!}\left(q_1^2+q_2^2\right)^{m+1} \tag{3.77a}$$

$$\frac{J_{k-1}(ke)}{e^{k-1}}=\sum_{m=0}^{\infty}\frac{(-1)^m\,k^{k+2m-1}}{2^{k+2m-1}\,m!\,(k+m-1)!}\left(q_1^2+q_2^2\right)^{m} \tag{3.77b}$$

3.9 Summary

This chapter studies the effects of eccentricity on the shape and size of relative orbits. No assumptions are made regarding the value of eccentricity, although nonlinearity is treated separately in Chapters V and VI. Parameters based upon the relative orbit shape and phase angle are used to study these effects, since these are more meaningful than the differential orbital elements by themselves. The key effects are identified as those that lead to amplitude and phase changes, and introduction of bias. Corrective schemes are proposed that exploit the effects of eccentricity, and in some cases, these lead to relative orbits very close or similar to those predicted by the HCW equations. Since the effects of eccentricity are studied both in a qualitative and quantitative fashion, these results can serve as excellent models for future mission design. The approach in this chapter unifies the solutions to the Tschauner-Hempel equations, and

the relative motion description using differential orbital elements. The linear mapping between the relative orbit parameters and differential orbital elements can be used to design impulsive or continuous maneuvers for the establishment of such formations, at low cost, since they include the full effects of eccentricity. Furthermore, tracking orbits obtained from the time-explicit formulation for periodic relative motion will result in lower costs than those obtained from the HCW equations.

CHAPTER IV

OPTIMAL RENDEZVOUS NEAR A KEPLERIAN ORBIT

4.1 Introduction

In this chapter, a novel analytical solution to the problem of optimal rendezvous is developed. The theory is also applicable to formation reconfiguration, since reconfiguration is simply a form of rendezvous where the final position and velocity are not the origin of the rotating Cartesian frame. The development does not assume small eccentricity of the reference orbit, and uses results developed in Chapter III.

The optimal rendezvous problem has been of historical interest, especially due to Lawden's primer vector theory (Lawden 1963). Billik (1964) used a differential games approach to design optimal thruster programming laws for the HCW equations. Edelbaum (1964) formulated and solved the optimal rendezvous problem in terms of small orbital element differences. Gobetz (1965) also used a similar linearization in orbital element space, with the additional assumption of a near-circular target orbit, but used a nonsingular element set that extended the validity of the laws to those cases where eccentricity and inclination are zero - known singularities in the classical orbital element set. The elements used by Gobetz are similar to the equinoctial elements (Broucke and Cefola 1972). Alfriend and Kashiwagi (1969) formulated the open-loop, minimum-time rendezvous problem for elliptic orbits, using the TH equations. Jezewski and Stoolz (1970) formulated the constant-thrust orbital transfer problem, by expressing the gravity field as a third-order polynomial in time by using two measurements of position and velocity and solving for the polynomial coefficients.

Solutions to the continuous-thrust optimal rendezvous problem in a linearized gravity field, using the TH equations as a base, have been explored extensively by Carter and Humi (1987); Carter and Brient (1992); Humi (1993), among others, although these references characterize the problem, but do not solve it. Euler (1969) approached the rendezvous problem by attempting to find an open-loop optimal control to the TH equations, for the standard low-thrust, limited-power quadratic cost function. However, a completely analytical solution could not be found, and results were obtained by restricting the equations to first order in eccentricity. Carter (1994) proposed a method to solve the problem posed by Euler (1969), but the procedure requires the numerical integration for a key matrix, for a complete solution. In this chapter, the problem posed by Euler (1969) is solved in closed form.

The problem of optimal bounded, low-thrust rendezvous, using the HCW equations, was solved by Guelman and Aleshin (2001). Recent work by Palmer (2006) provides an analytical formulation for optimal transfer paths, also based on the HCW equations. Zanon and Campbell (2006b) developed an approximate solution for optimal open-loop, bounded-input control for rendezvous near elliptic orbits, using Carter's solution (Carter 1998) to the TH equations as a basis. In this work, spline approximations were used for certain key integrals; however, as will be shown in this chapter, these integrals can be solved in closed form.

4.2 Problem Statement

The Tschauner-Hempel (TH) equations for rendezvous near a Keplerian orbit with arbitrary eccentricity, can be written in the following state-space representation:

$$\mathbf{x}' = \mathbf{A}(f)\mathbf{x} + \mathbf{B}(f)\mathbf{u} \tag{4.1}$$

where $\mathbf{x} \in X \subset \mathbb{R}^6$, $\mathbf{u} \in U \subset \mathbb{R}^3$, $\mathbf{A} : \mathbb{R}_{\geq 0} \to \mathbb{R}^{6\times 6}$, $\mathbf{B} : \mathbb{R}_{\geq 0} \to \mathbb{R}^{6\times 3}$, and the following hold:

$$\mathbf{x} = \left\{ \begin{array}{c} \boldsymbol{\rho} \\ \boldsymbol{\rho}' \end{array} \right\} = \{x \quad y \quad z \quad x' \quad y' \quad z'\}^\top, \quad \mathbf{B} = (1 + e\cos f)^{-3} \left[\begin{array}{c} \mathbb{O}_3 \\ \mathbb{1}_3 \end{array} \right]$$

$$\mathbf{A} = \left[\begin{array}{cc} \mathbb{O}_3 & \mathbb{1}_3 \\ \widetilde{\mathbf{A}} & \boldsymbol{\Omega} \end{array} \right], \quad \widetilde{\mathbf{A}} = \left[\begin{array}{ccc} 3/(1 + e\cos f) & 0 & 0 \\ 0 & 0 & 0 \\ 0 & 0 & -1 \end{array} \right], \quad \boldsymbol{\Omega} = \left[\begin{array}{ccc} 0 & 2 & 0 \\ -2 & 0 & 0 \\ 0 & 0 & 0 \end{array} \right]$$

In the above, $\mathbb{O}_3$ and $\mathbb{1}_3$ denote the 3×3 zero and identity matrices, respectively. It should also be noted that the actual control acceleration $\mathbf{u}_{\text{appl}}$ is obtained by the following transformation:

$$\mathbf{u}_{\text{appl}}(f) = \frac{\mu}{p^2}\mathbf{u}(f) \tag{4.2}$$

The optimal control problem is posed as the following:

$$\min \mathcal{J} = \frac{1}{2}\int_{f_0}^{f_T} \mathbf{u}^\top \mathbf{R}\mathbf{u}\, df \tag{4.3}$$

$$\mathbf{x}(f_0) = \mathbf{x}_0, \quad \mathbf{x}(f_T) = \mathbf{x}_T \tag{4.4}$$

with f_T specified, and where $\mathbf{R} \in \mathbb{R}^{3\times 3} > 0$. Althought this cost function is not strictly appropriate for low-thrust, high-specific impulse thrust devices (Marec 1979, chap. 1), the choice of true anomaly f instead of mean anomaly (time) l as the variable of integration is a natural choice for penalizing control effort at the perigee, and the difference between their use is only apparent at high eccentricities. Additionally, the use of f results in readily integrable functions, as will be shown later. For the linear-quadratic (LQ) problem posed, it can be shown that the necessary conditions for optimality (Lewis and Syrmos 1995) yield the following conditions for the control

and costates, denoted by $\boldsymbol{\lambda}$:

$$\boldsymbol{\lambda}' = -\mathbf{A}^\top(f)\boldsymbol{\lambda} \tag{4.5a}$$

$$\mathbf{u} = -\mathbf{R}^{-1}\mathbf{B}^\top\boldsymbol{\lambda} \tag{4.5b}$$

For the augmented linear system comprising states and costates, the values of $\mathbf{x}$ and $\boldsymbol{\lambda}$ at any time are given by the state transition matrix (STM) $\boldsymbol{\Phi}$. Consequently, the initial values of $\boldsymbol{\lambda}$ can be found by the following:

$$\begin{Bmatrix} \mathbf{x}' \\ \boldsymbol{\lambda}' \end{Bmatrix} = \begin{bmatrix} \mathbf{A} & -\mathbf{B}\mathbf{R}^{-1}\mathbf{B}^\top \\ \mathbb{O}_6 & -\mathbf{A}^\top \end{bmatrix} \begin{Bmatrix} \mathbf{x} \\ \boldsymbol{\lambda} \end{Bmatrix} \Rightarrow \begin{Bmatrix} \mathbf{x}(f) \\ \boldsymbol{\lambda}(f) \end{Bmatrix} = \boldsymbol{\Phi}(f, f_0) \begin{Bmatrix} \mathbf{x}(f_0) \\ \boldsymbol{\lambda}(f_0) \end{Bmatrix}$$

$$\boldsymbol{\Phi} = \begin{bmatrix} \boldsymbol{\Phi}_{xx} & \boldsymbol{\Phi}_{x\lambda} \\ \boldsymbol{\Phi}_{\lambda x} & \boldsymbol{\Phi}_{\lambda\lambda} \end{bmatrix} \Rightarrow \boldsymbol{\lambda}_0 = \boldsymbol{\Phi}_{x\lambda}^{-1}(f_T, f_0)\mathbf{x}_T - \boldsymbol{\Phi}_{x\lambda}^{-1}(f_T, f_0)\boldsymbol{\Phi}_{xx}(f_T, f_0)\,\mathbf{x}_0 \tag{4.6}$$

Thus, the LQ problem can be solved if $\boldsymbol{\Phi}_{xx}$, $\boldsymbol{\Phi}_{\lambda\lambda}$, and $\boldsymbol{\Phi}_{x\lambda}$ are determined.

4.3 Solution to the Problem

While not immediately obvious, the matrices can be evaluated analytically. This is possible because the TH equations themselves have closed-form solutions. The solutions to the unforced TH equations are given by (3.9) and (3.10). Let $\mathbf{c} = \{c_1 \cdots c_6\}^\top$ denote the vector of integration constants in (3.9) and (3.10). As shown in Chapter III, the relationship between the states and the integration constants can be expressed as $\mathbf{x} = \mathbf{L}(f)\mathbf{c}$ where the entries of the matrix $\mathbf{L}$ can be obtained from the terms corresponding to the constants of integration in (3.9) and (3.10). This matrix has determinant 1, and the constants of integration can then be calculated by its adjoint, as shown in (3.11), to yield the relation $\mathbf{c} = \mathbf{M}(f_0)\,\mathbf{x}_0$. The STM for the

unforced equations can then be written as:

$$\mathbf{x}(f) = \mathbf{L}(f)\mathbf{M}(f_0)\mathbf{x}_0 \tag{4.7}$$

$$\Rightarrow \qquad \mathbf{\Phi}_{xx}(f, f_0) = \mathbf{L}(f)\mathbf{M}(f_0) \tag{4.8}$$

The STM for the costates can be obtained by observing that the Hamiltonian system comprising $\mathbf{x}$ and $\boldsymbol{\lambda}$ leads to a state transition matrix that is symplectic in nature. If $\mathfrak{S}$ denotes the symplectic matrix of appropriate order, (4.6) implies

$$\mathbf{\Phi}\mathfrak{S}\mathbf{\Phi}^\top = \mathfrak{S} \tag{4.9}$$

$$\text{or,} \quad \begin{bmatrix} \mathbf{\Phi}_{xx} & \mathbf{\Phi}_{x\lambda} \\ \mathbf{\Phi}_{\lambda x} & \mathbf{\Phi}_{\lambda\lambda} \end{bmatrix} \begin{bmatrix} \mathbb{O}_6 & \mathbb{1}_6 \\ -\mathbb{1}_6 & \mathbb{O}_6 \end{bmatrix} \begin{bmatrix} \mathbf{\Phi}_{xx}^\top & \mathbf{\Phi}_{\lambda x}^\top \\ \mathbf{\Phi}_{x\lambda}^\top & \mathbf{\Phi}_{\lambda\lambda}^\top \end{bmatrix} = \begin{bmatrix} \mathbb{O}_6 & \mathbb{1}_6 \\ -\mathbb{1}_6 & \mathbb{O}_6 \end{bmatrix} \tag{4.10}$$

Resolving the matrix multiplication, and comparing the block matrices on both sides leads to four equations, one of which is:

$$\mathbf{\Phi}_{xx}\mathbf{\Phi}_{\lambda\lambda}^\top - \mathbf{\Phi}_{x\lambda}\mathbf{\Phi}_{\lambda x}^\top = \mathbb{1}_6 \tag{4.11}$$

However, if $\mathbf{x}$ is not present in the cost function (as is the case considered here), $\boldsymbol{\lambda}$ does not depend on $\mathbf{x}$, and $\mathbf{\Phi}_{\lambda x} = \mathbb{O}_6$. It follows that

$$\mathbf{\Phi}_{\lambda\lambda}(f, f_0) = \left[\mathbf{\Phi}_{xx}^\top(f, f_0)\right]^{-1} = \mathbf{M}^\top(f)\mathbf{L}^\top(f_0) \tag{4.12}$$

From (4.12) and (4.5*b*), the solution to the forced system is:

$$\begin{aligned} \mathbf{x}(f) &= \mathbf{\Phi}_{xx}(f, f_0)\mathbf{x}_0 - \int_{f_0}^{f} \mathbf{\Phi}_{xx}(f, s)\mathbf{B}(s)\mathbf{R}^{-1}\mathbf{B}^\top(s)\mathbf{\Phi}_{\lambda\lambda}(s, f_0)\boldsymbol{\lambda}_0\, ds \\ &= \mathbf{\Phi}_{xx}(f, f_0)\mathbf{x}_0 + \mathbf{\Phi}_{x\lambda}(f, f_0)\boldsymbol{\lambda}_0 \end{aligned} \tag{4.13}$$

It follows that:

$$\begin{aligned}
\boldsymbol{\Phi}_{x\lambda}(f, f_0) &= -\int_{f_0}^{f} \boldsymbol{\Phi}_{xx}(f, s)\mathbf{B}(s)\mathbf{R}^{-1}\mathbf{B}^{\top}(s)\boldsymbol{\Phi}_{\lambda\lambda}(s, f_0)\, ds \\
&= -\mathbf{L}(f)\left(\int_{f_0}^{f} \mathbf{M}(s)\mathbf{B}(s)\mathbf{R}^{-1}\mathbf{B}^{\top}(s)\mathbf{M}^{\top}(s)\, ds\right)\mathbf{L}^{\top}(f_0) \quad (4.14) \\
&= -\mathbf{L}(f)\left[\mathbf{W}(f) - \mathbf{W}(f_0)\right]\mathbf{L}^{\top}(f_0) \quad (4.15) \\
\text{where,} \quad \mathbf{W}(f) &= \int \mathbf{M}(f)\mathbf{B}(f)\mathbf{R}^{-1}\mathbf{B}^{\top}(f)\mathbf{M}^{\top}(f)\, df \quad (4.16)
\end{aligned}$$

It is evident that the problem can be solved completely if $\mathbf{W}(f)$ is evaluated. It is also worth noting that $\mathbf{W}(f)$ is symmetric. It can be shown that:

$$\mathbf{B}(f)\mathbf{R}^{-1}\mathbf{B}^{\top}(f) = (1 + e\cos f)^{-6}\begin{bmatrix} \mathbb{O} & \mathbb{O} \\ \mathbb{O} & \mathbf{R}^{-1} \end{bmatrix} \quad (4.17)$$

Though it appears at the outset that the integration process is complicated due to the presence of terms containing $(1 + e\cos f)$ in the denominator, integration can be performed by changing the independent variable to E. This step can also be used to solve the integrals presented by Zanon and Campbell (2006b), as was shown in Zanon and Campbell (2006a). The matrix $\mathbf{W}(f)$ may be rewritten as:

$$\mathbf{W}(f) = \mathbf{W}^{(3)}(f)\, K^3(f) + \mathbf{W}^{(2)}(f)\, K^2(f) + \mathbf{W}^{(1)}(f)\, K(f) + \mathbf{W}^{(0)}(f) \quad (4.18)$$

The components of $\mathbf{W}^{(0\ldots3)}(f)$ are presented in Appendix A, where it is also assumed that $\mathbf{R}$ is a diagonal matrix, with entries $R_{1\ldots3}$. For the sake of brevity,

$$\overline{\mathbf{W}}(f_T, f_0) \triangleq \mathbf{W}(f_T) - \mathbf{W}(f_0) \quad (4.19)$$

4.4 Dependence of Cost on Final Value of True Anomaly

For given initial and final conditions, $\mathbf{x}_0$ and $\mathbf{x}_T$, and epoch f_0, the cost is purely a function of the final value of the true anomaly, f_T. From (4.3) and (4.5b), the optimal cost is given by:

$$\begin{aligned}\mathcal{J}^*(f_T) &= \frac{1}{2}\int_{f_0}^{f_T} \boldsymbol{\lambda}^\top(f)\mathbf{B}(f)\mathbf{R}^{-1}\mathbf{B}^\top(f)\boldsymbol{\lambda}(f)\,df \\ &= \frac{1}{2}\int_{f_0}^{f_T} \boldsymbol{\lambda}_0^\top\boldsymbol{\Phi}_{\lambda\lambda}^\top(f,f_0)\mathbf{B}(f)\mathbf{R}^{-1}\mathbf{B}^\top(f)\boldsymbol{\Phi}_{\lambda\lambda}(f,f_0)\boldsymbol{\lambda}_0\,df\end{aligned}$$

To ease notation, $\mathbf{L}(f_0) = \mathbf{L}_0$, $\mathbf{L}(f_T) = \mathbf{L}_T$, $\mathbf{M}(f_0) = \mathbf{M}_0$, and $\mathbf{M}(f_T) = \mathbf{M}_T$. Furthermore, since $\boldsymbol{\lambda}_0$ is a constant, the use of (4.12) and (4.16) results in the following equation:

$$\mathcal{J}^* = \frac{1}{2}\boldsymbol{\lambda}_0^\top\mathbf{L}_0\overline{\mathbf{W}}\mathbf{L}_0^\top\boldsymbol{\lambda}_0 \tag{4.20}$$

Using (4.6) and (4.15) yields the following expression for the optimal cost:

$$\mathcal{J}^* = \frac{1}{2}\left(\mathbf{M}_T\mathbf{x}_T - \mathbf{M}_0\mathbf{x}_0\right)^\top\overline{\mathbf{W}}^{-1}\left(\mathbf{M}_T\mathbf{x}_T - \mathbf{M}_0\mathbf{x}_0\right) \tag{4.21}$$

Since $\mathcal{J}^* \geq 0$ for all possible choices of initial and final conditions $\mathbf{x}_T$ and $\mathbf{x}_0$, $\overline{\mathbf{W}}^{-1}$ must be positive semi-definite. In fact, $\mathcal{J}^* = 0$ implies that either 1) $\mathbf{M}_T\mathbf{x}_T = \mathbf{M}_0\mathbf{x}_0$, or 2) $\overline{\mathbf{W}}^{-1}$ is singular. The first case is only possible if $\mathbf{x}_T = \boldsymbol{\Phi}_{xx}(f_T, f_0)\mathbf{x}_0$, or if the desired states arise from the natural evolution of the state from the initial states. The second case arises if at least one eigenvalue of $\overline{\mathbf{W}}^{-1}$ is zero, or if at least one eigenvalue of $\overline{\mathbf{W}}$ is infinity. Since $\mathbf{W}$ comprises only bounded periodic terms and $K(f)$, which increases with f, this must mean $K(f_T) \to \infty$, and consequently, $f_T \to \infty$. This agrees with the physics of the problem, since in both cases, control required is zero. Therefore in the cases where control is required, $\overline{\mathbf{W}}^{-1}$ and $\overline{\mathbf{W}}$ are positive definite.

Furthermore, since $\overline{\mathbf{W}}$ is symmetric and block diagonal in structure, methods such as the Cholesky decomposition may be used to find the inverse.

4.5 Numerical Simulations

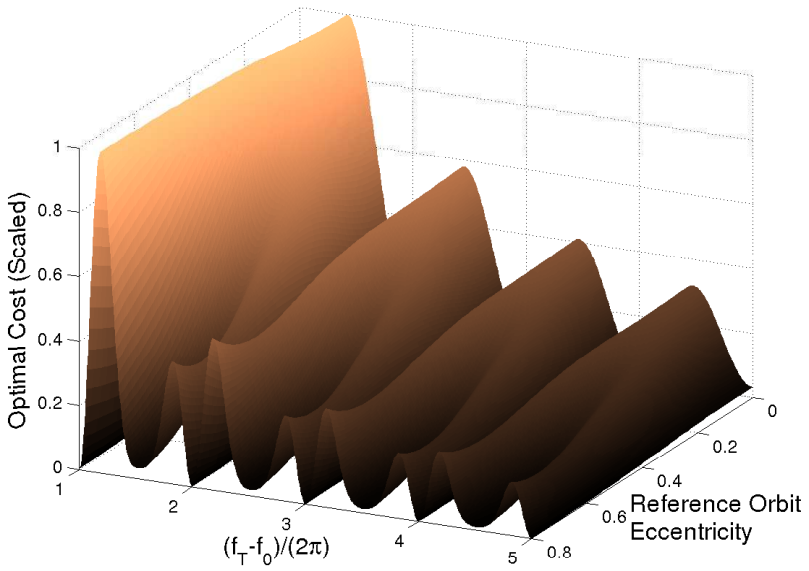

Fig. 4.1 Optimal Cost of Reconfiguration as a Function of Eccentricity of the Reference and True Anomaly Gap

The availability of the analytical solution to the LQ problem allows the examination of the dependence of the cost of rendezvous on the final value of the true anomaly. Since the control and costates are known functions, the Hamiltonian corresponding the LQ problem reduces to a function of one variable, f. Therefore, solving for the zeros of this Hamiltonian provides a necessary condition for a maneuver with the smallest true anomaly change, and as a consequences, a solution to the minimum-time problem. In this case, it is observed that solving for the zeros is particularly difficult due to the complicated nature of the Hamiltonian, because the true anomaly expresses itself through various orders of harmonics. However, additional insight

into the problem may be obtained by studying Figure 4.1. In this figure, a sample reconfiguration from $\mathbf{x}_0 = \{0\ 1\ 0\ 0.5\ 0\ 1\}^\top$ to $\mathbf{x}_T = \{0\ 2\ 0\ 1\ 0\ 2\}^\top$ is chosen, with $f_0 = 35°$. This figure shows the optimal cost for rendezvous, scaled by the maximum cost, as a function of the eccentricity of the reference orbit, and the final value of true anomaly. It is observed that the cost for rendezvous decreases as the gap between initial and final true anomaly increases. This is a consequence of the fact that $\overline{\mathbf{W}}$ comprises $K(f)$ which increases with true anomaly, and that the cost depends on $\overline{\mathbf{W}}^{-1}$. Furthermore, it can also be seen that depending on the final true anomaly, the cost for rendezvous can be significantly high. In this case, when $e \sim 0$, it is best to wait for target to complete one or more revolutions about the gravitational center, to obtain lower costs. Finally, it is observed that the rendezvous cost displays pitchfork bifurcation, with reference orbit eccentricity as a parameter. While it is apparent that for low eccentricities that the cost is minimum when the target completes one or more revolutions, for high eccentricities new minima appear approximately half-way between complete revolutions. In this case, these regions correspond to the apogee. Although Figure 4.1 is the result of just one set of initial and final conditions, the qualitative behavior of the cost does not change with other boundary conditions.

4.6 Summary

This chapter derives an analytical solution to the LQ rendezvous problem. The solution can be easily extended to intercept maneuvers, since in this case, one set of final conditions on relative velocity are exchanged for another set of final conditions on the costates corresponding the relative velocity, and state transition due to the forcing function will still require the evaluation of $\mathbf{W}$. Furthermore, the analytical solution

to the initial costate values can serve as an excellent guess to solve the nonlinear rendezvous problem using an open-loop control derived using shooting methods, or with higher-order methods for feedback control.

CHAPTER V

SECOND-ORDER STATE TRANSITION FOR RELATIVE MOTION NEAR PERTURBED, ELLIPTIC ORBITS

5.1 Introduction

In this chapter, the problem of nonlinear relative motion is analyzed. The purpose is to develop a suitable method for state transition that is valid for large relative orbits. In spite of the extensive literature related to the rendezvous problem and formation flight, the effects of nonlinearity are yet to be modeled fully. Nonlinearity in the HCW equations were treated as perturbations and the system was solved by Knollman and Pyron (1963); London (1963), and with particular application to formation flight and periodic motion, by Richardson and Mitchell (2003); Vaddi et al. (2003); Gurfil (2005b). By representing relative motion using spherical coordinates, and by the use of perturbation techniques, Karlgaard and Lutze (2003, 2004) solved the HCW equations perturbed by second-order differential gravity terms with a circular reference. In their approach, a frequency correction was introduced to ensure validity of the solution. Kasdin et al. (2005) used a Hamiltonian formulation to obtain solutions to a similar problem, but with J_2 perturbations, also with a circular orbit assumption. Gurfil and Kasdin (2004) presented differential equations that model nonlinear relative motion in the configuration space, assuming a central field, by using a series representation for eccentricity effects. Yan (2006) presented expressions for J_2-perturbed relative motion coordinates, correct to the second order in J_2, by using the higher-order generating function from Brouwer theory. Consequently, small element differences up to the third order were also included, to ensure consistency between the

magnitudes of second-order J_2, and nonlinearity effects. A map for relative position propagation using second partials from the unit-sphere approach, was also derived. However, the general case of nonlinear relative motion using state variables and one independent variable has not been solved.

This chapter solves the relative motion problem to the second-order, by formulating a nonlinear map that can be used to find the relative states from differential orbital elements, that is accurate to the second order, and can therefore be used for large relative orbits. A method for solving the inverse problem is also devised, thereby leading to the formulation of a linear-quadratic map between the initial relative states, and the relative states at a desired time, using differential orbital elements as an intermediary. Furthermore, it is shown that simply isolating the quadratic map is sufficient for use with STMs that take into account J_2 perturbations, since for many cases, quadratic terms and terms with J_2 are of the same order, and for large relative orbits, nonlinearity effects dominate. A nonsingular element set is used to ensure uniform validity even when the eccentricity of the reference orbit is small or zero.

5.2 Nonlinear Relative Motion

The nonlinear relative motion equations in a central field have been presented in Chapter II, and are given by (2.7), or their scaled equivalent, by (2.15), and in perturbed form, by (2.16). The system of equations restricted to quadratic terms were presented by Euler and Shulman (1967). For the special case of periodic relative motion, this system can be solved (Sengupta et al. 2006). However, for the more general case where periodicity conditions have not been enforced, it is not yet known whether a method using a frequency correction can successfully be applied.

A formulation for relative motion equations with a circular reference orbit has been presented by Bond (1999), where the only assumption on the chaser orbit is that its eccentricity is low. Using the methodology described therein, it can be shown that all solutions are stable and bounded, which is true for any two satellites orbiting around a central body. The local in-plane growth term, for the simplest case of relative motion between two circular orbits, is given by $\sin(\Delta n\, t)$, where Δn is the difference between the mean motions of the chaser and target. This term can be expanded using a Taylor series comprising terms up to an arbitrary order:

$$\sin(\Delta n\, t) = \Delta n\, t - \frac{1}{6}(\Delta n\, t)^3 + \ldots \tag{5.1}$$

Since terms comprising t^k, $k = 1 \ldots \infty$ arise from the expansion process, standard perturbation methods cannot be used successfully to obtain a uniformly valid solution (Alfriend et al. 2002).

To circumvent the problems associated with an analytical solution to the perturbed system, the geometric method is used. Each orbit is uniquely defined by a set of nonsingular orbital elements, $\mathbf{ns} = \{a\ \theta\ i\ q_1\ q_2\ h\}^\top$, as defined in Chapter II. Use is also made of the geometric equations, as given by (3.13). If it is assumed that the orbital elements of the deputy are not much different from those of the chief, then the direction cosine matrix of the deputy can be expanded in a Taylor series, using the chief as a reference. For example, the differential inclination δi, if assumed small, allows expansions of the type $\cos\delta i \approx 1 - \delta i^2/2$ and $\sin\delta i \approx \delta i$. Using these approximations, the relative position is given by:

$$\begin{aligned} \xi \;\approx\; & \delta r - \frac{r}{2}\left(\cos^2\theta + \cos^2 i\, \sin^2\theta\right)\delta h^2 - \frac{r}{2}\sin^2\theta\, \delta i^2 - \frac{r}{2}\,\delta\theta^2 \\ & + r\sin i \sin\theta\cos\theta\, \delta h\, \delta i - r\cos i\, \delta h\, \delta\theta \end{aligned} \tag{5.2a}$$

$$\begin{aligned}\vartheta &\approx (r+\delta r)\left(\delta\theta+\cos i\,\delta h\right)+\frac{r}{2}\sin^2 i\sin\theta\cos\theta\,\delta h^2-\frac{r}{2}\sin\theta\cos\theta\,\delta i^2\\ &\quad -r\sin i\sin^2\theta\,\delta h\,\delta i \qquad (5.2b)\\ \zeta &\approx (r+\delta r)\left(\sin\theta\,\delta i-\sin i\cos\theta\,\delta h\right)+\frac{r}{2}\sin i\cos i\sin\theta\,\delta h^2\\ &\quad +r\sin i\sin\theta\,\delta h\,\delta\theta+r\cos\theta\,\delta i\,\delta\theta \qquad (5.2c)\end{aligned}$$

It should be noted that if only linear terms are considered in (5.2), then the out-of-plane dynamics depend only on differential RAAN, δh, and differential inclination, δi, and are therefore uncoupled from the in-plane dynamics. The inclusion of second-order terms introduces coupling effects.

To obtain the second-order map for the position variables, the expansions of δr and $\delta\theta$, are required. The first quantity is obtained by considering the equation of the radius of a satellite, which is written in terms of a, q_1, q_2, and θ, as follows:

$$r=\frac{a(1-q_1^2-q_2^2)}{(1+q_1\cos\theta+q_2\sin\theta)} \qquad (5.3)$$

For the sake of brevity, the functions α and β, defined in (3.66) are used. Using these functions, it is easily shown that:

$$\frac{\partial\alpha}{\partial\theta}=-\beta,\quad \frac{\partial\alpha}{\partial q_1}=\cos\theta,\quad \frac{\partial\alpha}{\partial q_2}=\sin\theta \qquad (5.4a)$$

$$\frac{\partial\beta}{\partial\theta}=\alpha-1,\quad \frac{\partial\beta}{\partial q_1}=\sin\theta,\quad \frac{\partial\beta}{\partial q_2}=-\cos\theta \qquad (5.4b)$$

Using (3.66) and (5.4) to calculate the partials of r with respect to the orbital elements, the differential radius δr is obtained using a Taylor series expansion to the second order, in the differential elements δa, δq_1, δq_2, and $\delta\theta$:

$$\begin{aligned}\frac{\delta r}{r} &\approx \frac{\delta a}{a}+\frac{\beta}{\alpha}\,\delta\theta-\frac{1}{\eta^2\alpha}\left(2q_1\alpha+\eta^2\cos\theta\right)\,\delta q_1-\frac{1}{\eta^2\alpha}\left(2q_2\alpha+\eta^2\sin\theta\right)\,\delta q_2\\ &\quad -\frac{1}{2\alpha^2}(\alpha^2-3\alpha+2\eta^2)\,\delta\theta^2+\frac{1}{\eta^2\alpha^2}\left(\eta^2\cos^2\theta+2q_1\alpha\cos\theta-\alpha^2\right)\,\delta q_1^2\end{aligned}$$

$$
\begin{aligned}
&+\frac{1}{\eta^2\alpha^2}\left(\eta^2\sin^2\theta+2q_2\alpha\sin\theta-\alpha^2\right)\,\delta q_2^2+\frac{\beta}{\alpha}\,\frac{\delta a}{a}\,\delta\theta\\
&-\frac{1}{\eta^2\alpha}\left(2q_1\alpha+\eta^2\cos\theta\right)\,\frac{\delta a}{a}\,\delta q_1-\frac{1}{\eta^2\alpha}\left(2q_2\alpha+\eta^2\sin\theta\right)\,\frac{\delta a}{a}\,\delta q_2\\
&-\frac{1}{\eta^2\alpha^2}\left(2q_1\alpha\beta+2\eta^2\beta\cos\theta-\eta^2\alpha\sin\theta\right)\,\delta\theta\,\delta q_1\\
&-\frac{1}{\eta^2\alpha^2}\left(2q_2\alpha\beta+2\eta^2\beta\sin\theta+\eta^2\alpha\cos\theta\right)\,\delta\theta\,\delta q_2\\
&+\frac{2}{\eta^2\alpha^2}\left(q_1\alpha\sin\theta+q_2\alpha\cos\theta+\eta^2\sin\theta\cos\theta\right)\,\delta q_1\,\delta q_2
\end{aligned}
\tag{5.5}
$$

The second quantity, $\delta\theta$, is required in terms of its initial value, $\delta\theta_0$. Since $\theta = g + f$, it follows that $\delta\theta = \delta g + \delta f$. By the use of (2.1) and (2.2), the differential true anomaly, correct to the second order, is given by:

$$
\delta f \;=\; d_l\,\delta l + d_e\,\delta e + d_{ll}\,\delta l^2 + d_{ee}\,\delta e^2 + d_{le}\,\delta l\,\delta e \tag{5.6}
$$

where,

$$
d_l = \frac{1}{\eta^3}(1+e\cos f)^2 \tag{5.7a}
$$

$$
d_e = \frac{1}{\eta^2}\sin f\,(2+e\cos f) \tag{5.7b}
$$

$$
d_{ll} = -\frac{e}{\eta^6}\sin f\,(1+e\cos f)^3 \tag{5.7c}
$$

$$
d_{ee} = \frac{1}{2\eta^4}\sin f\,(2e+5\cos f+6e\cos^2 f+2e^2\cos^3 f) \tag{5.7d}
$$

$$
d_{le} = -\frac{1}{\eta^5}(e-2\cos f-2e\cos^2 f)(1+e\cos f)^2 \tag{5.7e}
$$

Use is made of the mean argument of latitude, λ, which allows one to use the relation $\delta l = \delta\lambda - \delta g$. The following equations are also required to obtain $\delta\theta$ in terms of nonsingular elements:

$$
\begin{aligned}
e^2\,\delta g \;\approx\; & -e\sin g\,\delta q_1 + e\cos g\,\delta q_2 + \sin g\,\cos g\left(\delta q_1^2-\delta q_2^2\right)\\
& -\cos 2g\,\delta q_1\,\delta q_2
\end{aligned}
\tag{5.8a}
$$

$$
\begin{aligned}
e\,\delta e &\approx e\cos g\,\delta q_1 + e\sin g\,\delta q_2 + \frac{1}{2}\sin^2 g\,\delta q_1^2 + \frac{1}{2}\cos^2 g\,\delta q_2^2 \\
&\quad -\frac{1}{2}\sin 2g\,\delta q_1\,\delta q_2 \qquad (5.8b)\\
\delta\lambda &= \delta\lambda_0 + \delta n\,\Delta t = \delta\lambda_0 + \left(-\frac{3}{2}\frac{\delta a}{a} + \frac{15}{8}\frac{\delta a^2}{a^2}\right) n\,\Delta t \qquad (5.8c)
\end{aligned}
$$

where $\delta\lambda_0$ is the initial mean argument of latitude difference. Kepler's equation using nonsingular elements is used to denote elapsed time:

$$
\begin{aligned}
K(\theta_2,\theta_1) &\triangleq \int_{\theta_1}^{\theta_2} \frac{\eta^3}{(1+q_1\cos\theta+q_2\sin\theta)^2}\,d\theta \\
&= (F_2 - q_1\sin F_2 + q_2\cos F_2) - (F_1 - q_1\sin F_1 + q_2\sin F_1) \\
&= \lambda_2 - \lambda_1 = \dot{\lambda}\,\Delta t \qquad (5.9)
\end{aligned}
$$

where F is the eccentric argument of latitude, and $\dot{\lambda} = \dot{g} + \dot{l} = n$, for the two-body problem. The following equations relate the true and eccentric arguments of latitude:

$$\cos F = \frac{(1+\eta-q_2^2)\cos\theta + q_1q_2\sin\theta + (1+\eta)q_1}{(1+\eta)(1+q_1\cos\theta+q_2\sin\theta)} \qquad (5.10a)$$

$$\sin F = \frac{(1+\eta-q_1^2)\sin\theta + q_1q_2\cos\theta + (1+\eta)q_2}{(1+\eta)(1+q_1\cos\theta+q_2\sin\theta)} \qquad (5.10b)$$

$$\cos\theta = \frac{(1+\eta-q_2^2)\cos F + q_1q_2\sin F - (1+\eta)q_1}{(1+\eta)(1-q_1\cos F-q_2\sin F)} \qquad (5.10c)$$

$$\sin\theta = \frac{(1+\eta-q_1^2)\sin F + q_1q_2\cos F - (1+\eta)q_2}{(1+\eta)(1-q_1\cos F-q_2\sin F)} \qquad (5.10d)$$

Let $\boldsymbol{\delta\mathfrak{ns}} = \{\delta a/a\ \delta\theta\ \delta i\ \delta q_1\ \delta q_2\ \delta h\}^\top$ denote the vector of differential orbital elements, as defined in (2.20). In the two-body problem, all orbital element differences are constant, except $\delta\theta$. Equation (5.6) and δg are used to compose $\delta\theta$, and (5.7) and (5.8) are used to write $\delta\theta$ in terms of the nonsingular element differences, δq_1, δq_2, and $\delta\lambda$. The quantity $\delta\lambda$ is rewritten in terms of its initial value, $\delta\lambda_0$, which can be obtained from $\delta\theta_0$, using the inverse of the process described above. Consequently, the propagation of the differential orbital elements can be written in the following

form:

$$\boldsymbol{\delta\mathfrak{ms}}(\theta_2) \approx \mathbf{G}(\theta_2, \theta_1)\, \boldsymbol{\delta\mathfrak{ms}}(\theta_1) + \frac{1}{2}\mathbf{H}(\theta_2, \theta_1) \otimes \boldsymbol{\delta\mathfrak{ms}}(\theta_1) \otimes \boldsymbol{\delta\mathfrak{ms}}(\theta_1) \tag{5.11}$$

where $\mathbf{G} \in \mathbb{R}^{6\times 6}$ is the transition matrix for the differential orbital elements, and $\mathbf{H} \in \mathbb{R}^{6\times 6\times 6}$ is the next-order tensor for transition. In (5.11), the operator $\otimes$ denotes the dyadic product, i.e., in indicial notation this equation is equivalent to:

$$\delta\mathfrak{ms}_i(\theta_2) = G_{ij}(\theta_2, \theta_1)\, \delta\mathfrak{ms}_j(\theta_1) + \frac{1}{2}H_{ijk}(\theta_2, \theta_1)\, \delta\mathfrak{ms}_j(\theta_1)\, \delta\mathfrak{ms}_k(\theta_1) \tag{5.12}$$

with repeated indices implying summation. The components of $\mathbf{G}$ and $\mathbf{H}$ are given in Appendix B.

The expressions for relative velocities require the formulation of the quantities $\delta\dot{\theta}$ and $\delta\dot{r}$. These quantities can be calculated by taking the variations upto the second order in $\dot{\theta} = \dot{f} = \sqrt{\mu/p^3}\,\alpha^2$, and $\dot{r} = \sqrt{\mu/p}\,\beta$.

5.3 Formulation of the State Transition Matrix and Tensor

Let $\mathbf{x} = \{x\ y\ z\ x'\ y'\ z'\}^\top$ denote the state vector. The nondimensional relative velocities are given by $\boldsymbol{\rho}' = d\boldsymbol{\rho}/d\theta$. In the two-body problem, θ and f differ by a constant, g; therefore a derivative with respect to θ is equivalent to a derivative with respect to f.

The objective is to obtain a mapping between the state vector at $\theta = \theta_2$, and the state vector at $\theta = \theta_1$, that includes quadratic nonlinearities. Consequently, an expression of the following type is required:

$$\mathbf{x}(\theta_2) = \boldsymbol{\Phi}^{(1)}(\theta_2, \theta_1)\, \mathbf{x}(\theta_1) + \frac{1}{2}\boldsymbol{\Phi}^{(2)}(\theta_2, \theta_1) \otimes \mathbf{x}(\theta_1) \otimes \mathbf{x}(\theta_1) \tag{5.13}$$

In this equation, $\mathbf{\Phi}^{(1)} \in \mathbb{R}^{6\times6}$ is the STM for linearized relative motion. The second term contains $\mathbf{\Phi}^{(2)} \in \mathbb{R}^{6\times6\times6}$, which is a third-order tensor for state transition, accounting for second-order nonlinearities. Since a matrix is also a second-order tensor, both $\mathbf{\Phi}^{(1)}$ and $\mathbf{\Phi}^{(2)}$ will be referred to as state-transition tensors (STTs).

The evaluation of the STTs is performed via the use of the mapping between the Cartesian LVLH states and differential orbital elements. Using (5.5) in (5.2), and using some more algebra, results in the following mapping between $\mathbf{x}(\theta)$ and $\boldsymbol{\delta\mathfrak{ns}}$:

$$\mathbf{x}(\theta) = \mathbf{P}(\theta)\boldsymbol{\delta\mathfrak{ns}}(\theta) + \frac{1}{2}\mathbf{Q}(\theta) \otimes \boldsymbol{\delta\mathfrak{ns}}(\theta) \otimes \boldsymbol{\delta\mathfrak{ns}}(\theta) + \mathcal{O}\left(|\boldsymbol{\delta\mathfrak{ns}}(\theta)|^3\right) \tag{5.14}$$

where $\mathbf{P} \in \mathbb{R}^{6\times6}$ and $\mathbf{Q} \in \mathbb{R}^{6\times6\times6}$ are provided in Appendix C. To formulate the expressions for $\mathbf{\Phi}^{(1)}$ and $\mathbf{\Phi}^{(2)}$, an inverse map from $\mathbf{x}$ to $\boldsymbol{\delta\mathfrak{ns}}$ is required. Therefore, the objective is to solve for $\boldsymbol{\delta\mathfrak{ns}}$ in terms of the given state vector, $\mathbf{x}$, at any value of θ.

5.3.1 Inverse Map from States to Differential Orbital Elements

It is stated at the outset, that an inverse map for the linear system has been provided by Gim and Alfriend (2003). However, for better accuracy, an inverse map that is quadratic in the states, is sought. From the *vis-viva* integral (Battin 1999, chap. 3), the relationship between a, orbit energy, $\mathcal{E}$, and the velocity and position of a satellite, is given by:

$$\mathcal{E} = \frac{v^2}{2} - \frac{\mu}{r} = -\frac{\mu}{2a} \tag{5.15}$$

It is shown in Sengupta et al. (2006), that by using position and velocity scaled in the sense of the TH equations, the energy difference between two neighboring orbits as a

function of the true anomaly of the reference orbit, can be written in the following form:

$$\begin{aligned}\frac{\eta^2}{2}\frac{\delta\mathcal{E}}{\mathcal{E}} &= (2+3e\cos f+e^2)\,x+e\sin f\,(1+e\cos f)\,x'+(1+e\cos f)^2\,y' \\ &\quad +\frac{1}{2}\Big[-(1-e^2)\,x^2+(2+3e\cos f+e^2)\,y^2+(1+e\cos f+e^2\sin^2 f)\,z^2 \\ &\quad +(1+e\cos f)^2(x'^2+y'^2+z'^2)+2e\sin f\,(1+e\cos f)(xx'+yy'+zz') \\ &\quad +2(1+e\cos f)^2(xy'-yx')\Big]+\mathcal{O}\left(|\boldsymbol{\rho}|^3\right) \qquad (5.16)\end{aligned}$$

where $\mathcal{E}$ is used to denote the orbital energy of the chief. The third- and higher-order terms in (5.16) are contributed by Legendre polynomials of equivalent order, and contribute relative position terms only. From (5.15), the semimajor axis difference can also be written in terms of the energy difference. To the second order, the equation relating the two quantities is as follows:

$$\delta a=\frac{\mu}{2\mathcal{E}^2}\,\delta\mathcal{E}-\frac{\mu}{2\mathcal{E}^3}\,\delta\mathcal{E}^2+\mathcal{O}(\delta\mathcal{E}^3) \qquad (5.17)$$

$$\text{or,}\qquad \frac{\delta a}{a}\approx-\frac{\delta\mathcal{E}}{\mathcal{E}}+\left(\frac{\delta\mathcal{E}}{\mathcal{E}}\right)^2 \qquad (5.18)$$

Upon substituting (5.16) in (5.18), and keeping terms up to the second order, an expression for the semimajor axis difference is obtained, in terms of the relative position and velocity components.

However, the procedure for determining expressions for the remaining five differential orbital elements is far more complicated, because the *vis-viva* integral is the only constant of two-body motion that relates a single orbital element to the states of a satellite. The remaining integrals - the eccentricity and angular momentum vectors - yield equations in multiple orbital elements, and furthermore, these equations have to be rewritten in inertial coordinates to introduce inclination and RAAN.

A related approach is to first solve for the position and velocity of the deputy in the ECI frame, given the relative states, and then convert the ECI position and velocity to the orbital elements of the chief. Vadali et al. (2002) present a set of nonlinear equations that can be used to calculate relative position and velocity in $\mathcal{B}$, when the relative position and velocity in $\mathcal{N}$, and position and velocity of the chief in $\mathcal{N}$, are provided. Consequently, for the inverse operation, as required by the first step of this approach, a series of nonlinear equations in relative states is obtained. The second step of conversion from the deputy's ECI position to the deputy's orbital elements, further complicates the approach.

Both methods discussed in this section result in a set of nonlinear equations, which can be solved using numerical techniques, but are not amenable to closed-form analysis. In this chapter, a reversion of series is chosen as a feasible transformation, since $|\boldsymbol{\rho}| \ll 1$, second-order terms in $|\boldsymbol{\rho}|$ are much smaller in magnitude than first-order terms.

5.3.2 Inverse Map Using Series Reversion

The reversion of series for a function of one or many variables (Feagin and Gottlieb 1971), can also be written using tensors of increasing order (Turner 2003). In the present case, following the development in Turner (2003), a reversion of series is applied on (5.14), comprising linear and quadratic terms only. Series reversion leads to the following approximate solution for $\boldsymbol{\delta\mathfrak{n}}(\theta)$, for a given state vector $\mathbf{x}(\theta)$, and θ:

$$\begin{aligned}\boldsymbol{\delta\mathfrak{n}}(\theta) = \mathbf{P}^{-1}(\theta)\,\mathbf{x}(\theta) - \frac{1}{2}\mathbf{P}^{-1}(\theta)\,\left\{\mathbf{Q}(\theta)\otimes\left[\mathbf{P}^{-1}(\theta)\,\mathbf{x}(\theta)\right]\otimes\left[\mathbf{P}^{-1}(\theta)\,\mathbf{x}(\theta)\right]\right\} \\ +\mathcal{O}\left(|\mathbf{x}(\theta)|^3\right)\end{aligned} \tag{5.19}$$

Let $\overline{\mathbf{R}}(\theta) = \mathbf{P}^{-1}(\theta)$. Furthermore, let $\mathbf{S}(\theta_2, \theta_1)$ be a tensor such that its operation on the vector $\mathbf{x}(\theta_1)$ is given by:

$$\begin{aligned}
&\mathbf{S}(\theta_2,\theta_1)\otimes\mathbf{x}(\theta_1)\otimes\mathbf{x}(\theta_1)\\
&= \mathbf{Q}(\theta_2)\otimes\left[\mathbf{G}(\theta_2,\theta_1)\,\mathbf{P}^{-1}(\theta_1)\,\mathbf{x}(\theta_1)\right]\otimes\left[\mathbf{G}(\theta_2,\theta_1)\,\mathbf{P}^{-1}(\theta_1)\,\mathbf{x}(\theta_1)\right]\\
&= \mathbf{Q}(\theta_2)\otimes\left[\mathbf{G}(\theta_2,\theta_1)\,\overline{\mathbf{R}}(\theta_1)\,\mathbf{x}(\theta_1)\right]\otimes\left[\mathbf{G}(\theta_2,\theta_1)\,\overline{\mathbf{R}}(\theta_1)\,\mathbf{x}(\theta_1)\right] \qquad (5.20)
\end{aligned}$$

From Appendix B, it is observed that when $\theta_2 = \theta_1$, $\mathbf{G}(\theta_2, \theta_1)$ is the identity matrix. The matrix $\mathbf{G}(\theta_2, \theta_1)$ is introduced to facilitate the formulation of the STT, as will be made clear later. The above equation can be written in indicial notation as follows:

$$\begin{aligned}
&S_{ijk}(\theta_2,\theta_1)\,x_j(\theta_1)\,x_k(\theta_1)\\
&= Q_{ijk}(\theta_2)\,G_{jn}(\theta_2,\theta_1)\overline{R}_{nl}(\theta_1)\,x_l(\theta_1)\,G_{ko}(\theta_2,\theta_1)\overline{R}_{om}(\theta_1)\,x_m(\theta_1)\\
&= Q_{ilm}(\theta_2)\,G_{ln}(\theta_2,\theta_1)\overline{R}_{nj}(\theta_1)\,G_{mo}(\theta_2,\theta_1)\overline{R}_{ok}(\theta_1)\,x_j(\theta_1)\,x_k(\theta_1) \qquad (5.21)
\end{aligned}$$

In the above expression, j, k, l and m are repeated indices and can therefore be interchanged. It follows that:

$$S_{ijk}(\theta_2,\theta_1) \;=\; Q_{ilm}(\theta_2)\,G_{ln}(\theta_2,\theta_1)\overline{R}_{nj}(\theta_1)\,G_{mo}(\theta_2,\theta_1)\overline{R}_{ok}(\theta_1) \qquad (5.22)$$

In matrix notation, this is rewritten as:

$$\mathbf{S}_i(\theta_2,\theta_1) = \left[\mathbf{G}(\theta_2,\theta_1)\,\overline{\mathbf{R}}(\theta_1)\right]^{\top}\mathbf{Q}_i(\theta_2)\left[\mathbf{G}(\theta_2,\theta_1)\,\overline{\mathbf{R}}(\theta_1)\right] \qquad (5.23)$$

$$\text{where,}\quad \mathbf{S}_i = \begin{bmatrix} S_{i11} & \cdots & S_{i16} \\ \vdots & & \vdots \\ S_{i61} & \cdots & S_{i66} \end{bmatrix}, \quad \mathbf{Q}_i = \begin{bmatrix} Q_{i11} & \cdots & Q_{i16} \\ \vdots & & \vdots \\ Q_{i61} & \cdots & Q_{i66} \end{bmatrix}$$

It is obvious that $S_{ijk} = S_{ikj}$. Upon substituting the tensor $\mathbf{S}(\theta_1, \theta_1)$ from (5.22) in (5.19), the following equation is obtained from which $\boldsymbol{\delta\mathfrak{n}\mathfrak{s}}$ can be calculated from the

state vector at $\theta = \theta_1$:

$$\boldsymbol{\delta\mathfrak{ns}}(\theta_1) = \overline{\mathbf{R}}(\theta_1)\,\mathbf{x}(\theta_1) - \frac{1}{2}\overline{\mathbf{R}}(\theta_1)\,[\mathbf{S}(\theta_1,\theta_1)\otimes\mathbf{x}(\theta_1)\otimes\mathbf{x}(\theta_1)] + \mathcal{O}\left(|\mathbf{x}(\theta_1)|^3\right) \quad (5.24)$$

Substituting (5.24) and (5.11) in (5.14) evaluated at $\theta = \theta_2$ leads to the following expression:

$$\begin{aligned}
\mathbf{x}(\theta_2) &= \mathbf{P}(\theta_2)\,\mathbf{G}(\theta_2,\theta_1)\,\boldsymbol{\delta\mathfrak{ns}}(\theta_1) + \frac{1}{2}\mathbf{P}(\theta_2)\,\mathbf{H}(\theta_2,\theta_1)\otimes\boldsymbol{\delta\mathfrak{ns}}(\theta_1)\otimes\boldsymbol{\delta\mathfrak{ns}}(\theta_1) \\
&\quad + \frac{1}{2}\mathbf{Q}(\theta_2)\otimes[\mathbf{G}(\theta_2,\theta_1)\,\boldsymbol{\delta\mathfrak{ns}}(\theta_1)]\otimes[\mathbf{G}(\theta_2,\theta_1)\,\boldsymbol{\delta\mathfrak{ns}}(\theta_1)] \\
&\quad + \mathcal{O}\left(|\boldsymbol{\delta\mathfrak{ns}}(\theta_1)|^3\right) \qquad (5.25) \\
&= \mathbf{P}(\theta_2)\,\mathbf{G}(\theta_2,\theta_1)\,\overline{\mathbf{R}}(\theta_1)\,\mathbf{x}(\theta_1) \\
&\quad - \frac{1}{2}\mathbf{P}(\theta_2)\,\mathbf{G}(\theta_2,\theta_1)\,\overline{\mathbf{R}}(\theta_1)\,[\mathbf{S}(\theta_1,\theta_1)\otimes\mathbf{x}(\theta_1)\otimes\mathbf{x}(\theta_1)] \\
&\quad + \frac{1}{2}\mathbf{P}(\theta_2)\,\mathbf{H}(\theta_2,\theta_1)\otimes\left[\overline{\mathbf{R}}(\theta_1)\,\mathbf{x}(\theta_1)\right]\otimes\left[\overline{\mathbf{R}}(\theta_1)\,\mathbf{x}(\theta_1)\right] \\
&\quad + \frac{1}{2}\mathbf{Q}(\theta_2)\otimes\left[\mathbf{G}(\theta_2,\theta_1)\,\overline{\mathbf{R}}(\theta_1)\,\mathbf{x}(\theta_1)\right]\otimes\left[\mathbf{G}(\theta_2,\theta_1)\,\overline{\mathbf{R}}(\theta_1)\,\mathbf{x}(\theta_1)\right] \\
&\quad + \mathcal{O}(|\mathbf{x}(\theta_1)|^3) \qquad (5.26)
\end{aligned}$$

Upon comparing (5.26) with (5.13), and by using (5.22), the following expressions for the STTs are obtained:

$$\begin{aligned}
\Phi^{(1)}_{ij}(\theta_2,\theta_1) &= P_{ik}(\theta_2)\,G_{kl}(\theta_2,\theta_1)\,\overline{R}_{lj}(\theta_1) \qquad (5.27a) \\
\Phi^{(2)}_{ijk}(\theta_2,\theta_1) &= S_{ijk}(\theta_2,\theta_1) - P_{in}(\theta_2)\,G_{nm}(\theta_2,\theta_1)\,\overline{R}_{ml}(\theta_1)\,S_{ljk}(\theta_1,\theta_1) \\
&\quad + P_{in}(\theta_2)\,H_{nlm}(\theta_2,\theta_1)\,\overline{R}_{lj}(\theta_1)\,\overline{R}_{mk}(\theta_1) \qquad (5.27b)
\end{aligned}$$

Thus, $\mathbf{x}(\theta_2)$ can be obtained in terms of $\mathbf{x}(\theta_1)$, if the matrices $\mathbf{P}$, $\overline{\mathbf{R}}$, and tensor $\mathbf{Q}$ are known. Furthermore, let $\overline{\mathbf{S}}(\theta)$ denote a tensor such that $\overline{S}_{ijk}(\theta) = -\overline{R}_{il}(\theta)\,S_{ljk}(\theta,\theta)$.

Then, (5.24) reduces to the following form:

$$\boldsymbol{\delta\mathfrak{ns}}(\theta) = \overline{\mathbf{R}}(\theta)\,\mathbf{x}(\theta) + \frac{1}{2}\overline{\mathbf{S}}(\theta,\theta) \otimes \mathbf{x}(\theta) \otimes \mathbf{x}(\theta) + \mathcal{O}\left(|\mathbf{x}(\theta)|^3\right) \tag{5.28}$$

The tensors $\overline{\mathbf{R}}$ and $\overline{\mathbf{S}}$ are presented in Appendix C. It is worth noting that $\delta a/a$ obtained from (5.28) matches the expression obtained from (5.18).

The properties of the state transition matrices and tensors can easily be verified. For example, the first-order STT has the following properties:

1. $\boldsymbol{\Phi}^{(1)}(\theta_1,\theta_1) = \mathbb{1}_6$
2. $\boldsymbol{\Phi}^{(1)}(\theta_2,\theta_1) = \left[\boldsymbol{\Phi}^{(1)}(\theta_1,\theta_2)\right]^{-1}$
3. $\boldsymbol{\Phi}^{(1)}(\theta_3,\theta_1) = \boldsymbol{\Phi}^{(1)}(\theta_3,\theta_2)\,\boldsymbol{\Phi}^{(1)}(\theta_2,\theta_1)$

Noting from (5.27*b*) that $\boldsymbol{\Phi}^{(1)}(\theta_2,\theta_1) = \mathbf{P}(\theta_2)\,\mathbf{G}(\theta_2,\theta_1)\,\overline{\mathbf{R}}(\theta_1)$, the first property is verified, if it can be shown that $\mathbf{G}(\theta_1,\theta_1) = \mathbb{1}_6$. This can easily be observed from Appendix B, wherein the fact that $K(\theta_1,\theta_1) = 0$ is used. The second property can be verified, if it can be shown that $[\mathbf{G}(\theta_2,\theta_1)]^{-1} = \mathbf{G}(\theta_1,\theta_2)$. This can also be observed by using $K(\theta_2,\theta_1) = -K(\theta_1,\theta_2)$, in Appendix B. The third property may be verified by the following steps:

$$\begin{aligned}
\boldsymbol{\Phi}^{(1)}(\theta_3,\theta_1) &= \mathbf{P}(\theta_3)\,\mathbf{G}(\theta_3,\theta_1)\,\overline{\mathbf{R}}(\theta_1) \\
&= \mathbf{P}(\theta_3)\,\mathbf{G}(\theta_3,\theta_2)\,\mathbf{G}(\theta_2,\theta_1)\,\mathbf{R}(\theta_1) \\
&= \mathbf{P}(\theta_3)\,\mathbf{G}(\theta_3,\theta_2)\,\overline{\mathbf{R}}(\theta_2)\,\mathbf{P}(\theta_2)\,\mathbf{G}(\theta_2,\theta_1)\,\overline{\mathbf{R}}(\theta_1) \\
&= \boldsymbol{\Phi}^{(1)}(\theta_3,\theta_2)\,\boldsymbol{\Phi}^{(1)}(\theta_2,\theta_1)
\end{aligned} \tag{5.29}$$

where the fact that $\mathbf{G}(\theta_3,\theta_1) = \mathbf{G}(\theta_3,\theta_2)\,\mathbf{G}(\theta_2,\theta_1)$ is easily demonstrated by observing that $K(\theta_3,\theta_1) = K(\theta_3,\theta_2) + K(\theta_2,\theta_1)$.

The properties of the second-order STT can also be verified using similar steps. In particular, the following can be shown:

1. $\Phi^{(2)}_{ijk}(\theta_1, \theta_1) = 0$
2. $\Phi^{(2)}_{ijk}(\theta_1, \theta_2) = -\Phi^{(1)}_{il}(\theta_1, \theta_2)\, \Phi^{(2)}_{lmn}(\theta_2, \theta_1)\, \Phi^{(1)}_{mj}(\theta_1, \theta_2)\, \Phi^{(1)}_{nk}(\theta_1, \theta_2)$
3. $\Phi^{(2)}_{ijk}(\theta_3, \theta_1) = \Phi^{(1)}_{il}(\theta_3, \theta_2)\, \Phi^{(2)}_{ljk}(\theta_2, \theta_1) + \Phi^{(2)}_{ilm}(\theta_3, \theta_2)\, \Phi^{(1)}_{lj}(\theta_2, \theta_1)\, \Phi^{(1)}_{mk}(\theta_2, \theta_1)$

For the sake of completeness, the following relations can be used to transform between the dimensional and scaled states:

$$\begin{Bmatrix} \boldsymbol{\varrho} \\ \dot{\boldsymbol{\varrho}} \end{Bmatrix} = \begin{bmatrix} p/\alpha\, \mathbb{1}_3 & \mathbb{O}_3 \\ \sqrt{(\mu/p)}\, \beta, \mathbb{1}_3 & \sqrt{(\mu/p)}\, \alpha\, \mathbb{1}_3 \end{bmatrix} \begin{Bmatrix} \boldsymbol{\rho} \\ \boldsymbol{\rho}' \end{Bmatrix} \tag{5.30a}$$

$$\begin{Bmatrix} \boldsymbol{\rho} \\ \boldsymbol{\rho}' \end{Bmatrix} = \begin{bmatrix} (1/p)\, \alpha\, \mathbb{1}_3 & \mathbb{O}_3 \\ -(1/p)\, \beta\, \mathbb{1}_3 & \sqrt{(p/\mu)}/\alpha\, \mathbb{1}_3 \end{bmatrix} \begin{Bmatrix} \boldsymbol{\varrho} \\ \dot{\boldsymbol{\varrho}} \end{Bmatrix} \tag{5.30b}$$

where α and β are defined in (3.66). The matrices in (5.30) are denoted by $\mathbf{T}(\theta)$ and $\mathbf{T}^{-1}(\theta)$, respectively.

Since the analysis in this chapter uses nonsingular orbital elements, evaluation of the intermediate tensors are still singular for equatorial orbits. This is easily observed from the expressions in Appendix C, some of which comprise $\cot i$ and $\csc i$. The formulation using either equinoctial elements or kinematic states is more complicated and is beyond the scope of this dissertation. A state transition matrix for the linear, J_2-perturbed case, that uses equinoctial elements, is presented in Gim and Alfriend (2005).

5.4 Oblateness Effects

The most significant advantage of the formulation in the previous section is that the second-order STT can very easily be used with more accurate first-order STTs that also account for J_2-induced oblateness effects.

It is first necessary to compare the order of the terms arising due to J_2 and nonlinear differential gravity. Sengupta et al. (2006) show that if the states of the TH equations are scaled by $\varrho_0/(1+\overline{e}\cos f)$, instead of $\overline{p}/(1+\overline{e}\cos f)$, where ϱ_0 represents the size of the relative orbit, then the second-order terms in x, y, and z have $\epsilon = \varrho_0/\overline{p}$ as a coefficient, where the overbar indicates the use of mean elements. Consequently, ϵ is a measure of nonlinearity. Similarly, as shown in Kasdin et al. (2005), the linear terms that arise due to the inclusion of terms with J_2 in the gravitational potential, have $\overline{J} = J_2(R_\oplus/\overline{p})^2$ as their coefficient, where $R_\oplus$ is the radius of the Earth. Scaling the states by $\varrho_0/(1+\overline{e}\cos f)$ leads to $|\boldsymbol{\rho}| = \mathcal{O}(1)$, and consequently both linear and quadratic terms are of the same order, and the effect of J_2 and nonlinearity can be studied by comparing ϵ and $\overline{J}$. Assuming a reference orbit with $a = 13,000\,\text{km}$, and $e = 0.3$, and using the values from Table 2.1, calculations show that $\overline{J} = 3 \times 10^{-4}$. For small relative orbits, the inclusion of second-order terms may not lead to significant improvement in the accuracy of the propagated states, since oblateness effects dominate. However, second-order terms may be required when the chief's orbit is highly eccentric, even when the relative orbit is small, since the nonlinear terms also have $(1 + e\cos f)$ in the denominator of (2.16), and can be significantly dominant. In all cases of relative motion involving large relative orbits, the inclusion of second-order terms is necessary for an accurate description of relative motion.

The above analysis also shows that the second-order terms can be limited to their representation in mean elements, and the inclusion of short-periodic and long-periodic variations are not necessary. If $\overline{\mathfrak{os}}$ denotes a mean element, then the corresponding osculating element is given by $\mathfrak{os} = \overline{\mathfrak{os}}\,[1 + \mathcal{O}(J_2)]$. Consequently, $\mathfrak{os}^2 = \mathcal{O}(\epsilon)+\mathcal{O}(\epsilon J_2)+\mathcal{O}(J_2^2)$. Since the mean to osculating conversion employed in Gim and Alfriend (2003) is correct to first order in J_2, and $\epsilon J_2 \approx J_2^2$, only secular growth terms need to be incorporated in the higher-order terms. Therefore, in $\mathbf{Q}$, the mean elements $\overline{a}$, $\overline{e}$, and $\overline{i}$ are used instead of the osculating semimajor axis, eccentricity, and inclination, respectively. Furthermore, the RAAN, argument of periapsis, and mean anomaly, are propagated by their respective mean secular rates, denoted by $\dot{h}_s$, $\dot{g}_s$, and $\dot{l}_s$. In terms of nonsingular elements, the following equations are obtained (Gim and Alfriend 2003):

$$\overline{q}_1 = e\cos(g_0 + \dot{g}_s\Delta t) = \overline{q}_{10}\cos(\dot{g}_s\,\Delta t) - \overline{q}_{20}\sin(\dot{g}_s\,\Delta t) \tag{5.31a}$$

$$\overline{q}_2 = e\sin(g_0 + \dot{g}_s\Delta t) = \overline{q}_{10}\sin(\dot{g}_s\,\Delta t) + \overline{q}_{20}\cos(\dot{g}_s\,\Delta t) \tag{5.31b}$$

$$\overline{\lambda} = \overline{\lambda}_0 + (\dot{g}_s + \dot{l}_s)\,\Delta t \tag{5.31c}$$

where

$$\dot{g}_s = -\frac{3}{4}\,\overline{J}\,\overline{n}(1 - 5\cos^2\overline{i}) \tag{5.32a}$$

$$\dot{M}_s = \overline{n}\,\left[1 + \frac{3}{4}\,\overline{J}\eta\,(-1 + 3\cos^2\overline{i}^2)\right] \tag{5.32b}$$

and $\overline{n} = \sqrt{(\mu/\overline{a}^3)}$. It should be noted that since the RAAN does not appear in of the elements of $\mathbf{Q}$, its secular rate is not required.

For consistent analysis, notation is borrowed from Gim and Alfriend (2003), with the understanding that the true argument of latitude is the independent variable, instead of time. This is easily accommodated for, as the time can be obtained from the true

argument of latitude without the inverse solution to Kepler's equation, by using (5.9) and (5.10). Additionally, the state vector in Gim and Alfriend (2003) is defined as $\{\xi\ \vartheta\ \zeta\ \dot{\xi}\ \dot{\vartheta}\ \dot{\zeta}\}^\top$; consequently it is necessary to use the matrix $\mathbf{T}$ as defined in (5.30) to transform between scaled and unscaled states, as well as to define the permutation matrix $\mathbf{\Pi}$, whose nonzero entries are:

$$\Pi_{11} = \Pi_{23} = \Pi_{35} = \Pi_{42} = \Pi_{54} = \Pi_{66} = 1 \tag{5.33}$$

Lastly, the differential orbital element set used in Gim and Alfriend (2003) does not scale the differential semimajor axis. Therefore, the scaling matrix $\mathbf{\Gamma}(\mathfrak{ns})$ is also defined, whose nonzero entries are:

$$\Gamma_{11} = a,\ \Gamma_{22} = \Gamma_{33} = \Gamma_{44} = \Gamma_{55} = \Gamma_{66} = 1 \tag{5.34}$$

The inverse matrices $\mathbf{\Pi}^{-1}$ and $\mathbf{\Gamma}^{-1}$ are easily obtained by inspection.

Let $\mathbf{\Sigma}(\theta)$ be the first-order geometric map between $\boldsymbol{\delta}\mathfrak{ns}(\theta)$, and the unscaled states, as defined in Gim and Alfriend (2003). It follows that the map between $\mathbf{x}(\theta)$ and $\boldsymbol{\delta}\mathfrak{ns}(\theta)$ is given by:

$$\mathbf{x}(\theta) = \mathbf{T}^{-1}(\theta)\,\mathbf{\Pi}\,\mathbf{\Sigma}(\theta)\,\mathbf{\Gamma}(\mathfrak{ns})\,\boldsymbol{\delta}\mathfrak{ns}(\theta) \tag{5.35}$$

The osculating differential nonsingular elements can be written in terms of the initial mean differential nonsingular elements, denoted by $\boldsymbol{\delta}\overline{\mathfrak{ns}}(\theta_1)$, by the following equation:

$$\mathbf{\Gamma}(\mathfrak{ns})\,\boldsymbol{\delta}\mathfrak{ns}(\theta_2) = \mathbf{D}(\theta_2)\,\overline{\mathbf{\Phi}}_{\bar{\varepsilon}}(\theta_2,\theta_1)\,\mathbf{\Gamma}(\overline{\mathfrak{ns}})\,\boldsymbol{\delta}\overline{\mathfrak{ns}}(\theta_1) \tag{5.36}$$

where $\mathbf{D}(\theta) = \partial\boldsymbol{\delta}\mathfrak{ns}(\theta)/\partial\boldsymbol{\delta}\overline{\mathfrak{ns}}(\theta)$, and $\overline{\mathbf{\Phi}}_{\bar{\varepsilon}}$ is the state transition matrix mapping initial mean nonsingular element differences at θ_1, to the element differences at θ_2, as given in Gim and Alfriend (2003). In the absence of J_2 perturbations, $\overline{\mathbf{\Phi}}_{\bar{\varepsilon}} = \mathbf{G}$, and $\mathbf{\Sigma} = \mathbf{P}$,

as defined in the appendices.

To include second-order terms in the map from initial mean orbital element differences to the osculating relative states, it is first necessary to define $\boldsymbol{\Xi}$ as the following matrix:

$$\boldsymbol{\Xi} = \overline{\boldsymbol{\Gamma}}^{-1} \overline{\boldsymbol{\Phi}}_{\bar{e}} \overline{\boldsymbol{\Gamma}} \tag{5.37}$$

where $\overline{\boldsymbol{\Gamma}} = \boldsymbol{\Gamma}(\overline{\mathbf{n}\mathbf{s}})$. It can be shown that:

$$\Xi_{ij} = \begin{cases} \overline{\Phi}_{\bar{e}_{ij}}, & i = 2 \ldots 6,\ j = 2 \ldots 6 \text{ and } i = j = 1 \\ \overline{\Phi}_{\bar{e}_{ij}} / \overline{a}, & i = 1, j = 2 \ldots 6 \\ \overline{a}\, \overline{\Phi}_{\bar{e}_{ij}}, & j = 1, i = 2 \ldots 6 \end{cases} \tag{5.38}$$

Appending the tensors $\overline{\mathbf{Q}}$ and $\overline{\mathbf{H}}$ to (5.35), where the overbar denotes mean elements, and using (5.37):

$$\begin{aligned} \mathbf{x}(\theta_2) &= \mathbf{T}^{-1}(\theta_2)\, \boldsymbol{\Pi}\, \boldsymbol{\Sigma}(\theta_2)\, \mathbf{D}(\theta_2)\, \overline{\boldsymbol{\Phi}}_{\bar{e}}(\theta_2, \theta_1)\, \overline{\boldsymbol{\Gamma}}\, \boldsymbol{\delta}\overline{\mathbf{n}\mathbf{s}}(\theta_1) \\ &\quad + \frac{1}{2} \overline{\boldsymbol{\Sigma}}(\theta_2)\, \overline{\mathbf{H}}(\theta_2, \theta_1) \otimes \boldsymbol{\delta}\overline{\mathbf{n}\mathbf{s}}(\theta_1) \otimes \boldsymbol{\delta}\overline{\mathbf{n}\mathbf{s}}(\theta_1) \\ &\quad + \frac{1}{2} \overline{\mathbf{Q}}(\theta_2) \otimes [\boldsymbol{\Xi}\, \boldsymbol{\delta}\overline{\mathbf{n}\mathbf{s}}(\theta_1)] \otimes [\boldsymbol{\Xi}\, \boldsymbol{\delta}\overline{\mathbf{n}\mathbf{s}}(\theta_1)] \qquad (5.39) \\ &= \widetilde{\mathbf{P}}(\theta_2, \theta_1)\, \boldsymbol{\delta}\overline{\mathbf{n}\mathbf{s}}(\theta_1) + \frac{1}{2} \widetilde{\mathbf{Q}}(\theta_2, \theta_1) \otimes \boldsymbol{\delta}\overline{\mathbf{n}\mathbf{s}}(\theta_1) \otimes \boldsymbol{\delta}\overline{\mathbf{n}\mathbf{s}}(\theta_1) \qquad (5.40) \end{aligned}$$

where,

$$\widetilde{\mathbf{P}}(\theta_2, \theta_1) = \mathbf{T}^{-1}(\theta_2)\, \boldsymbol{\Pi}\, \boldsymbol{\Sigma}(\theta_2)\, \mathbf{D}(\theta_2)\, \overline{\boldsymbol{\Phi}}_{\bar{e}}(\theta_2, \theta_1)\, \overline{\boldsymbol{\Gamma}} \tag{5.41a}$$

$$\widetilde{Q}_{ijk}(\theta_2, \theta_1) = \overline{\Sigma}_{il}(\theta_2)\, \overline{H}_{ljk}(\theta_2, \theta_1) + \overline{Q}_{ilm}(\theta_2)\, \Xi_{lj}\, \Xi_{mk} \tag{5.41b}$$

In (5.37), it is necessary to use $\overline{\boldsymbol{\Phi}}_{\bar{e}}$, instead of $\overline{\mathbf{G}}$, even though it appears at the quadratic level in (5.41b). This occurs because the structure of $\overline{\boldsymbol{\Phi}}_{\bar{e}}$ in Gim and Alfriend (2003) introduces terms of the order of $\overline{J}^2 K(\theta_2, \theta_1)^2 / \overline{n}^2$, which can become $\mathcal{O}(\overline{J})$ after

a few orbits.

The structure of (5.40) allows a straightforward application of a reversion of series on (5.40), as outlined in the chapter, by using $\widetilde{\mathbf{P}}$ and $\widetilde{\mathbf{Q}}$ in place of $\mathbf{P}$ and $\mathbf{Q}$, in (5.24). It should be noted that for the initial conditions, $\overline{\mathbf{\Phi}}_{\bar{e}} = \mathbb{1}_6$ and $\overline{H}_{ijk} = 0$.

The propagation of the states using the second-order tensor does not require additional computation, since the matrices $\mathbf{\Sigma}$, $\mathbf{D}$, and $\overline{\mathbf{\Phi}}_{\bar{e}}$ are already available in the literature, and are required even in the linear case for the perturbed model.

5.5 Numerical Simulations

5.5.1 Validation of the Inverse Transformation from Relative States to Differential Orbital Elements (No Oblateness Effects)

The effectiveness of series reversion to obtain initial differential orbital elements, using $\mathbf{P}$, $\mathbf{Q}$, $\overline{\mathbf{R}}$ and $\mathbf{S}$ in (5.19) is tested in this section by way of an example. Consider a reference orbit with the following orbital elements:

$$\begin{aligned} a = 13,000\,\text{km}, \quad \theta_0 = 0.1\,\text{rad}, \quad i = 0.87266\,\text{rad} \\ q_1 = 0.29886, \quad q_2 = 0.02615, \quad h = 0.34907\,\text{rad} \end{aligned} \tag{5.42}$$

Relative motion is established by selecting the following arbitrary initial relative position and velocity in the LVLH frame:

$$\begin{aligned} \xi_0 = -3.0331\,\text{km}, \quad \vartheta_0 = -12.967\,\text{km}, \quad \zeta_0 = 3.0837\,\text{km} \\ \dot{\xi}_0 = -10.3931\,\text{m/s}, \quad \dot{\vartheta}_0 = 4.3801\,\text{m/s}, \quad \dot{\zeta}_0 = 37.6743\,\text{m/s} \end{aligned} \tag{5.43}$$

The relative position and velocity of the deputy are converted to the position and velocity in the ECI frame, using the procedure outlined in Vadali et al. (2002). These

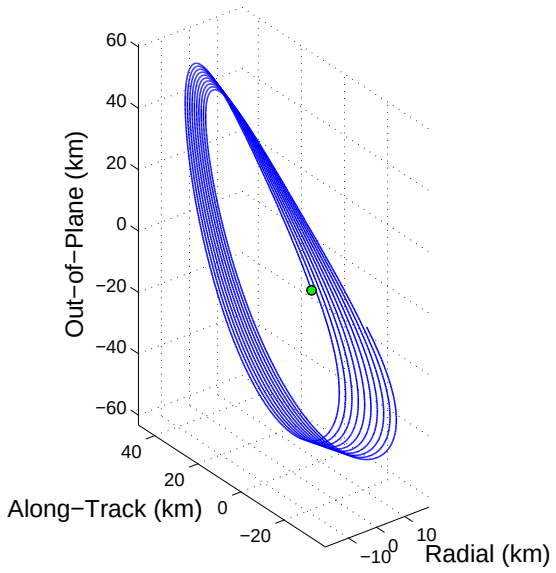

Fig. 5.1 Trajectory in the Rotating Frame

are used as initial conditions to integrate the ECI equations of motion due to a central field without J_2 accelerations. At each instant, the ECI position and velocity of the chief and deputy are converted to their respective orbital elements, and the former is subtracted from the latter to provide the true differential orbital elements. The ECI positions and velocities of the two satellites are also converted to the relative position and velocity in the LVLH frame of the chief. This relative trajectory is shown in Figure 5.1, with the circle denoting epoch. The relative distance involved is more than 50 km and the chief's eccentricity is 0.3. For a relative orbit of this size, it is not expected that linear analysis, for either the inverse transformation from relative states to differential orbital elements, or as a tool for state transition, will provide satisfactory results.

The orbital elements are now calculated over a period of 10 orbits of the chief, using the inverse mapping derived, as shown in (5.24). The results are shown in Figures 5.2a-5.2f. In all figures, the solid line indicates differential orbital elements

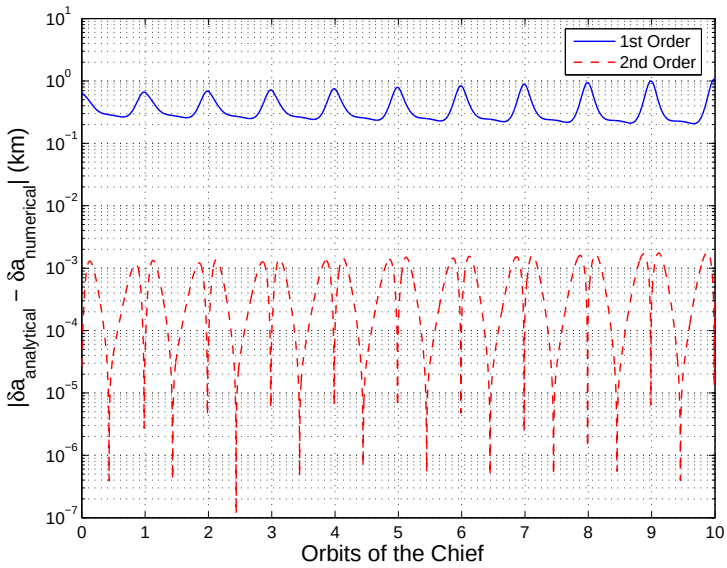

(a) Differential Semimajor Axis Error

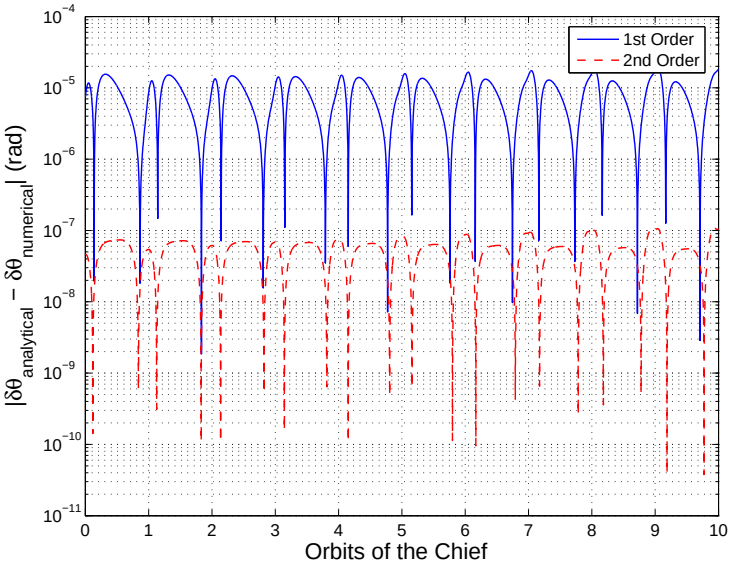

(b) Differential True Argument of Latitude Error

Fig. 5.2 Errors in Differential Orbital Elements Obtained from First-Order and Second-Order Maps

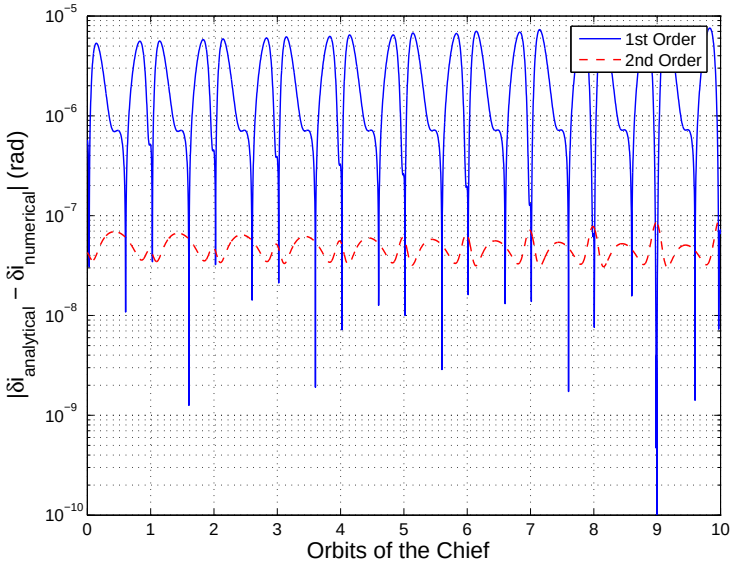

(c) Differential Inclination Error

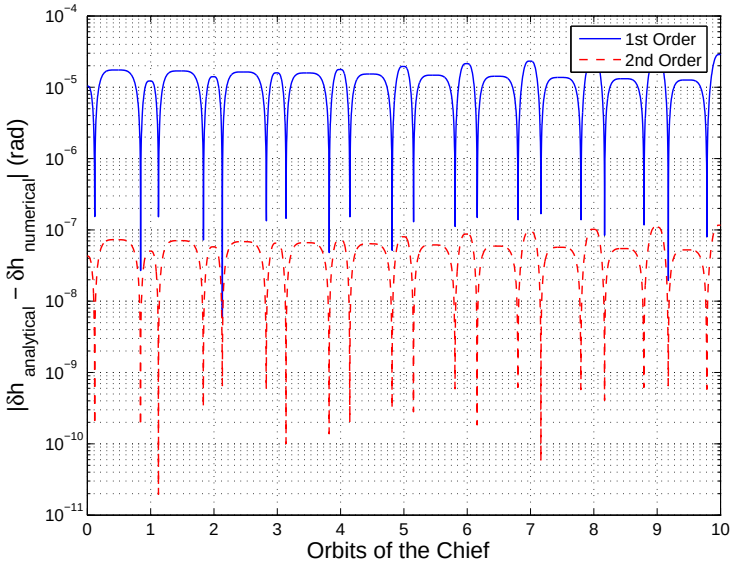

(d) Differential RAAN Error

Fig. 5.2 Continued

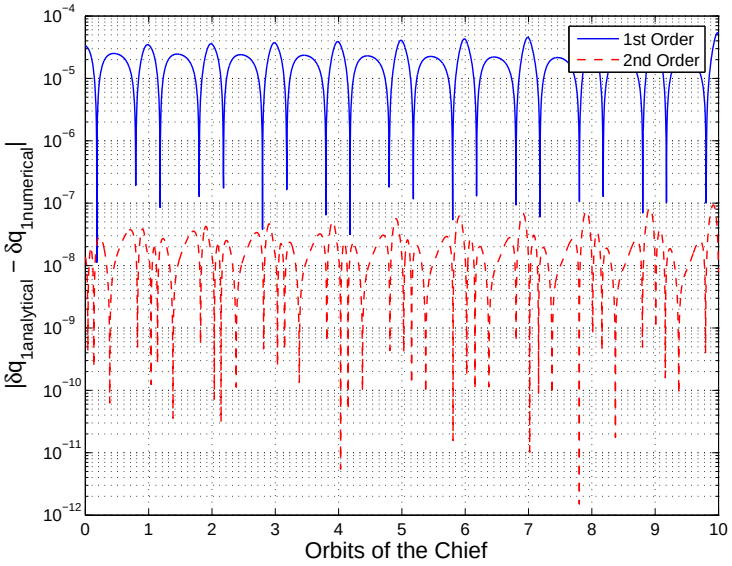

(e) δq_1 Error

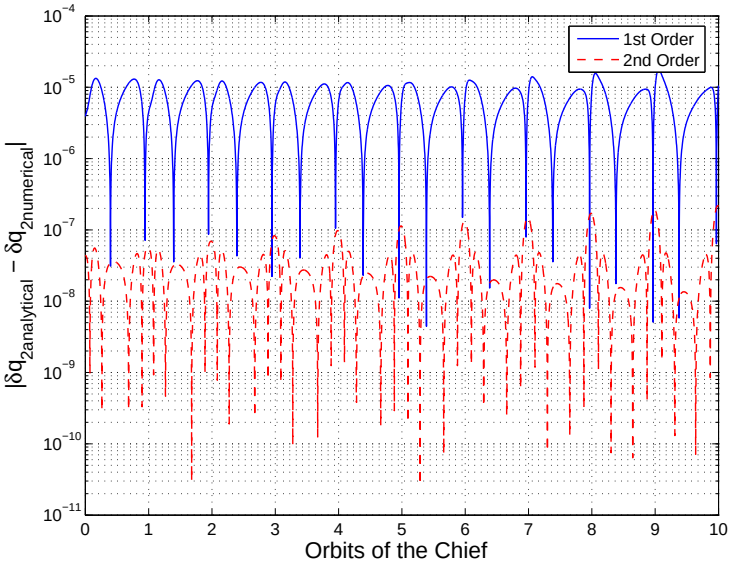

(f) δq_2 Error

Fig. 5.2 Continued

obtained using only the linear part of the transformation, given by $\overline{\mathbf{R}}(\theta)\,\mathbf{x}(\theta)$. The broken line shows the differential orbital elements obtained using the second-order map. The errors are shown on a logarithmic scale to bring out the accuracy of the second-order method. The relative distance is large, and the second-order map reduces errors by three magnitudes on an average.

5.5.2 State Transition Including Oblateness Effects

To account for oblateness effects, the initial mean orbital elements of the chief's trajectory are selected as shown in (5.42). These are converted to osculating elements using Brouwer theory, and then to ECI position and velocity. Relative position and velocity of the deputy are selected as shown in (5.43). The integration of the ECI equations include the J_2 accelerations, and is performed for 10 orbits of the chief. The relative trajectory in this case is not expected to match Figure 5.1 due to the inclusion of J_2 effects; it is sufficient to note that the relative orbit size is of the same order as that in the non-J_2 case.

The initial mean orbital element differences are calculated using series reversion on (5.40). This reversion is straightforward since $\theta_2 = \theta_1$, and the inverse of the matrices are known. The mean differential orbital elements obtained from the linear transformation are denoted by $\boldsymbol{\delta}\mathbf{m}\mathbf{s}_1$, and those obtained using the quadratic correction are denoted by $\boldsymbol{\delta}\mathbf{m}\mathbf{s}_2$. These are shown as the second and third columns of Table 5.1. When compared with the exact mean differential orbital elements (Column 4 of Table 5.1), it is obvious that the second-order transformation shows a marked improvement over the linear inverse transformation. The position and velocity for 10 orbits are obtained by using $\boldsymbol{\delta}\mathbf{m}\mathbf{s}_1$ and the linear part of (5.40), and $\boldsymbol{\delta}\mathbf{m}\mathbf{s}_2$ with

Table 5.1 Comparison of Initial Mean Differential Orbital Elements

Mean Element Difference	1st-Order ($\boldsymbol{\delta}\mathbf{n}\mathbf{s}_1$)	2nd-Order ($\boldsymbol{\delta}\mathbf{n}\mathbf{s}_2$)	Exact
$\overline{\delta a}$	$-0.43937\,\mathrm{km}$	$0.19993\,\mathrm{km}$	$0.20000\,\mathrm{km}$
$\overline{\delta\theta}_0$	$-0.15601 \times 10^{-2}\,\mathrm{rad}$	$-0.15526 \times 10^{-2}\,\mathrm{rad}$	$-0.15526 \times 10^{-2}\,\mathrm{rad}$
$\overline{\delta i}$	$0.50006 \times 10^{-2}\,\mathrm{rad}$	$0.50000 \times 10^{-2}\,\mathrm{rad}$	$0.50000 \times 10^{-2}\,\mathrm{rad}$
$\overline{\delta q_{1_0}}$	0.81355×10^{-4}	0.11479×10^{-3}	0.11452×10^{-3}
$\overline{\delta q_{2_0}}$	0.13376×10^{-2}	0.13415×10^{-2}	0.13415×10^{-2}
$\overline{\delta h}_0$	$0.21037 \times 10^{-3}\,\mathrm{rad}$	$0.19994 \times 10^{-3}\,\mathrm{rad}$	$0.20000 \times 10^{-3}\,\mathrm{rad}$

the complete linear-quadratic map in (5.40). The position error from either map is calculated from the norm of the individual radial, along-track, and out-of-plane errors, and is shown in Figure 5.3. It is immediately obvious that the linear map quickly loses validity, as indicated by the solid, blue line. The error using the linear-quadratic map (broken, red line) is approximately 10 m after 10 orbits, or approximately 0.03 per cent. The lack of accuracy of $\boldsymbol{\delta}\mathbf{n}\mathbf{s}_1$ results in the large errors for the linear map seen in Figure 5.3.

5.5.3 State Transition with Exact Initial Differential Orbital Elements

If it is now assumed that the initial mean differential orbital elements are known exactly, as given by Column 4 of Table 5.1, then propagation of these elements to obtain relative position and velocity results in the errors shown in Figure 5.4. The

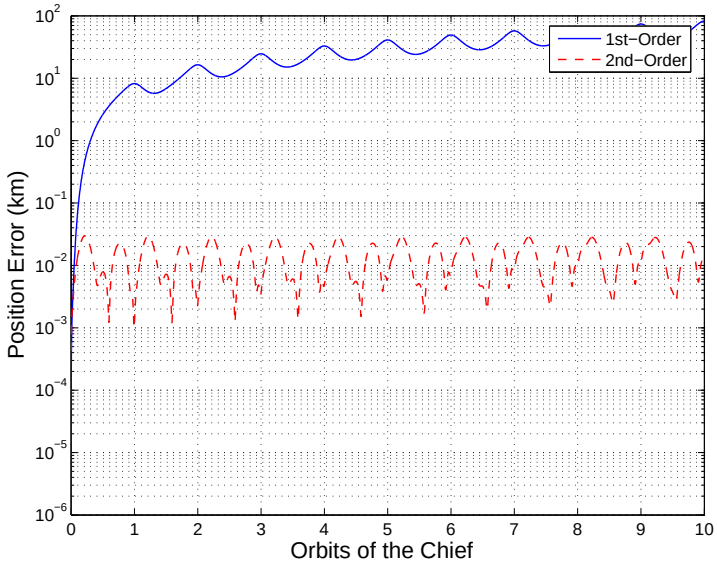

Fig. 5.3 Position Errors from First-Order and Second-Order STTs, with Oblateness Effects

solid, blue line, indicating the use of the linear map, shows a marked improvement from Figure 5.3. The error after 10 orbits is approximately 200 m, which is approximately 0.44 per cent of the orbit size. The error from the second-order map (broken, red line) does not show improvement over Figure 5.3, although it is still one order of magnitude lower than that from the linear map. The position error with the inclusion of the quadratic map, as shown in Figure 5.3 and Figure 5.4, are nearly identical, because the initial mean differential orbital elements used in both cases, as shown in Column 3 and Column 4 of Table 5.1 are nearly equal to each other. The remaining error, although small in magnitude, is a result of ignoring third- and higher-order terms in the development of the theory in this chapter, as well as second- and higher-order J_2 perturbations.

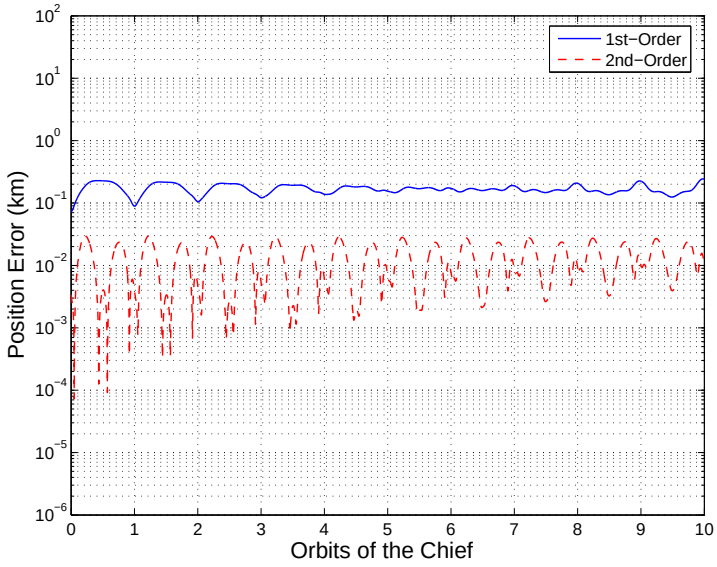

Fig. 5.4 Position Errors from First-Order and Second-Order STTs, with Oblateness Effects, with Accurate Initial Conditions

5.6 Summary

A second-order tensor suitable for satellite relative motion calculations has been developed using reversion of a vector series relating differential orbital elements, to relative position and velocity. This tensor can be used to obtain state transition representations, accurate to second-order, and it is shown that its use reduces position errors between analytical propagation and integration by upto two orders of magnitude in comparison with the errors from the linear propagation. The tensor is applicable to cases where a two-body model for satellite motion has been assumed, as well as one perturbed by oblateness effects. In the latter case, no modification to the theory is necessary since the effects of second-order nonlinearities can be of the same order as perturbations due to oblateness effects, and higher-order coupling between these two effects can be neglected. Finally, the use of nonsingular elements extends the validity of state transition to any value of eccentricity of an elliptic reference orbit.

CHAPTER VI

PERIODIC RELATIVE MOTION NEAR A KEPLERIAN ELLIPTIC ORBIT WITH NONLINEAR DIFFERENTIAL GRAVITY

6.1 Introduction

As shown in Chapter III, The HCW equations, (2.12), admit a special set of solutions that result in bounded relative motion. The applicability of the HCW conditions is limited in the same sense as the HCW solutions, to a circular reference orbit with a linearized gravitation field without perturbations. Modifications to the model must be made to account for the realities of the system, which manifest themselves as a violation to the underlying assumptions. In this chapter[1], the conditions for periodicity are derived when these assumptions are violated.

Previous work, limiting attention only to the two-body problem, may be categorized into those that deal with 1) nonlinear differential gravity, 2) noncircular reference orbit, and 3) the combination of nonlinearity and noncircular orbits. Assuming a circular reference orbit, conditions for periodic motion correct through the third order in differential gravitation terms were derived by Richardson and Mitchell (2003). A condition for the linear, eccentric case was derived by Inalhan et al. (2002); although an explicit formulation was only provided for orbit initiation at apogee or perigee, the condition for epoch at any other location on the chief's orbit could be obtained by a matrix inversion. In Chapter III, a generalized linear condition was derived, using the TH equations.

---

[1]Portions of this chapter were published by Sengupta et al. (2006). The author of this dissertation retains copyright.

Literature on establishing initial conditions for formations amply shows the importance of addressing the effects of eccentricity as well as nonlinearity. To this end, Anthony and Sasaki (1965) obtained approximate solutions to the HCW equations by including quadratic nonlinearities and first-order eccentricity effects. Vaddi et al. (2003) studied the combined problem of eccentricity and nonlinearity and obtained periodicity conditions in the presence of these effects. However, these conditions lose validity even for intermediate eccentricities, primarily because of the higher-order coupling between eccentricity and nonlinearity. Recent work by Gurfil (2005b) poses the bounded-motion problem in terms of the energy-matching condition. Since the velocity appears in a quadratic fashion in this equation, velocity corrections to the full, nonlinear problem can be obtained in an analytical manner, without assumptions on relative orbit size. However, the more general problem of period-matching is reduced to the solution of a sixth-order algebraic equation in any of the states, assuming the other five states are known. This approach requires a numerical procedure to obtain a solution, starting with an initial guess. The sixth-order polynomial has multiple roots, some of which have no physical significance. Euler and Shulman (1967) first presented the TH equations perturbed by nonlinear differential gravity with no assumptions on eccentricity. It was claimed in their work, that these equations could not be solved analytically.

If orbital elements are used to describe relative motion, then the boundedness condition is straightforward since the only requirement is that the semimajor axes of all satellites in the formation be equal. Though much work has been done on the problem of formation flight using orbital elements, in many ways, the use of relative motion equations in the LVLH frame is preferred over orbital element differences. It is easier to obtain local ranging data directly, than to have the position and

velocity of either satellite reported to a terrestrial station and translated into orbital elements. This also allows the use of decentralized control algorithms for the control of formations.

The work in this chapter studies the perturbed TH equations by treating second-order nonlinearities. In effect, the problem posed in Euler and Shulman (1967) is solved, for the case of bounded relative motion. These results are valid for arbitrary eccentricities and implicitly account for eccentricity-nonlinearity effects. The exact analytical solution, while complicated in appearance at first, leads to an elegant form of expressions for relative motion. Furthermore, the terms that lead to secular growth in the perturbed equations are easily identified as those that also lead to secular growth in the unperturbed equation, as observed in Carter (1990). Consequently, collecting these terms and negating their effects leads to a valid condition for periodic orbits.

6.2 Problem Description

A modified form of (2.16) is used in this chapter. Upon scaling the true position by the radius of the chief satellite, an additional scaling by the following dimensionless parameter is introduced:

$$\epsilon = \frac{\varrho_0}{p} \tag{6.1}$$

where, ϱ_0 is some measure of the relative orbit size. This is similar to the approach followed by Alfriend and Kashiwagi (1969), although only the linear TH equations were considered in their work. For low eccentricities, ϱ_0 may be the circular orbit radius as predicted by the HCW solutions. Without loss of generality,

$\varrho_0 = \sqrt{(}\xi_0^2 + \vartheta_0^2 + \zeta_0^2) \ll a$. The scaled relative position vector is now defined as

$$\boldsymbol{\rho} = \frac{\boldsymbol{\varrho}}{\varrho_0}(1 + e\cos f) \tag{6.2}$$

The use of this new parameter as a scaling factor slightly modifies (2.16). In this case, the equations of motion are as follows:

$$\begin{Bmatrix} x'' \\ y'' \\ z'' \end{Bmatrix} + \begin{bmatrix} 0 & -2 & 0 \\ 2 & 0 & 0 \\ 0 & 0 & 0 \end{bmatrix} \begin{Bmatrix} x' \\ y' \\ z' \end{Bmatrix} + \begin{bmatrix} -3/(1+e\cos f) & 0 & 0 \\ 0 & 0 & 0 \\ 0 & 0 & 1 \end{bmatrix} \begin{Bmatrix} x \\ y \\ z \end{Bmatrix}$$
$$= \epsilon\frac{3}{2}(1 + e\cos f)^{-1} \begin{Bmatrix} y^2 + z^2 - 2x^2 \\ 2xy \\ 2xz \end{Bmatrix} + \mathcal{O}(\epsilon^2) \tag{6.3}$$

From (6.3), it is evident that if the terms of order ϵ and higher are ignored, then the equations reduce to the unperturbed TH equations. It should be noted that the small parameter ϵ, as shown in (6.1) depends not only on the size of the relative orbit, but also on the eccentricity of the reference. Furthermore, the quantity $(1 + e\cos f)$ appears in the denominator of the nonlinear terms. These reflect the fact that eccentricity and nonlinearity effects in formation flight are coupled.

6.3 Solution Using a Perturbation Approach

A straightforward expansion (Nayfeh 1973, chap. 2) of the following form is considered:

$$\begin{aligned} x(f) &= x_0(f) + \epsilon x_1(f) + \cdots \\ y(f) &= y_0(f) + \epsilon y_1(f) + \cdots \\ z(f) &= z_0(f) + \epsilon z_1(f) + \cdots \end{aligned} \tag{6.4}$$

Lindstedt-Poincaré or renormalization techniques are not required since a frequency correction is not necessary. As shown in Chapter III, the linear TH system is 2π-periodic. Furthermore, in fully nonlinear relative motion, periodic motion between two satellites is only possible when the two satellites have the same mean motion and the period of relative motion is also 2π-periodic[2]. Consequently, higher-order corrections to the frequency must necessarily be zero, since the coefficient corresponding to each correction is an increasing power of the small parameter.

Equation (6.4) is substituted in (6.3), with perturbations up to order ϵ included. Collecting terms of the same order, the following two systems are obtained:

$$x_0'' - 2y_0' - \frac{3x_0}{(1 + e\cos f)} = 0 \tag{6.5a}$$

$$y_0'' + 2x_0' = 0 \tag{6.5b}$$

$$z_0'' + z_0 = 0 \tag{6.5c}$$

[2]In all other cases, motion, though bounded, is quasi-periodic (Gurfil and Kholshevnikov 2006)

and,

$$x_1'' - 2y_1' - \frac{3x_1}{(1+e\cos f)} = \frac{3}{2}\frac{(y_0^2+z_0^2-2x_0^2)}{(1+e\cos f)} \tag{6.6a}$$

$$y_1'' + 2x_1' = \frac{3x_0y_0}{(1+e\cos f)} \tag{6.6b}$$

$$z_1'' + z_1 = \frac{3x_0z_0}{(1+e\cos f)} \tag{6.6c}$$

6.3.1 Solution to the Unperturbed System

The approach followed in this section is for epoch at a general initial value of true anomaly f_i. In a later section, the explicit formulation for $f_i = 0$ (periapsis) and $f_i = \pi$ (apoapsis) will be presented. This considerably simplifies the expressions obtained.

Following the approach in Chapter III, use is made of the function $J(f)$ to write the following solution to the homogeneous zeroth-order system:

$$\begin{aligned} x_0(f) &= c_1\cos f\ (1+e\cos f) + c_2\sin f\ (1+e\cos f) \\ &\quad + c_3\left[2e\sin f\ (1+e\cos f)J(f) - \frac{\cos f}{(1+e\cos f)}\right] && (6.7a) \\ y_0(f) &= -c_1\sin f\ (2+e\cos f) + c_2\cos f\ (2+e\cos f) \\ &\quad + 2c_3(1+e\cos f)^2J(f) + c_4 && (6.7b) \\ z_0(f) &= c_5\cos f + c_6\sin f && (6.7c) \\ x_0'(f) &= -c_1(\sin f + e\sin 2f) + c_2(\cos f + e\cos 2f) \\ &\quad + c_3\left[2e(\cos f + e\cos 2f)J(f) + \frac{(\sin f + e\sin 2f)}{(1+e\cos f)^2}\right] && (6.7d) \\ y_0'(f) &= -c_1(2\cos f + e\cos 2f) - c_2(2\sin f + e\sin 2f) \\ &\quad - 2c_3\left[e(2\sin f + e\sin 2f)J(f) - \frac{\cos f}{(1+e\cos f)}\right] && (6.7e) \\ z_0'(f) &= -c_5\sin f + c_6\cos f && (6.7f) \end{aligned}$$

The function $J(f)$ is used rather than $K(f)$, since it is consistent with the development of the forced TH model as shown in Carter and Humi (1987); Carter (1990). In terms of the eccentric anomaly, this function is given by:

$$\begin{aligned} J(f) &= \int \frac{\cos f}{(1+e\cos f)^3}\, df \\ &= -(1-e^2)^{-5/2}\left[\frac{3e}{2}E - (1+e^2)\sin E + \frac{e}{4}\sin 2E\right] \end{aligned} \tag{6.8}$$

The first-order periodicity condition, (3.27), is satisfied for infinite combinations of initial conditions, and for resolution, a constraint is required. One suitable constraint may be to keep the initial states as a given and calculate the minimum velocity impulse required to obtain a periodic orbit. A similar approach has been used by Inalhan et al. (2002), wherein the Δv for formation insertion is minimized by posing the problem as a linear program. The problem may also be posed as one where the 2-norm of the impulse, with components $\Delta x_0'$ and $\Delta y_0'$, is minimized:

$$\begin{aligned} &\min\ \Phi(\Delta x_0', \Delta y_0') = \left(\ \Delta x_0'^2 + \Delta y_0'^2\right)^{1/2} \\ &\text{subject to : } \Psi(\Delta x_0', \Delta y_0') = \ l_1 x_{0_i} + l_2\left(x_{0_i}' + \Delta x_0'\right) + l_3\left(y_{0_i}' + \Delta y_0'\right) = 0 \end{aligned} \tag{6.9}$$

where

$$\begin{aligned} l_1 &= e^2 + 3e\cos f_i + 2 \\ l_2 &= e\sin f_i(1 + e\cos f_i) \\ l_3 &= (1 + e\cos f_i)^2 \end{aligned}$$

By minimizing $\Phi + \ell\,\Psi$, where ℓ is a Lagrange multiplier, the following unique solution is obtained:

$$\Delta x_0' = -\frac{l_2}{l_2^2 + l_3^2}(l_1 x_{0_i} + l_2 x_{0_i}' + l_3 y_{0_i}') \tag{6.10a}$$

$$\Delta y_0' = -\frac{l_3}{l_2^2 + l_3^2}(l_1 x_{0_i} + l_2 x_{0_i}' + l_3 y_{0_i}') \tag{6.10b}$$

Irrespective of the manner in which the initial conditions are established, the result is the most general (linear) periodic solution, as shown in (3.32).

6.3.2 Solution to the Perturbed System

Having obtained initial conditions for periodicity in the unperturbed system, its periodic form is now substituted in (6.6). The solutions to these equations are similar to (6.7), with additional particular integrals. The equation in $z_1(f)$ is considered separately, due to its tractable nature:

$$z_1'' + z_1 = \frac{3 x_p z_p}{(1 + e\cos f)} = 3\rho_1\rho_3 \sin(f + \psi_0)\sin(f + \phi_0) \tag{6.11}$$

Solving (6.11) yields:

$$z_1(f) = b_5 \cos f + b_6 \sin f + \frac{1}{2}\rho_1\rho_3 \left[3\cos(\psi_0 - \phi_0) + \cos(2f + \psi_0 + \phi_0)\right] \tag{6.12}$$

Since there are no secular growth terms in (6.12), an arbitrary choice may be made for the constants of integration b_5 and b_6. Although not necessariy, one option is to remove terms with $\cos(f)$ and $\sin(f)$, i.e., to ensure that the mean value of the z amplitude is the same as that predicted by the linear equations. Therefore, the following choices for the initial conditions are made:

$$z_{1_i} = \frac{1}{2}\rho_1\rho_3 \cos(2f_i + \psi_0 + \phi_0) + \frac{3}{2}\rho_1\rho_3 \cos(\psi_0 - \phi_0) \tag{6.13a}$$

$$z_{1_i}' = -\rho_1\rho_3 \sin(2f_i + \psi_0 + \phi_0) \tag{6.13b}$$

As a result,

$$z_1(f) = \frac{3}{2}\rho_1\rho_3\cos(\psi_0 - \phi_0) + \frac{1}{2}\rho_1\rho_3\cos(2f + \psi_0 + \phi_0) \tag{6.14}$$

Carter and Humi (1987) developed the TH equations in the presence of a forcing function. Utilizing this result, it can be shown that the x_1 and y_1 solutions are:

$$\begin{aligned} x_1(f) &= b_1\cos f\ (1 + e\cos f) + b_2\sin f\ (1 + e\cos f) \qquad (6.15a)\\ &\quad + b_3\left[2e\sin f\ (1 + e\cos f)J(f) - \frac{\cos f}{(1 + e\cos f)}\right] + \phi\int\frac{\Lambda}{\phi^2}\ df \\ y_1(f) &= -b_1\sin f\ (2 + e\cos f) + b_2\cos f\ (2 + e\cos f) \qquad (6.15b)\\ &\quad + 2b_3(1 + e\cos f)^2 J(f) + b_4 + 3\iint\frac{x_p y_p}{(1 + e\cos f)}\ df \\ &\quad + \frac{1}{e}\left[(1 + e\cos f)^2\int\frac{\Lambda}{\phi^2}\ df - \int\frac{\Lambda}{\sin^2 f}\ df\right] \end{aligned}$$

where $\phi = \sin f\ (1 + e\cos f)$, and

$$\begin{aligned} \Lambda &= \frac{3}{2}\int(y_p^2 + z_p^2 - 2x_p^2)\sin f\ df - \frac{3}{e}(1 + e\cos f)^2\int\frac{x_p y_p}{(1 + e\cos f)}\ df \\ &\quad + \frac{3}{e}\int x_p y_p(1 + e\cos f)\ df \\ &= \Lambda_0 + \sum_{k=1}^{5}(\Lambda_{c_k}\cos kf + \Lambda_{s_k}\sin kf) \qquad (6.16) \end{aligned}$$

The coefficients, $\{\Lambda_0, \Lambda_{c_1}\cdots\Lambda_{c_5}, \Lambda_{s_1}\cdots\Lambda_{s_5}\}$ are provided in Appendix D. The complete solution of (6.15) requires the evaluation of the integrals of $\cos(kf)/\phi^2$, $\sin(kf)/\phi^2$, $\cos(kf)/\sin^2 f$, and $\sin(kf)/\sin^2 f$, $k = 1\ldots5$. These integrals can also be evaluated in terms of $J(f)$ and sinusoidal functions of the true anomaly, and are presented in Appendix D. Though it may appear that the terms in the appendix are not defined for $f = n\pi$, it should be noted that when multiplied by the appropriate coefficient, the logarithmic terms, and terms containing f explicitly, cancel each other for and value of f, and are therefore ignored from further analysis. Consequently, the

analytical solution to the perturbed system can be constructed.

From Appendix D and the solution to (6.15a), the secular growth terms are identified as those which contain $J(f)$. It follows that setting the combined coefficient of $J(f)$ to zero will prevent secular growth to the second order. Collecting the coefficients of $J(f)$ in $x_1(f)$ results in the following condition:

$$\begin{aligned} & 2eb_3 + 2e\Lambda_0 - \frac{2}{3}(2+e^2)\Lambda_{c_1} + \frac{2}{3e}(2+e^2)\Lambda_{c_2} - 2(2-e^2)\Lambda_{c_3} \\ & -\frac{2}{3e^3}(8-24e^2+13e^4)\Lambda_{c_4} - \frac{2}{3e^4}(32-80e^2+50e^4-5e^6)\Lambda_{c_5} = 0 \qquad (6.17) \\ \text{or} \qquad & b_3 = -\frac{e}{4}\left(2\rho_1^2\cos 2\psi_0 + \rho_3^2\cos 2\phi_0\right) - 2\rho_1\rho_2\cos\psi_0 - \frac{e}{4}\left(\rho_1^2+2\rho_2^2+\rho_3^2\right) \\ & \quad -\frac{1}{2e}\left(2\rho_1^2+2\rho_2^2+\rho_3^2\right) \qquad (6.18) \end{aligned}$$

The seemingly complex integrals involved in the equation actually reduce to fairly simple expressions. Ignoring the terms containing $J(f)$, since they are rendered absent by the choice of b_3 in (6.18), the integrals may be rewritten as the following:

$$\begin{aligned} p_1(f) &= \phi\int\frac{\Lambda}{\phi^2}\,df = \sum_{k=1}^{3}G_k\sin kf + \frac{1}{(1+e\cos f)}\sum_{k=0}^{4}H_k\cos kf \qquad (6.19a) \\ s_1(f) &= 3\iint\frac{x_p y_p}{(1+e\cos f)}\,df = \sum_{k=1}^{3}(E_k\,\sin kf + F_k\cos kf) \qquad (6.19b) \\ s_2(f) &= \frac{1}{e}\left[(1+e\cos f)^2\int\frac{\Lambda}{\phi^2}\,df - \int\frac{\Lambda}{\sin^2 f}\,df\right] \\ &= \overline{Q}_0 + \sum_{k=1}^{3}\left(Q_k\sin kf + \overline{Q}_k\cos kf\right) \qquad (6.19c) \end{aligned}$$

The coefficients are presented in Appendix D.

The initial conditions for the perturbed system, $\mathbf{x}_{1_i} = \{x_{1_i}\ y_{1_i}\ x'_{1_i}\ y'_{1_i}\}^\top$, integration constants $\mathbf{b} = \{b_1 \cdots b_4\}^\top$, and initial values of the forcing function, are related by

the following:

$$\mathbf{x}_{1_i} = \widetilde{\mathbf{\Lambda}}\mathbf{b} + \mathbf{w} \tag{6.20}$$

It follows that:

$$\widetilde{\mathbf{\Lambda}} = \begin{bmatrix} L_{11} & L_{12} & L_{13} & 0 \\ L_{21} & L_{22} & L_{23} & 1 \\ L_{41} & L_{42} & L_{43} & 0 \\ L_{51} & L_{52} & L_{53} & 0 \end{bmatrix} \tag{6.21}$$

It can be shown using the matrix $\mathbf{L}$ from Chapter III, that $\det\widetilde{\mathbf{\Lambda}} = 1$. The initial values of the forcing functions are given by $\mathbf{w} = \{p_1 \quad (s_1 + s_2) \quad p_1' \quad (-2p_1 + s_1')\}^\top$ evaluated at $f = f_i$.

Initial conditions are required that will lead to the particular value of b_3 specified in (6.18). This provides one constraint on the initial conditions. If only a velocity correction is required, one may choose $x_{1_i} = y_{1_i} = x'_{1_i} = 0$. By substituting the $b_{1\ldots3}$ obtained from solving (6.20) into the last equation for y'_{1_i}, the following is obtained:

$$\begin{aligned} \Delta \triangleq y'_{1_i} &= \frac{l_1}{l_3}(p_1 + L_{13}b_3) + \frac{l_2}{l_3}(p_1' + L_{43}b_3) + L_{53}b_3 - 2p_1 + s_1' \\ &= -\frac{e(\cos f_i + e\cos 2f_i)}{(1 + e\cos f_i)^2}p_1 + \frac{e\sin f_i}{(1 + e\cos f_i)}p_1' + s_1' + \frac{eb_3}{(1 + e\cos f_i)^2} \end{aligned} \tag{6.22}$$

It should be noted that the apparent zero-eccentricity singularity in (6.18) is removed by the e multiplier in (6.22). The quantity Δ specifies the correction to the initial conditions required to negate secular growth arising from second-order differential gravity. Consequently,

$$\Delta x' = -\frac{l_2}{l_2^2 + l_3^2}\left[l_1 x(f_i) + l_2 x'(f_i) + l_3 y'(f_i)\right] \tag{6.23a}$$

$$\Delta y' = -\frac{l_3}{l_2^2 + l_3^2}\left[l_1 x(f_i) + l_2 x'(f_i) + l_3 y'(f_i)\right] + \epsilon\Delta \tag{6.23b}$$

To convert this to initial dimensional relative position and velocity, (ξ_i, ϑ_i, ζ_i, $\dot{\xi}_i$, $\dot{\vartheta}_i$, $\dot{\zeta}_i$), the following transformation may be used:

$$\begin{Bmatrix} \xi_i \\ \vartheta_i \\ \zeta_i \end{Bmatrix} = \frac{\varrho_0}{(1 + e\cos f_i)} \begin{Bmatrix} x_i \\ y_i \\ z_i \end{Bmatrix} \tag{6.24a}$$

$$\begin{Bmatrix} \dot{\xi}_i \\ \dot{\vartheta}_i \\ \dot{\zeta}_i \end{Bmatrix} = \varrho_0\sqrt{\frac{\mu}{p^3}}(1 + e\cos f_i) \begin{Bmatrix} x_i' \\ y_i' \\ z_i' \end{Bmatrix} + \varrho_0\sqrt{\frac{\mu}{p^3}} e\sin f_i \begin{Bmatrix} x_i \\ y_i \\ z_i \end{Bmatrix} \tag{6.24b}$$

6.3.3 Epoch at Periapsis/Apoapsis

The expressions are simplified greatly if it is assumed that $f_i = 0$ or $f_i = \pi$. At these values of f_i, $l_2 = 0$. The condition for periodicity in the linearized field reduces to:

$$y'_{0_i} = -\frac{(2 \pm e)}{(1 \pm e)} x_{0_i} \tag{6.25}$$

where the positive and negative signs denote $f_i = 0$ and $f_i = \pi$, respectively. These are obtained in an equivalent fashion by Inalhan et al. (2002). Since $l_2 = 0$, it is now unnecessary to evaluate p_1'. From the expressions for L_0, Λ_{c_k} and Λ_{s_k} that are presented in the appendix, it is observed that:

$$\begin{aligned} p_1(0) &= -\frac{1}{(1+e)}\left(\Lambda_0 + \sum_{k=1}^{5}\Lambda_{c_k}\right) \qquad (6.26a) \\ &= \frac{1}{(1+e)}\left[\frac{1}{4}{\rho_3}^2\cos 2\,\phi_0 - \frac{1}{4}{\rho_1}^2\left(5\,e + e^2 + 2\right)\cos 2\,\psi_0\right. \\ &\quad \left. -\rho_1\rho_2\,(3+e)\cos\psi_0 + \frac{3}{2}{\rho_1}^2 - \frac{1}{4}{\rho_1}^2 e^2 + \frac{3}{4}{\rho_3}^2 + \frac{3}{2}{\rho_2}^2\right] \end{aligned}$$

$$
\begin{aligned}
p_1(\pi) &= \frac{1}{(1-e)}\left(\Lambda_0 + \sum_{k=1}^{5}(-1)^k \Lambda_{c_k}\right) \qquad (6.26b)\\
&= \frac{1}{(1-e)}\left[\frac{1}{4}\,{\rho_3}^2 \cos 2\,\phi_0 - \frac{1}{4}\,{\rho_1}^2\left(-5\,e + e^2 + 2\right)\cos 2\,\psi_0\right.\\
&\quad \left. +\rho_1\rho_2\,(3-e)\cos\psi_0 + \frac{3}{2}\,{\rho_1}^2 - \frac{1}{4}\,{\rho_1}^2 e^2 + \frac{3}{4}\,{\rho_3}^2 + \frac{3}{2}\,{\rho_2}^2\right]
\end{aligned}
$$

By substituting p_1, $s_1' = E_1 + 2E_2 + 3E_3$ and b_3 in (6.22), the initial condition correction is:

$$
\begin{aligned}
y_{1_i}' &= \frac{1}{4}\,\frac{(e^2 \mp 2\,e - 4)\,{\rho_1}^2}{1 \pm e} - \frac{1}{4}\,\frac{(2 \pm e)}{(1 \pm e)}\left(2\rho_2^2 + \rho_3^2\right) \mp \frac{1}{4}\,\frac{e{\rho_3}^2\cos 2\,\phi_0}{1 \pm e}\\
&\quad -\frac{1}{4}\,\frac{{\rho_1}^2\,(3\,e^2 \pm 8\,e + 6)\cos 2\,\psi_0}{1 \pm e} - \frac{\rho_1\rho_2\,(2\,e \pm 3)\cos\psi_0}{1 \pm e} \qquad (6.27)
\end{aligned}
$$

6.3.4 Second-Order Analytical Expressions for Relative Motion

Since the the choice of the constants b_1, b_2, and b_4 is arbitrary, they may be chosen to yield a suitable second-order equation for relative motion. Equation (6.15b) is now reconsidered. Upon substituting (6.18) in (6.15b), it can be shown that:

$$
\begin{aligned}
y_1(f) &= (-2b_1 + Q_1 + E_1)\sin f + \left(-\frac{eb_1}{2} + Q_2 + E_2\right)\sin 2f + (Q_3 + E_3)\sin 3f\\
&\quad + \left(2b_2 + \overline{Q}_1 + F_1\right)\cos f + \left(\frac{eb_2}{2} + \overline{Q}_2 + F_2\right)\cos 2f + (\overline{Q}_3 + F_3)\cos 3f\\
&\quad + \left(\frac{eb_2}{2} + b_4 + \overline{Q}_0\right) \qquad (6.28)
\end{aligned}
$$

It is observed that $Q_3 = -E_3$ and $\overline{Q}_3 = -F_3$. The values of b_1, b_2, and b_4 can be chosen such that the coefficients of $\sin f$ and $\cos f$, and the constant term are zero. In this event,

$$
\begin{aligned}
b_1 &= \frac{1}{2}\,(Q_1 + E_1) \qquad (6.29a)\\
b_2 &= -\frac{1}{2}\left(\overline{Q}_1 + F_1\right) \qquad (6.29b)
\end{aligned}
$$

$$b_4 = -\overline{Q}_0 - \frac{eb_2}{2} \tag{6.29c}$$

Consequently,

$$\begin{aligned} y_1(f) &= \left(-\frac{eQ_1}{4} - \frac{eE_1}{4} + Q_2 + E_2\right)\sin 2f + \left(-\frac{e\overline{Q}_1}{4} - \frac{eF_1}{4} + \overline{Q}_2 + F_2\right)\cos 2f \\ &= -\frac{e^2}{8}\rho_1^2 \sin 2f + \frac{e}{4}\rho_1\rho_2 \sin(2f+\psi_0) - \frac{1}{8}(2-e^2)\rho_1^2 \sin(2f+2\psi_0) \\ &\quad -\frac{1}{4}\rho_3^2 \sin(2f+2\phi_0) \end{aligned} \tag{6.30}$$

Now, (6.15a) is considered, after the removal of secular terms. In this case,

$$\begin{aligned} x_1(f) &= b_1\cos f\,(1+e\cos f) + b_2 \sin f\,(1+e\cos f) \\ &\quad +G_1 \sin f + G_2 \sin 2f + G_3 \sin 3f \\ &\quad +\frac{1}{(1+e\cos f)}\left[H_0 + (H_1 - b_3)\cos f + H_2 \cos 2f\right. \\ &\quad \left. +H_3 \cos 3f + H_4 \cos 4f\right] \end{aligned} \tag{6.31}$$

It can be shown that

$$\begin{aligned} &\frac{1}{(1+e\cos f)}\left[H_0 + (H_1 - b_3)\cos f + H_2\cos 2f + H_3\cos 3f + H_4\cos 4f\right] \\ &= N_1\cos f + N_2 \cos 2f + N_3 \cos 3f \end{aligned} \tag{6.32}$$

where $N_1 = -Q_1/2$, $N_2 = -Q_2$, and $N_3 = -3Q_3/2$. It follows that:

$$\begin{aligned} x_1(f) &= \frac{eb_1}{2} + (b_1+N_1)\cos f + (b_2+G_1)\sin f + \left(\frac{eb_1}{2} + N_2\right)\cos 2f \\ &\quad + \left(\frac{eb_2}{2} + G_2\right)\sin 2f + N_3\cos 3f + G_3 \cos 3f \\ &= -\frac{1}{8}\left[\left(4-e^2\right)\rho_1^2 + 4\rho_2^2 + 2\rho_3^2\right] - \frac{e}{4}\rho_1\rho_2\cos\psi_0 - \frac{e^2}{8}\rho_1^2\cos 2\psi_0 \\ &\quad -\frac{3}{2}\rho_1\rho_2\cos(f+\psi_0) - \frac{3e}{8}\rho_1^2\cos(f+2\psi_0) - \frac{e}{4}\,\rho_1\,\rho_2\cos\left(2f+\psi_0\right) \\ &\quad +\frac{e^2}{8}\,{\rho_1}^2\cos 2f - \frac{1}{8}(4+e^2)\,{\rho_1}^2\cos\left(2f+2\psi_0\right) + \frac{1}{4}\,{\rho_3}^2\cos\left(2f+2\phi_0\right) \end{aligned}$$

$$-\frac{e}{8}\rho_1^2\cos(3f+2\psi_0) \tag{6.33}$$

The analytical solution for a relative orbit near a Keplerian orbit, accounting for second-order terms, is thus given by (6.4), with $x_0(f)$, $y_0(f)$, and $z_0(f)$ given by (3.32), and $x_1(f)$, $y_1(f)$, and $z_1(f)$ by (6.33), (6.30), and (6.12), respectively.

6.4 Periodic Orbits and the Energy-Matching Condition

Two spacecraft in Keplerian elliptic orbits will have periodic relative motion if the total energy $\mathcal{E}$ of each spacecraft (and consequently, the semi-major axis of each spacecraft) is the same. Denoting the quantities of the Deputy with subscript 'D' and those of the Chief with subscript 'C', the *vis-viva* equation (Battin 1999, chap. 3) for each spacecraft leads to the following condition for periodic relative motion:

$$\begin{aligned}\Delta\mathcal{E}(\xi,\vartheta,\zeta,\dot\xi,\dot\vartheta,\dot\zeta) &\triangleq \mathcal{E}_D-\mathcal{E}_C\\ &= -\left(\frac{\mu}{2a_D}-\frac{\mu}{2a_c}\right)=\left(\frac{v_D^2}{2}-\frac{\mu}{r_D}\right)-\left(\frac{v_C^2}{2}-\frac{\mu}{r_C}\right)\\ &= 0\end{aligned} \tag{6.34}$$

Using $\mathbf{r}_D=(r+\xi)\mathbf{i}_r+\vartheta\mathbf{i}_\theta+\zeta\mathbf{i}_h$, and $\mathbf{v}_D=(\dot r+\dot\xi-\dot\theta\vartheta)\mathbf{i}_r+(\dot\vartheta+\dot\theta\xi+\dot\theta r)\mathbf{i}_\theta+\dot\zeta\mathbf{i}_h$, and normalizing these quantities in the same manner as the TH equations, (6.34) can be rewritten as:

$$\begin{aligned}\Delta\mathcal{E}(\boldsymbol{\rho},\boldsymbol{\rho}') &= \frac{(2+3ec_f+e^2)}{(1+ec_f)}x+es_fx'+(1+ec_f)y'\\ &\quad+\frac{\epsilon}{2(1+ec_f)}\Big[-(1-e^2)x^2+(2+3ec_f+e^2)y^2+(1+ec_f+e^2s_f^2)z^2\\ &\quad+(1+ec_f)^2(x'^2+y'^2+z'^2)+2es_f(1+ec_f)(xx'+yy'+zz')\\ &\quad+2(1+ec_f)^2(xy'-yx')\Big]+\sum_{n=2}^{\infty}(-1)^n\epsilon^n\rho^{n+1}P_{n+1}\left(\frac{x}{\rho}\right)=0\end{aligned} \tag{6.35}$$

where c_f and s_f denote the cosine and sine of f, respectively. If terms of $\mathcal{O}(\epsilon)$ and higher are neglected, then (6.35) is exactly the same as (3.27). Appending the correction scheme developed in this chapter, to the initial conditions leads to $\Delta\mathcal{E}(\boldsymbol{\rho}, \boldsymbol{\rho}') = \mathcal{O}(\epsilon^2)$. This may be observed by using (6.27), and setting $f = 0$ in (6.35). Consequently,

$$\Delta\mathcal{E} \approx \frac{\mu}{2a^2}\Delta a \approx \varrho_0 a(1-e^2)\sqrt{\frac{\mu}{p^3}}^2 \epsilon^2 \tag{6.36a}$$

$$\Delta a = \frac{2\varrho_0^3}{a^2(1-e^2)^4} \tag{6.36b}$$

The effect of eccentricity on the semi-major axis difference is thus clearly evident.

The formation-keeping problem may be posed by appending $\Delta\mathcal{E}(\boldsymbol{\rho}, \boldsymbol{\rho}') = 0$ as a constraint to a cost function comprising velocity increments. In Gurfil (2005b) it is shown that instead of expanding the period-matching condition in terms of Legendre polynomials, the velocity increments can be solved for the complete nonlinear system analytically. This is possible because the relative velocity terms appear only up to the second order in (6.35).

6.5 Drift Measurement

To measure the efficacy of the initial condition corrections developed in this chapter, an index is desired that captures secular drift and periodic motion behavior. Unlike the solutions to the linear, autonomous HCW equations, circular relative orbits in the general elliptic case cannot be obtained. Consequently, a new measure of deviation from the nominal solution is desired, which can be used to compare the results in this chapter, with existing results in the literature. Therefore, the following measure of

error is defined:

$$\delta(t) \triangleq \left[\frac{1}{t}\int_0^t \left[\rho(t) - \rho_p(t)\right]^2 \, dt\right]^{\frac{1}{2}} \tag{6.37}$$

where $\rho = \sqrt{(x^2 + y^2 + z^2)}$ and $\rho_p = \sqrt{(x_p^2 + y_p^2 + z_p^2)}$. The advantage of using this function is in its behavior in the presence of various forms of error. Phase, frequency or amplitude errors lead to a constant value of $\delta(t)$ as t increases, as can be shown by taking $\rho_p(t) = A\sin\omega t$, and $\rho(t) = (A + \varepsilon_1)\sin\left[(\omega + \varepsilon_2)t + \varepsilon_3\right]$, where $\varepsilon_{1\ldots3}$ are constant errors. Then it can be shown that

$$\lim_{t\to\infty} \delta = \left[A^2 + \frac{1}{2}\varepsilon_1^2 + A\varepsilon_1\right]^{1/2} \tag{6.38}$$

the term A^2 arises due to frequency and phase errors, while the rest of the terms arise due to amplitude errors. Therefore, as long as the function δ is observed to approach a constant value, the solution $\rho(t)$ is considered bounded. However, a secular drift from the nominal solution will lead to an increasing $\delta(t)$.

6.6 Numerical Simulations

6.6.1 Periodicity Condition

The efficacy of the initial condition result derived is demonstrated in this section. All simulations are performed by integrating the sixth-order ECI system of equations for each satellite. Furthermore, the periapsis for all examples is kept constant at $r_p = 7,100\,\text{km}$, so that a can be obtained for any given e from the relation $a = r_p/(1 - e)$. The purpose of this approach is to ensure that the satellite never approaches too near the surface of the Earth, for very high eccentricities.

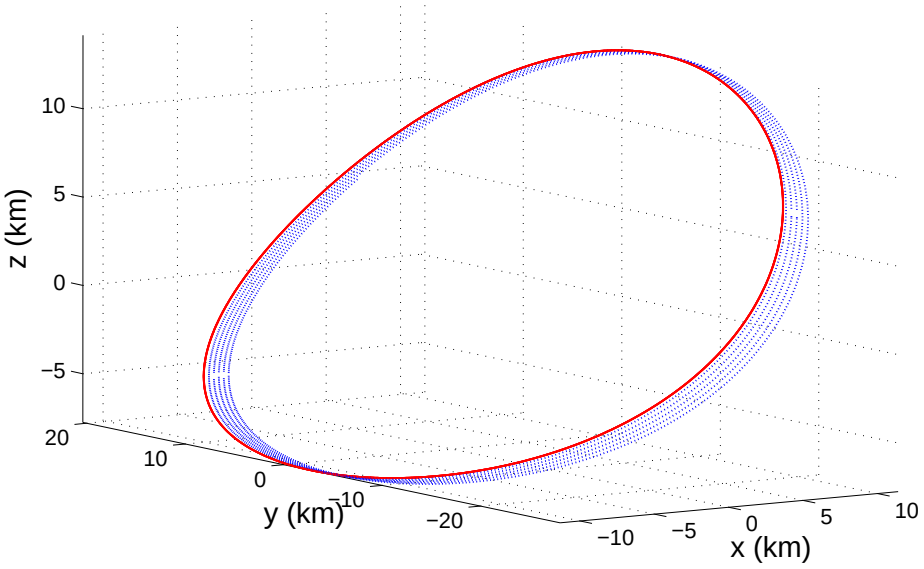

Fig. 6.1 Corrected and Uncorrected Relative Orbit, $e = 0.3$, $f_i = 105°$

First, the results derived will be used to set up a periodic relative orbit at an arbitrary epoch. For convenience, nondimensional units are chosen, although the simulations are based upon dimensional coordinates with time as the independent variable. The initial true anomaly, orbit size, and eccentricity, are chosen as $f_i = 105°$, $e = 0.3$, $\varrho_0 = 10\,\text{km}$, respectively. The initial values of the states of the Deputy satellite, denoted by $\mathbf{x}_i$, are chosen from the HCW initial conditions by setting $e = 0$, $\rho_1 = \rho_3 = 1$, $\rho_2 = 0$, and $\psi_0 = \phi_0 = 30°$ in (3.32). Therefore, $\mathbf{x}_{0_i} = \{0.5\ 1.732\ 0.5\ 0.866\ -1\ 0.866\}^\top$ (nondimensional). Equations (6.10) can be used to obtain their values for a periodic orbit. Upon correction

$$x'_{0_i} = 0.762, \quad y'_{0_i} = -1.331$$

By using the formulae derived, the correction required to negate secular drift induced by second-order differential gravity is found to be $y'_{1_i} = -2.386$. The trajectory with

and without this correction is shown in Figure 6.1. The broken blue line indicates the trajectory without the correction, and considerable drift can be seen after 5 orbits. The solid red line indicates that the corrected trajectory effectively accounts for the second-order differential gravity terms and remains bounded.

To analyze the extent of efficiency of the correction developed, various cases are drawn from existing works in the literature. The following cases assume epoch at $f_i = 0$. First, comparisons are made with the eccentricity/nonlinearity correction from Vaddi et al. (2003). A reference orbit with $e = 0.05$ is chosen with $\varrho_0 = 10\,\text{km}$. The initial conditions are chosen such that $\psi_0 = \phi_0 = 0^\circ$, $\rho_1 = 2\rho_3 = 1$, and $\rho_2 = 0$. Figure 6.2a shows the relative orbit using Hill's initial conditions (without eccentricity and/or nonlinearity conditions), and using the correction developed in this chapter. The broken line indicates the propagation using the HCW conditions, for a period of 20 orbits, and it is evident that a large amount of drift is present. However, by using the corrected initial conditions, the orbit shows negligible deviation even after 20 orbits. Figure 6.2b shows the percentage drift calculated by using (6.37). It is observed that the uncorrected condition shows about 80% error, which is also directly observed from Figure 6.2a. By using the correction for nonlinearity and eccentricity developed in Vaddi et al. (2003), this error is reduced to 10% (correction 1). These errors agree with those from Vaddi et al. (2003), for similar initial conditions. By using (6.27), this error is approximately 0.2% (correction 2).

Next, a comparison is made for a reference orbit with moderate eccentricity, where the result obtained by Vaddi et al. (2003) fails, but where the zeroth-order eccentricity correction, also presented by Inalhan et al. (2002), is expected to be valid. Figure 6.3a shows the relative orbit for $e = 0.2$ and $\varrho_0 = 10\,\text{km}$. The Deputy's orbit is initiated using the periodic equations in (3.32), setting $\rho_1 = 0.5$, $\rho_2 = 0.1$, $\rho_3 = 1.2$, and

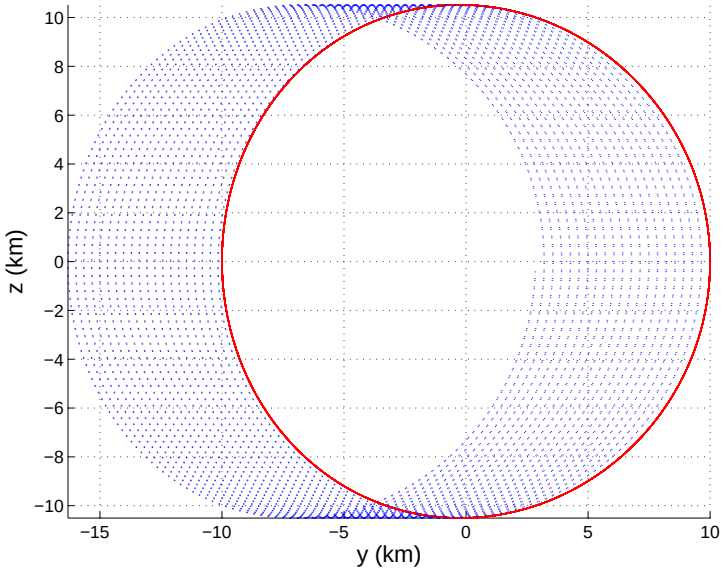

(a) Relative Motion

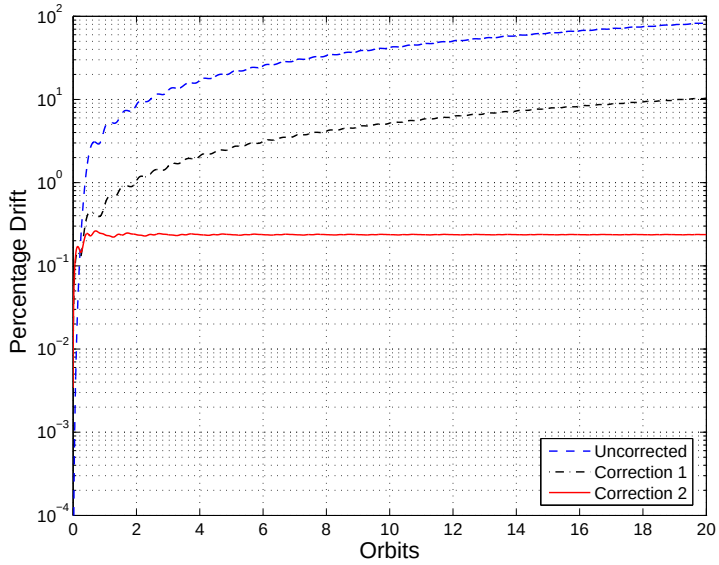

(b) Drift from Nominal Solution

Fig. 6.2 Relative Motion with Corrected and Uncorrected Initial Conditions, $e = 0.05,\ f_i = 0$

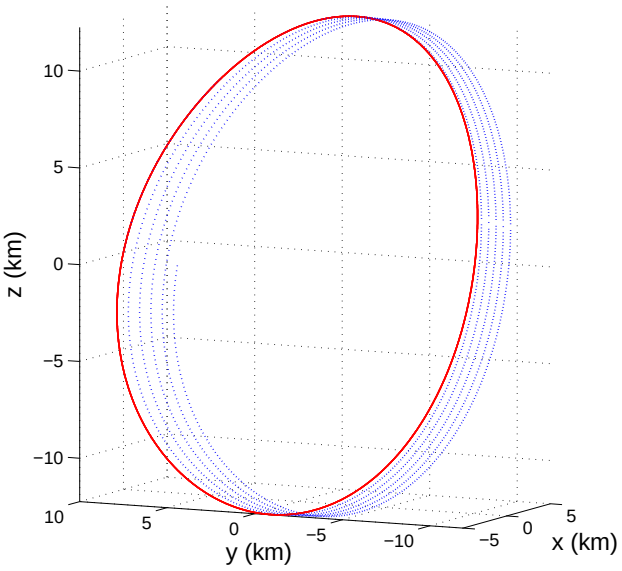

(a) Relative Motion

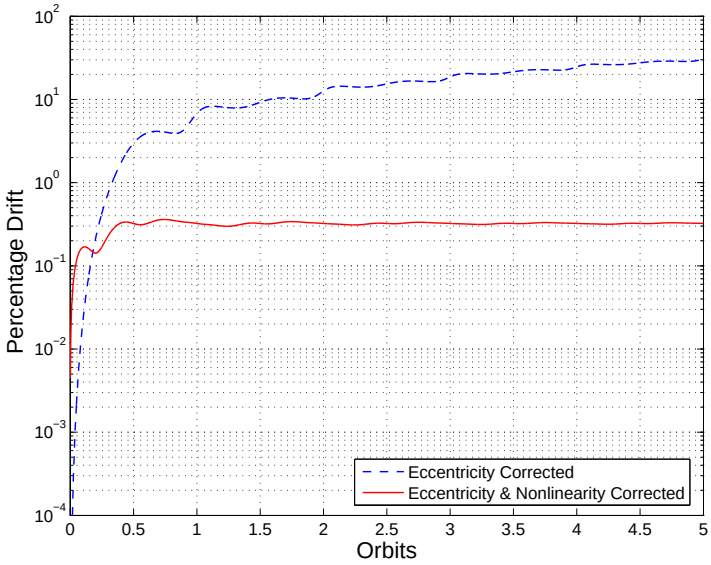

(b) Drift from Nominal Solution

Fig. 6.3 Relative Motion with Corrected and Uncorrected Initial Conditions, $e = 0.2,\ f_i = 0$

$\psi_0 = \phi_0 = 0°$. It is evident that these initial conditions show secular drift due to nonlinear differential gravity, as indicated by the broken line. However, by employing the correction derived, the drift is negligible even after 5 orbit periods, as indicated by the solid line. A study of the drift as shown in Figure 6.3b shows that the nonlinearity correction results in an error of approximately 0.3% of the orbit size, as opposed to the linear condition, which shows approximately 12% drift and continues to increase.

Figure 6.4a shows an orbit with Chief's eccentricity selected as $e = 0.8$, all other values kept the same as in the previous case. In this case it is observed that the initial conditions that satisfy the linearized periodicity condition do not even lead to bounded motion, and the relative motion quickly diverges within one orbit period in the presence of nonlinear terms, as indicated by the broken line. The solid line shows that by using the correction developed in this chapter, periodicity is maintained. As shown in Figure 6.4b, the error after the correction is approximately 2% of the orbit size. Keeping in mind that the error functions for the corrected solution, as depicted in Figures 6.2b, 6.3b and 6.4b, approach constant values, these values only indicate the amplitude error as a result of the correction. The orbits themselves show negligible drift.

6.6.2 Accuracy of the Analytical Solution

The second-order analytical solution which has been developed in this chapter, is tested against numerical integration in a fully nonlinear differential gravity environment. The reference orbit has $e = 0.4$ and $a = 12,000\,\text{km}$. The relative orbit is of dimension $\varrho_0 = 20\,\text{km}$, and the formation is initiated at $f_i = 30°$. The parameters for the relative orbit are: $\rho_1 = 0.4782$, $\rho_2 = 0.1729$, $\rho_3 = 0.9165$, $\psi_0 = -0.5236$

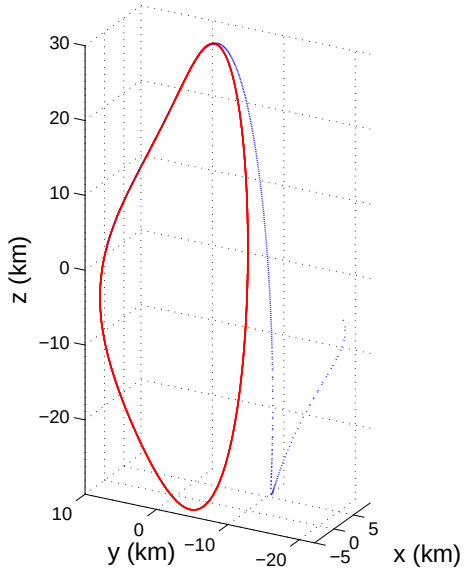

(a) Relative Motion

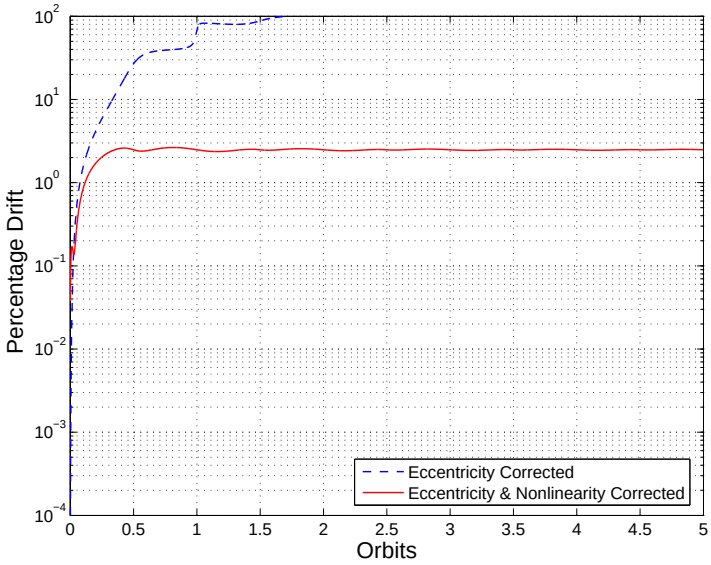

(b) Drift from Nominal Solution

Fig. 6.4 Relative Motion with Corrected and Uncorrected Initial Conditions, $e = 0.8,\ f_i = 0$

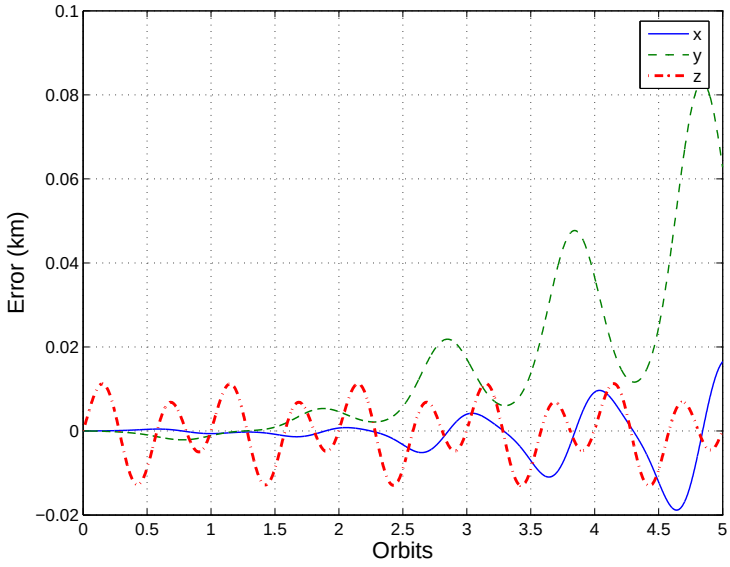

Fig. 6.5 Accuracy of the Analytical Solution

and $\phi_0 = -0.5136$. The errors between integrated relative position, and the relative position as predicted by the second-order analytical equations, is shown in Figure 6.5. It is observed that after 5 orbits, the error in position prediction is within 100m. This is an error of less than 1%. Growth is observed in the error due to the contribution of terms of third and higher order.

6.6.3 Energy-Matching Criterion

The exact periodicity condition for formation flight is $\Delta a = 0$, or when the time periods of the Chief and Deputy are equal. However, the periodicity conditions based on the unperturbed TH equations and the perturbed TH equations, only approximately satisfy the equation $\Delta a = 0$. The extent to which this condition is satisfied can be measured if the initial conditions of the Chief's and Deputy's

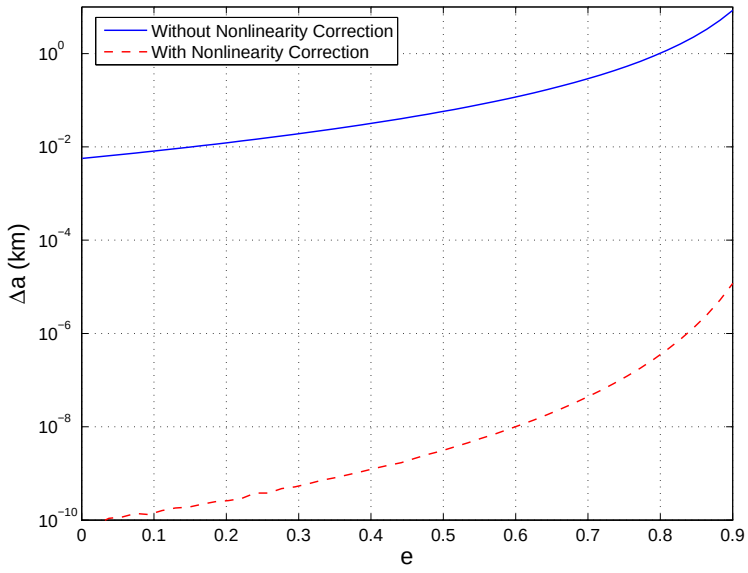

Fig. 6.6 Energy-Matching Criterion Satisfaction using Corrected and Uncorrected Initial Conditions

states in the local reference frame are converted to their respective inertial positions and velocities, and then to their respective orbital elements. A comparison of the uncorrected and nonlinear-corrected initial conditions is shown in Figure 6.6. These results are for a reference orbit with $a = 40,000\,\text{km}$, and $\varrho_0 = 10\,\text{km}$, with epoch at $f_i = 0$. It is observed that even if the Chief's eccentricity is 0.9, the difference between the Deputy and Chief semi-major axes is of the order of millimeters. Given the limitations of navigation technology, this is almost exact. In contrast, the uncorrected initial conditions lead to semi-major axis differences of hundreds of meters even for intermediate eccentricities, which lead to considerable drift in relative motion.

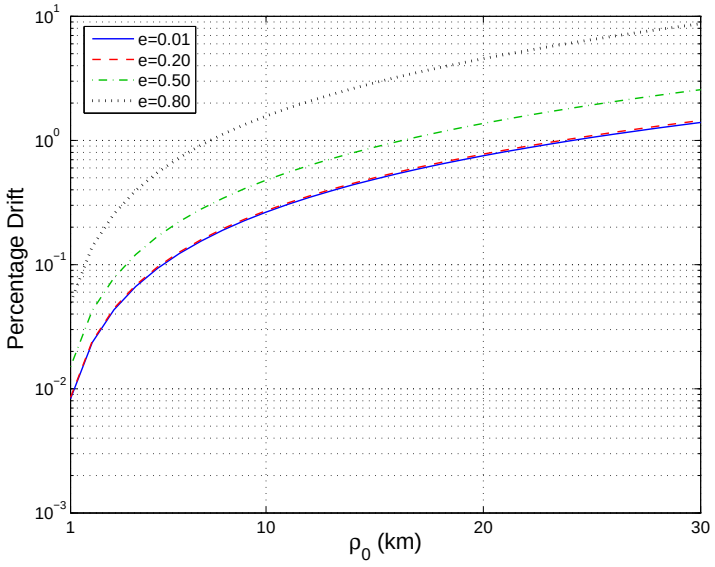

Fig. 6.7 Effect of Nonlinearity and Eccentricity on Errors

6.6.4 Effect of Eccentricity and Nonlinearity on Boundedness

It is now desired to study the efficacy of the correction under the effect of increasing ϱ_0. This is shown in Figure 6.7. These simulations were carried out for 10 time periods of the reference, for a variety of eccentricity values, as indicated. The figure shows that for ϱ_0 up to 30 km, and even with moderate values of eccentricity, the error is less than 1%. However, for high eccentricities, such as those greater than 0.8, the error is shown to increase markedly. This is due to the fact that the combined effect of large ϱ_0 and large e leads to ϵ^2 and ϵ being of the same order, and thus third-order terms in (6.3) are no longer negligible in comparison with the second-order terms.

6.7 Summary

Phase space initial conditions for periodic relative motion have been developed for an orbit with arbitrary eccentricity, by treating second-order nonlinear differential gravity terms as perturbations to the Tschauner-Hempel equations. By identifying only those terms that contribute to secular growth in relative motion, a condition for ensuring periodic motion is easily obtained. These initial conditions are shown to work remarkably well under the most general conditions, including those with very high eccentricities, and can serve as excellent guesses for initiating a numerical procedure for matching the semi-major axes of the two satellites by correcting one of the relative motion initial conditions. The removal of secular growth terms leads to the formulation of analytical, second-order relative motion equations, that very accurately model relative orbits in terms of its parameters. These expressions can be used for stationkeeping algorithms and will require less fuel for relative orbit maintenance.

CHAPTER VII

AVERAGE RELATIVE POSITION AND VELOCITY IN HILL'S FRAME DUE TO OBLATENESS EFFECTS

7.1 Introduction

In this chapter, expressions for averaged relative motion are derived. Relative motion is examined in the linear sense, but with oblateness effects due to J_2 accounted for. Instead of the state-space approach that has been followed in the previous chapters, the geometric method is found useful here.

It is first necessary to distinguish between the *average* of a function of the Delaunay elements, and the *mean* function of the Delaunay elements. Let $\boldsymbol{\alpha}$ be any osculating element set describing an orbit, and $\overline{\boldsymbol{\alpha}}$ be the corresponding mean element set. The osculating elements corresponding to $\overline{\boldsymbol{\alpha}}$ are obtained using a first-order transformation due to Brouwer (1959). Let $\kappa(\boldsymbol{\alpha})$ be any function of the orbital elements. Then, in general,

$$\overline{\kappa(\boldsymbol{\alpha})} \neq \kappa(\overline{\boldsymbol{\alpha}}) \tag{7.1}$$

The value of the operation on the LHS of (7.1) is the average of the function, and the value of the operation on the RHS is a function of the mean. Since the latter is simply obtained by substituting mean elements in place of the corresponding osculating elements, it is easier to calculate, but physically less meaningful than the former.

7.2 Averaged Relative Motion

A complete description of generating functions in the Hamiltonian framework can be found in Goldstein (1965). As shown by Brouwer (1959), if the potential due J_2 is treated as a perturbation to the the two-body Hamiltonian using the Delaunay element set given by (2.3), then a series of canonical transformations result in the mean elements, of which $\overline{L}$, $\overline{G}$, and $\overline{H}$ are constants, and $\bar{l}$, $\bar{g}$, and $\bar{h}$ are linear functions of time. The inverse transformation to obtain short- and long-periodic variations, is obtained by the use of generating functions that are also functions of the mean elements. Consequently, the osculating elements can be obtained from the mean elements.

The average of the function, including only short-periodic variations due to J_2, is calculated as follows:

$$\overline{\kappa(\mathbf{oe})} = \kappa(\overline{\mathbf{oe}}) + \frac{1}{2\pi}\int_0^{2\pi} \kappa_{\mathrm{sp}}(\overline{\mathbf{oe}})\, dl \tag{7.2}$$

where

$$\kappa_{\mathrm{sp}}(\overline{\mathbf{oe}}) = -J_2 R_\oplus^2 \left(\kappa, W_{\mathrm{sp}_1} + W_{\mathrm{sp}_2}\right) \tag{7.3}$$

where $(\cdot,\cdot)$ denotes the Lie bracket operator, and W_{sp_1} and W_{sp_2} are the short-periodic generating functions, as shown in Brouwer (1959):

$$W_{\mathrm{sp}_1} = -\frac{1}{4\overline{G}^3}\left(1 - 3\frac{\overline{H}^2}{\overline{G}^2}\right)\left(\overline{f} - \bar{l} + \overline{e}\sin\overline{f}\right) \tag{7.4a}$$

$$W_{\mathrm{sp}_2} = \frac{3}{8\overline{G}^3}\left(1 - \frac{\overline{H}^2}{\overline{G}^2}\right)\left[\sin(2\overline{f} + 2\overline{g}) + \overline{e}\sin(\overline{f} + 2\overline{g}) + \frac{\overline{e}}{3}\sin(3\overline{f} + 2\overline{g})\right] \tag{7.4b}$$

Of interest is the averaged relative position and velocity, due to J_2 effects. In this case,

short-periodic perturbations are accomodated by averaging them over one orbit. For a limited number of orbits, long-periodic perturbations exhibit themselves as secular growth of $\mathcal{O}(J_2^2)$, and are therefore neglected in this chapter.

The non-dimensional state vector for relative motion in a Local-Vertical Local-Horizontal frame, with origin on the chief satellite, is redefined as $\mathbf{x} = \{\xi/\overline{a}\ \vartheta/\overline{a}\ \zeta/\overline{a}\ \dot{\xi}/(\overline{n}\,\overline{a})\ \dot{\vartheta}/(\overline{n}\,\overline{a})\ \dot{\zeta}/(\overline{n}\,\overline{a})\}^\top$, where the relative position coordinates along the radial, along-track, and out-of-plane directions, are scaled by the mean semimajor axis of the chief, and the relative velocities are scaled by the velocity-like quantity $\overline{n}\,\overline{a}$, where $\overline{n}$ is the mean motion using mean elements, given by $\sqrt{(\mu/\overline{a}^3)}$. The vector $\overline{\mathbf{x}}$ denotes the averaged value of the state vector. Consequently, one seeks a description of the form:

$$\overline{\mathbf{x}} = (\mathbf{P}_0 + \overline{J}\mathbf{P}_J)\boldsymbol{\delta}\overline{\boldsymbol{\alpha}\mathbf{e}} \tag{7.5}$$

where $\overline{J} = J_2(R_\oplus/\overline{p})^2$, $\mathbf{P}_0$ is the transformation matrix corresponding to the non-J_2 problem, and $\mathbf{P}_J = \mathcal{O}(J_2)$ is a correction that is added to calculate the averaged relative motion. The advantage of this approach is that mean elements of the chief, and mean differential orbital elements can be used everywhere, to yield concise results.

A nonsingular element set is chosen to describe the orbit: $\boldsymbol{\alpha}\mathbf{e} = \{a\ \lambda_0\ i\ q_{10}\ q_{20}\ h_0\}^\top$. As discussed in Chapter II, λ is used instead of θ, because by using mean elements, the former is a linear function of time. The subscript '0' is used to denote the value of the respective quantity at epoch. The differential orbital element set is defined as, $\boldsymbol{\delta}\boldsymbol{\alpha}\mathbf{e} \triangleq \{\delta a/a\ \delta\lambda_0\ \delta i\ \delta q_{10}\ \delta q_{20}\ \delta h_0\}^\top$.

From the geometric description of relative motion (Gim and Alfriend 2003), it can be

shown that:

$$\xi = \delta r \tag{7.6a}$$

$$\vartheta = r(\delta\theta + \delta h \cos i) \tag{7.6b}$$

$$\zeta = r(\delta i \sin\theta - \delta h \sin i \cos\theta) \tag{7.6c}$$

$$\dot{\xi} = \delta v_r \tag{7.6d}$$

$$\dot{\vartheta} = \delta v_\theta + v_r(\delta\theta + \delta h \cos i) - v_h(\delta i \cos\theta + \delta h \sin i \sin\theta) - \omega_h \xi + \omega_r \zeta \tag{7.6e}$$

$$\dot{\zeta} = \delta v_h + v_r(\delta i \sin\theta - \delta h \sin i \cos\theta) + v_\theta(\delta i \cos\theta + \delta h \sin i \sin\theta) - \omega_r \vartheta + \omega_\theta \xi \tag{7.6f}$$

where r is the radial distance of the chief, v_r, v_θ, and v_h are the components of the chief's velocity in the LVLH frame, and ω_r, ω_θ, and ω_h are the components of the rotation rate of the LVLH frame. By using (3.66), it can be shown that:

$$r = \frac{a\eta^2}{\alpha} \tag{7.7a}$$

$$\omega_r = \dot{h}\sin i \sin\theta + \dot{i}\cos\theta = \mathcal{O}(J_2) \tag{7.7b}$$

$$\omega_\theta = \dot{h}\sin i \cos\theta - \dot{i}\sin\theta = \mathcal{O}(J_2) \tag{7.7c}$$

$$\omega_h = \frac{n\alpha^2}{\eta^3} \tag{7.7d}$$

$$v_r = \frac{na\beta}{\eta} \tag{7.7e}$$

$$v_\theta = r\omega_h = \frac{na\alpha}{\eta} \tag{7.7f}$$

$$v_h = -r\omega_\theta \tag{7.7g}$$

It should be noted from (7.7b) and (7.7c) that mean elements can be used in the expressions for ω_r and ω_θ without significant loss of accuracy, since the short- and long-periodic effects of J_2 will only result in contributions of $\mathcal{O}(J_2^2)$. The other quantities may be expressed as the sum of a function using direct substitution of mean elements,

and short-periodic variations using the generating functions. For example,

$$r = r_{\text{mean}} + \overline{J} r_{\text{sp}} \tag{7.8a}$$

$$r_{\text{mean}} = \frac{\overline{a}\,\overline{\eta}^2}{\overline{\alpha}} \tag{7.8b}$$

$$r_{\text{sp}} = -\overline{a}^2\,\overline{\eta}^2\left(r_{\text{mean}}, W_{\text{sp}_1} + W_{\text{sp}_2}\right) \tag{7.8c}$$

To this end, the following expressions are obtained:

$$r_{\text{sp}} = \overline{a\eta}^2(1-3\cos^2\bar{i})\left(\frac{\overline{\eta}+\overline{\alpha}}{4(1+\overline{\eta})}+\frac{\overline{\eta}}{2\overline{\alpha}}\right)+\frac{\overline{a\eta}^2}{4}\sin^2\bar{i}\,\cos 2\overline{\theta} \tag{7.9a}$$

$$\begin{aligned} w_{h_{\text{sp}}} &= \frac{1}{2}\overline{n}\,(1-3\cos\bar{i}^2)\overline{\alpha}^2\frac{[\overline{\alpha}^2+\overline{\eta\alpha}+2\overline{\eta}(1+\overline{\eta})]}{\overline{\eta}^3(1+\overline{\eta})} \\ &\quad +\frac{1}{4\overline{\eta}^3}\overline{n}\sin^2\bar{i}\,\overline{\alpha}^2(\cos 2\overline{\theta}+2\overline{q}_1\cos\overline{\theta}-2\overline{q}_2\sin\overline{\theta}) \end{aligned} \tag{7.9b}$$

$$v_{r_{\text{sp}}} = -\frac{\overline{a}\,\overline{n}}{4\overline{\eta}(1+\overline{\eta})}(1-3\cos^2\bar{i})\overline{\beta}(\overline{\alpha}^2+\overline{\eta}+\overline{\eta}^2)-\frac{\overline{a}\,\overline{n}}{2\overline{\eta}}\sin^2\bar{i}\,\overline{\alpha}^2\sin 2\overline{\theta} \tag{7.9c}$$

$$\begin{aligned} v_{\theta_{\text{sp}}} &= -\frac{\overline{a}\,\overline{n}}{4\eta(1+\eta)}(1-3\cos^2\bar{i})\overline{\alpha}\,[\overline{\alpha}(\overline{\eta}+\overline{\alpha})+2\overline{\eta}(1+\overline{\eta})] \\ &\quad +\frac{\overline{a}\,\overline{n}}{4\overline{\eta}}\sin^2\bar{i}\,\left[\overline{\alpha}(1+\overline{\alpha})\cos 2\overline{\theta}+2\overline{\alpha}(\overline{q}_1\cos\overline{\theta}-\overline{q}_2\sin\overline{\theta})\right] \end{aligned} \tag{7.9d}$$

$$i_{\text{sp}} = \frac{1}{4}\sin\bar{i}\,\cos\bar{i}\,\left(3\cos 2\overline{\theta}+3\overline{q}_1\cos\overline{\theta}-3\overline{q}_2\sin\overline{\theta}+\overline{q}_1\cos 3\overline{\theta}+\overline{q}_2\sin 3\overline{\theta}\right) \tag{7.9e}$$

$$\begin{aligned} h_{\text{sp}} &= -\frac{3}{2}\cos\bar{i}\,\left(\overline{\theta}-\overline{\lambda}+\overline{\beta}\right) \\ &\quad +\frac{1}{4}\cos\bar{i}\,\left(3\sin 2\overline{\theta}+3\overline{q}_1\sin\overline{\theta}+3\overline{q}_2\cos\overline{\theta}+\overline{q}_1\sin 3\overline{\theta}-\overline{q}_2\cos 3\overline{\theta}\right) \end{aligned} \tag{7.9f}$$

$$\begin{aligned} \theta_{\text{sp}} &= \frac{\overline{\beta}}{2}-\frac{3}{4}(1-5\cos^2\bar{i})(\overline{\theta}-\overline{\lambda})-\frac{1}{4}(1-3\cos^2\bar{i})\frac{\overline{\beta}}{(1+\overline{\eta})}(\overline{\alpha}+4\overline{\eta}+5) \\ &\quad -\frac{1}{4}\cos^2\bar{i}\,(\overline{q}_1\sin 3\overline{\theta}-\overline{q}_2\cos 3\overline{\theta})+\frac{1}{8}(1-7\cos^2\bar{i})\sin 2\overline{\theta} \\ &\quad +\frac{1}{4}(2-5\cos^2\bar{i})(\overline{q}_1\sin\overline{\theta}+\overline{q}_2\cos\overline{\theta}) \end{aligned} \tag{7.9g}$$

A few interesting points are noted here. First, $v_{r_{\text{sp}}} \neq \dot{r}_{\text{sp}}$. Second, the expression for θ_{sp} is more concise than what is provided by Gim and Alfriend (2003). Third, expressions for short-periodic variations in r have appeared in other works. For

example, Kozai (1959) obtained a similar expression as shown above; however, numerical computations show that his expression is incorrect since it fails to remove a bias. The use of Hill's variables by Aksnes (1972) also results in expressions for short-periodic behavior of r and $\dot{r}$. Even though the derivation presented therein is nonsingular (no eccentricity divisor), the relevant expressions are nevertheless written in terms of the classical orbital elements. The expressions in this chapter are written in nonsingular form and use (3.66) for conciseness. A low-eccentricity approximation for the average radius has also been derived by Born et al. (2001). The development of expressions for short-periodic variations in r, v_r, and v_θ is essential to obtain simplified, mean relative position and velocity. The only other alternative is to individually find the average values of the short-periodic variations in all the orbital elements, in their various functional forms, as shown in Gim and Alfriend (2003).

7.3 Special Integrals

It is evident that finding the mean values of expressions involving short-periodic variations, as shown in (7.9), requires the solutions to integrals of the following form:

$$\frac{1}{2\pi}\int_0^{2\pi}(f-l)\,p(f)\,dl, \quad \frac{1}{2\pi}\int_0^{2\pi}\frac{\cos kf}{(1+e\cos f)^2}\,dl, \quad \text{etc.} \tag{7.10}$$

where $p(f)$ is any even or odd 2π-periodic function. In this section, the solutions to these integrals are shown.

The following integral is considered first:

$$I_0 = \frac{1}{2\pi}\int_0^{2\pi}(f-l)\,p(f)\,dl \tag{7.11}$$

Integrals of this form occur when the average of a quantity comprising θ, $\delta\theta$, or δh is

required. Déprit and Rom (1970) noted that closed-form solutions to the indefinite integral corresponding to (7.11) could not be found, and there was a possibility that such a solution does not exist. However, it is shown here that a series solution to the indefinite form of (7.11) involving Bessel functions exists, and in particular, that $I_0 = 0$.

From Battin (1999), the following expansion is presented for $f - l$, known as the equation of the center:

$$f - l = 2\sum_{k=1}^{\infty} \frac{1}{k} \left[\sum_{m=-\infty}^{\infty} J_m(-ke)\varepsilon^{|k+m|} \right] \sin kl \tag{7.12}$$

where $\varepsilon = \sqrt{[(1-\eta)/(1+\eta)]}$, and J_m is the mth-order Bessel function of the first kind. Furthermore, also shown in Battin (1999), is the following:

$$\sin kl = \sum_{j=-\infty}^{\infty} J_j(-ke)\, \sin[(j+k)E] \tag{7.13}$$

Finally, from Kepler's equation,

$$l = E - e\sin E \Rightarrow dl = (1 - e\cos E)\, dE \tag{7.14}$$

The use of (2.1), (7.13), and (7.14) reduces the problem of solving for I_0, to one of solving for the following integral:

$$\int_0^{2\pi} \sin[(j+k)E]\, \widetilde{p}(E)\, (1 - e\cos E)\, dE \tag{7.15}$$

where $\widetilde{p}(E)$ is simply obtained by substituting (2.1) in $p(f)$. It follows that $\widetilde{p}(E)$ is also 2π-periodic. Consequently, it is only necessary to show that:

$$\int_0^{2\pi} \sin \overline{m}E\, \widetilde{p}(E)\, dE = 0, \quad \overline{m} \in \mathbb{Z} \tag{7.16}$$

This is true irrespective of whether $\widetilde{p}$ (or p) is even or odd, as can easily be verified

by integrating the above expression by parts.

Next, a solution is found to integrals of the following type:

$$I_{mk} = \frac{1}{2\pi} \int_0^{2\pi} \frac{\exp(\jmath k f)}{(1 + e\cos f)^m}\, dl \tag{7.17}$$

where $k, m \in \mathbb{Z}$. Integrals of this form are encountered, when the average value of a term comprising the mean radius is required, or when $(1 + e\cos f)$ appears in the denominator of a term. Hoots (1981b) presented solutions to I_{mk}, for specific values of m and k. It is observed that for the derivations in this chapter, it is sufficient to obtain expressions for I_{mk} for $m = 0, 1, 2$, although values of k of upto 9 are required, which were not given by Hoots (1981b). Consequently, a general form for I_{mk} as a function of k is presented here, with $m = 0, 1, 2$. The procedure for obtaining the solution is demonstrated for $m = 2$; for other values the procedure is similar and more straightforward.

The key step in solving these integrals, is the complex change of variable, $\exp(\jmath f) = \chi$, as shown in Chapter III. Also used is the relation $dl = \eta^3\, df/(1 + e\cos f)^2$. After some algebra, it can be shown that:

$$I_{2k} = -\frac{\jmath}{2\pi} \frac{16\eta^3}{e^4} \oint_C \frac{\chi^{k+3}\, d\chi}{(\chi + \varepsilon)^4 (\chi + 1/\varepsilon)^4} \tag{7.18}$$

The integrand in the above expression can be split into partial fractions. Noting that $\varepsilon < 1$ and $1/\varepsilon > 1$, Cauchy's integral theorem is then used to show that:

$$\oint_C \frac{\chi^{k+3}\, d\chi}{(\chi + \varepsilon)} = 2\pi\jmath(-\varepsilon)^{k+3}, \quad \oint_C \frac{\chi^{k+3}\, d\chi}{(\chi + 1/\varepsilon)} = 0 \tag{7.19a}$$

$$\oint_C \frac{\chi^{k+3}\, d\chi}{(\chi + \varepsilon)^2} = 2\pi\jmath(k+3)(-\varepsilon)^{k+2}, \quad \oint_C \frac{\chi^{k+3}\, d\chi}{(\chi + 1/\varepsilon)^2} = 0 \tag{7.19b}$$

$$\oint_C \frac{\chi^{k+3}\, d\chi}{(\chi + \varepsilon)^3} = \pi\jmath(k+3)(k+2)(-\varepsilon)^{k+1}, \quad \oint_C \frac{\chi^{k+3}\, d\chi}{(\chi + 1/\varepsilon)^3} = 0 \tag{7.19c}$$

$$\oint_C \frac{\chi^{k+3}\,d\chi}{(\chi+\varepsilon)^4} = \frac{\pi}{3}\jmath(k+3)(k+2)(k+1)(-\varepsilon)^k, \quad \oint_C \frac{\chi^{k+3}\,d\chi}{(\chi+1/\varepsilon)^4} = 0 \tag{7.19d}$$

Substituting the above equations in (7.18), and noting that $\exp(\jmath kf) = \cos kf + \jmath \sin kf$, the following results are obtained:

$$\frac{1}{2\pi}\int_0^{2\pi} \frac{\cos kf\,dl}{(1+e\cos f)^2} = \frac{1}{6\eta^4}(-\varepsilon)^k\left[k^3\eta^3 + 6k^2\eta^2 + k\eta(15-4\eta^2) + (15-9\eta^2)\right] \tag{7.20a}$$

$$\frac{1}{2\pi}\int_0^{2\pi} \frac{\sin kf\,dl}{(1+e\cos f)^2} = 0 \tag{7.20b}$$

Using the above methodology, the following can also be shown:

$$\frac{1}{2\pi}\int_0^{2\pi} \frac{\cos kf\,dl}{(1+e\cos f)} = \frac{1}{2\eta^2}(-\varepsilon)^k\left[k^2\eta^2 + 3k\eta + (3-\eta^2)\right] \tag{7.21a}$$

$$\frac{1}{2\pi}\int_0^{2\pi} \frac{\sin kf\,dl}{(1+e\cos f)} = 0 \tag{7.21b}$$

and,

$$\frac{1}{2\pi}\int_0^{2\pi} \cos kf\,dl = (-\varepsilon)^k\left[k\eta + 1\right] \tag{7.22a}$$

$$\frac{1}{2\pi}\int_0^{2\pi} \sin kf\,dl = 0 \tag{7.22b}$$

7.4 Average Position and Velocity

Some amount of algebra, performed easily via symbolic computation, is required to obtain the averaged position and velocity. For example, since $r = r_{\text{mean}} + \overline{J} r_{\text{sp}}$, it follows that:

$$\xi = \delta r_{\text{mean}} + \delta\left(\overline{J}\, r_{\text{sp}}\right) \tag{7.23}$$

and consequently,

$$\overline{\xi} = \delta r_{\text{mean}} + \frac{1}{2\pi} \int_0^{2\pi} \delta(\overline{J}\, r_{\text{sp}})\, dl \tag{7.24}$$

From (5.5), δr_{mean} is easily obtained to the first order in differential orbital elements. Additionally, use is made of the functions $g_{1\ldots3}(\theta)$ from Appendix B, to yield the following relation:

$$\delta\theta = g_1(\theta)\, \delta\lambda + g_2(\theta)\, \delta q_1 + g_3(\theta)\, \delta q_2 \tag{7.25}$$

To propagate the mean orbital element differences, the following vector is defined:

$$\widetilde{\mathbf{\Phi}}_{\overline{e}}(t_2, t_1) = \mathbf{P}_e(t_2)\, \overline{\mathbf{\Phi}}_{\overline{e}}(t_2, t_1)\, \mathbf{P}_e^{-1}(t_1) \tag{7.26}$$

where $\overline{\mathbf{\Phi}}_{\overline{e}}$ is the transition matrix for mean elements as given by Gim and Alfriend (2003), and the matrix $\mathbf{P}_e$ is used to scale the semimajor axis difference, and convert from $\delta\theta$ to δl. The non-zero components of $\mathbf{P}_e$ are given by:

$$P_{e_{11}} = 1/a \tag{7.27a}$$

$$P_{e_{22}} = \frac{1}{g_1(\theta)} \tag{7.27b}$$

$$P_{e_{24}} = -\frac{g_2(\theta)}{g_1(\theta)} \tag{7.27c}$$

$$P_{e_{25}} = -\frac{g_3(\theta)}{g_1(\theta)} \tag{7.27d}$$

$$P_{e_{33}} = P_{e_{44}} = P_{e_{55}} = P_{e_{66}} = 1 \tag{7.27e}$$

The inverse matrix is easily obtained by inspection:

$$P_{e_{11}}^{-1} = a \tag{7.28a}$$

$$P_{e_{22}}^{-1} = g_1(\theta) \tag{7.28b}$$

$$P_{e_{24}}^{-1} = g_2(\theta) \tag{7.28c}$$

$$P_{e_{25}}^{-1} = g_3(\theta) \tag{7.28d}$$

$$P_{e_{33}}^{-1} = P_{e_{44}}^{-1} = P_{e_{55}}^{-1} = P_{e_{66}}^{-1} = 1 \tag{7.28e}$$

From (7.5) and (7.26), the following transformation is obtained, that can be used to find the average states in terms of mean elements:

$$\overline{\mathbf{x}} = (\mathbf{P}_0 + \overline{J}\mathbf{P}_J)\,\widetilde{\mathbf{\Phi}}_{\overline{e}}\,\boldsymbol{\delta}\overline{\boldsymbol{\alpha}}_0 \tag{7.29}$$

The matrices $\mathbf{P}_0$ and $\mathbf{P}_J$ are given in Appendix E.

7.5 Numerical Simulations

An example from Gim and Alfriend (2003) is considered, to test the results of this chapter. Consider a reference orbit with the following initial mean orbital elements:

$$\begin{gathered} \overline{a} = 7,091.870\,\text{km}, \quad \overline{\theta}_0 = 3.141596\,\text{rad}, \quad \overline{i} = 1.221521\,\text{rad} \\ \overline{q}_1 = 0.00523, \qquad \overline{q}_2 = 0.001709, \qquad \overline{h} = 0.7853999\,\text{rad} \end{gathered} \tag{7.30}$$

Relative motion is established by selecting the following initial mean differential orbital elements

$$\begin{gathered} \overline{\delta a} = 0.415\,\text{m}, \qquad \overline{\delta\lambda}_0 = -6.195769 \times 10^{-7}\,\text{rad} \\ \overline{\delta q_{1_0}} = 1.601 \times 10^{-7}, \qquad \overline{\delta q_{2_0}} = 3.561 \times 10^{-5} \\ \overline{\delta i} = -7.079055 \times 10^{-5}\,\text{rad} \qquad \overline{\delta h}_0 = 0\,\text{rad} \end{gathered} \tag{7.31}$$

Similar to the procedure in Chapter V, the mean elements of the deputy and chief are converted to osculating elements using Brouwer theory, and then converted to ECI position and velocity. These are used as initial conditions to integrate over the

satellite orbit.

For comparison, three errors are defined. The *osculating* error refers to the error between the states as predicted by the Gim-Alfriend STM. The *mean* error refers to the error between the states obtained by using the transformation matrix $\mathbf{P}_0$, by using mean elements only. This would have the same results as using mean elements in any of the existing STMs that assume a central gravitation field. The *average* error is obtained by adding the correction matrix $\mathbf{P}_J$ to the transformation.

The three errors are shown for the radial, along-track and out-of-plane directions, in Figure 7.1, Figure 7.2, and Figure 7.3, respectively. In these figures, the solid blue line indicates the osculating error over 20 orbits, and these are identical to the results shown in Gim and Alfriend (2003). The broken green line indicates the mean error, and the dashed-dotted red line indicates the error after correction. It is observed that the radial correction is the most beneficial, and this a consequence of the short-periodic correction to the satellite radius, presented in this chapter. It is also observed that the bias is not completely removed, and is also present in the osculating error. This is a consequence of linearization, and can be removed if the higher-order STT developed in Chapter V is used. These figures also show the usefulness of the matrices $\mathbf{P}_0$ and $\mathbf{P}_J$. If a tracking controller design is desired such that short-periodic perturbations due to J_2 (or any perturbation that can be obtained via a generating function) are ignored, then in effect, what is desired is a tracking profile indicated by the dashed-dotted red line in Figures 7.1-7.3. The mean error as shown by this indicator, is essentially the difference between the actual state that contains short- and long-periodic variations, and the average state as obtained by the matrices $\mathbf{P}_0$ and $\mathbf{P}_J$.

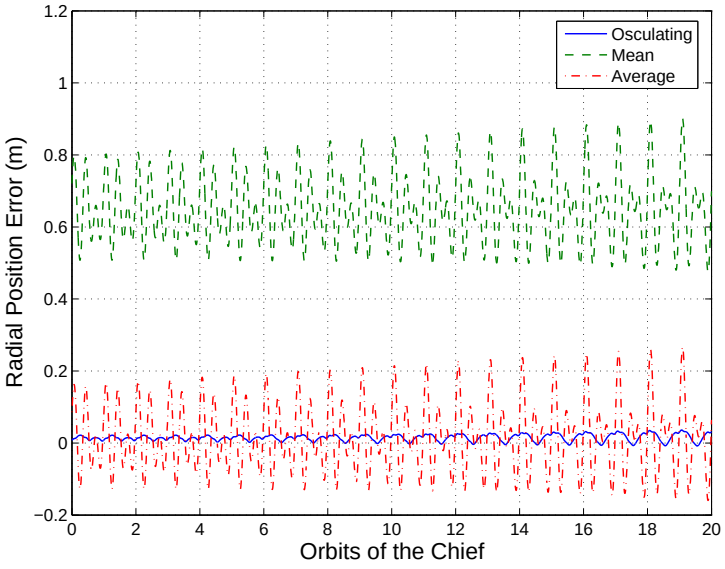

Fig. 7.1 Osculating, Mean and Average Position Error, Radial

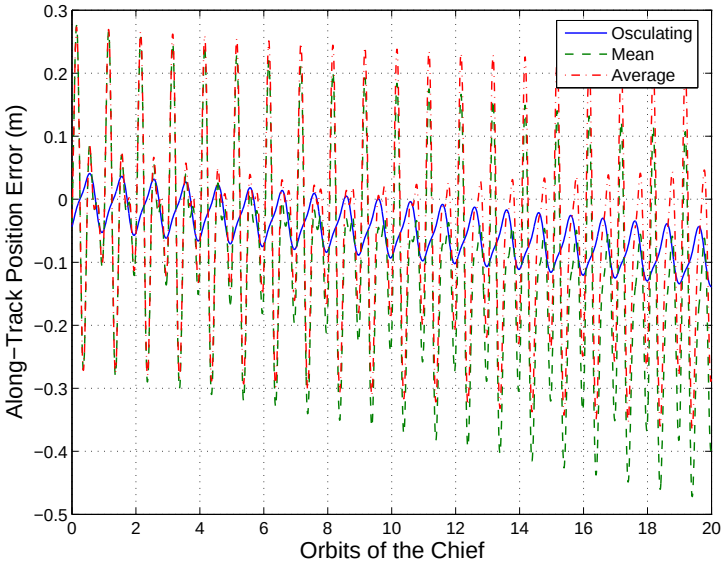

Fig. 7.2 Osculating, Mean and Average Position Error, Along-Track

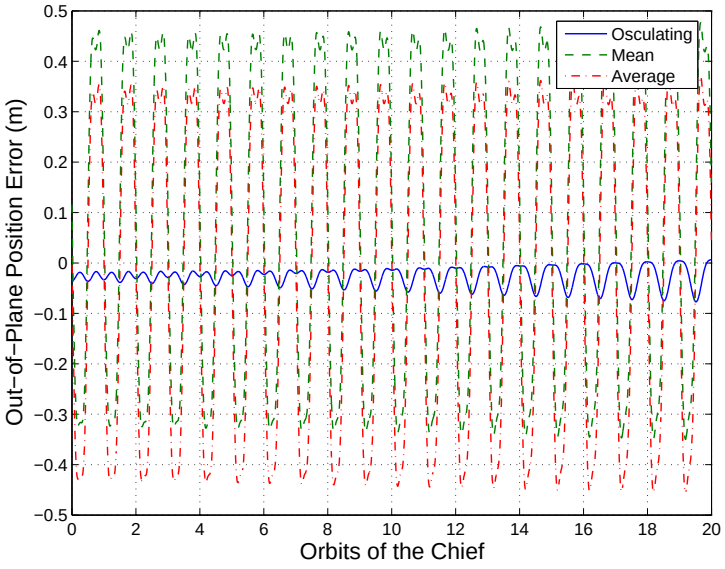

Fig. 7.3 Osculating, Mean and Average Position Error, Out-of-Plane

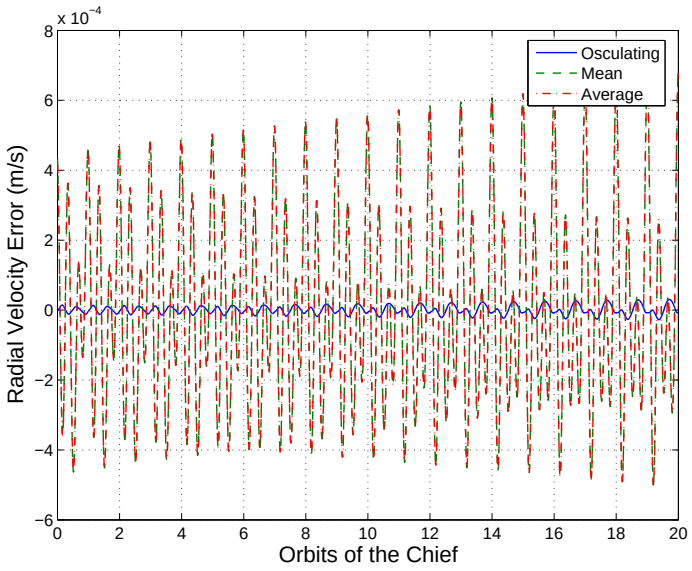

Fig. 7.4 Osculating, Mean and Average Velocity Error, Radial

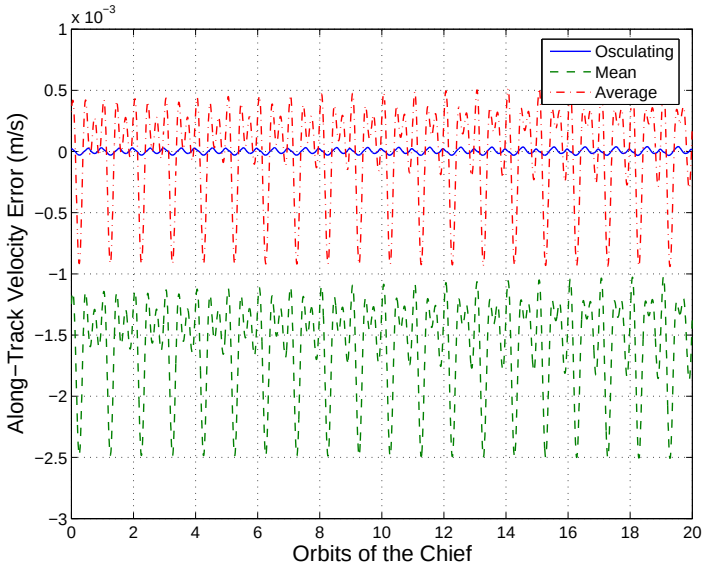

Fig. 7.5 Osculating, Mean and Average Velocity Error, Along-Track

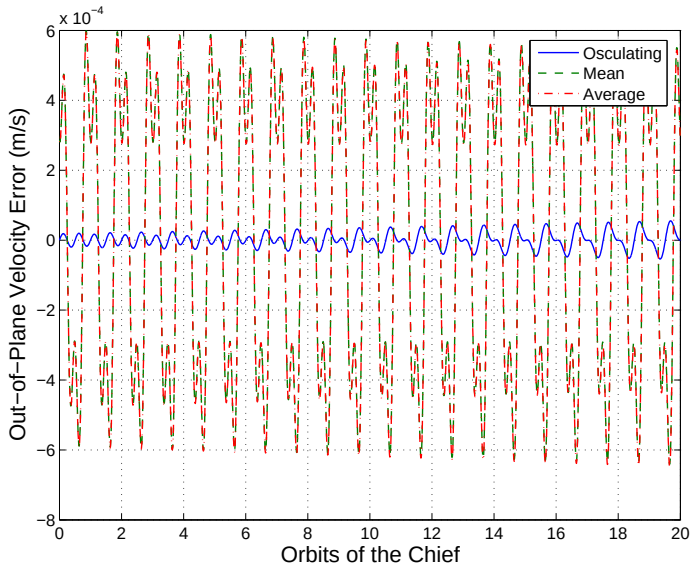

Fig. 7.6 Osculating, Mean and Average Velocity Error, Out-of-Plane

The velocity errors are shown in Figure 7.4, Figure 7.5, and Figure 7.6. There is no improvement in the radial velocity; in fact the bias correction is found to be zero. It can also be shown that the average short-periodic variation in radial velocity is zero. The improvement in the out-of-plane direction is also minimal, since the use of mean elements does not appear to create a non-zero bias error. As shown in Figure 7.5, the along-track velocity correction is the most significant among the three.

7.6 Summary

The average expressions for relative motion that have been derived in this section, can prove useful for different purposes. The number of computations required to calculate the average states are far lower than those required to calculate the osculating states. For small orbits, the errors between the two are of the order of centimeters. As the orbit size increases, the bias introduced by the use of mean elements will also increase, and the use of the correction matrix $\mathbf{P}_J$ becomes more important. However, the bias due to linearization also increases, so it may be necessary to introduce second-order terms. The advantage, as shown in Chapter V, is that the higher-order terms can be introduced using mean elements only, thereby resulting in a complete, mean-element description of relative motion.

The matrices $\mathbf{P}_0$ and $\mathbf{P}_J$ can also be used as an analytical filter to remove J_2-induced short-periodic perturbations from the osculating (actual) states, if the elements of the chief are known. From the inverse maps developed by Gim and Alfriend (2003) and in Chapter V, the osculating - and by extension - mean differential orbital elements corresponding to the osculating states can be determined. This mean differential orbital elements can then be used to find the corresponding average states.

CHAPTER VIII

CONCLUSIONS AND RECOMMENDATIONS FOR FUTURE WORK

In this dissertation, the problem of relative motion was analyzed by relaxing the underlying assumptions of the HCW equations. The extensive literature review revealed the need for analytical solutions to model equations for rendezvous and formation flight, near arbitrarily eccentric orbits, for large relative orbits, and/or near an oblate planet. This dissertation has addressed this need, by providing analytical solutions to all these problems.

In the process of developing the theory in the preceding chapters, several interesting quantities and integrals have been encountered. The first is the eccentricity-like quantity ε, which not only expressed itself in the Fourier expansions when modeling eccentricity effects on formation geometry, but also appeared in the process of averaging the short-periodic effects due to J_2. Similarly, several integrals were encountered in the process of modeling nonlinear perturbations, and when averaging short-periodic effects due to J_2, which were previously not solved. Some of these integrals included Kepler's equation as an integrand, especially in the rendezvous problem.

There are several extensions to this problem that have not been explored in this dissertation. Perturbations due to atmospheric drag have not been accounted for in the analysis. They will be required when modeling the long-term dynamics of satellite relative motion. These perturbations have been explored to some extent by Kechichian (1998); Carter and Humi (2002); Humi and Carter (2002); Mishne (2004).

More complicated models for relative motion, that also include lunisolar perturbations have been presented in recent work by Wnuk and Golebiewska (2005, 2006), although a state transition matrix that includes these effects has not been derived.

Following the development of an optimal control for rendezvous as shown in Chapter IV, it may be possible to use similar theory to obtain an optimal multi-impulsive control, that is useful for high-thrust engine mechanisms, near an arbitrarily eccentric orbit. Similar schemes have been proposed by Schaub and Alfriend (2001), that exploit the dynamics of relative motion to obtain locations where impulses are most effective in changing a given orbital element. A numerical procedure that was useful for highly eccentric orbits was also presented by Sengupta et al. (2004). However, an analytical solution to the multi-impulse rendezvous or reconfiguration problem has not yet been obtained.

The use of the analytical solution to the LQ problem of Chapter IV, as a basis for the development of optimal feedback controls that include nonlinear effects is also currently being explored.

Several aspects of the theory developed in this dissertation can possibly be used for formation flight problems in other environments, such as deep-space gravity-free problems, or the restricted three-body problem.

REFERENCES

Aksnes, K.: On the use of Hill's variables in artificial satellite theory; Brouwer's theory. Astron. Astrophys. **17**, 70–75 (1972)

Alfriend, K. T., Kashiwagi, Y.: Minimum time optimal rendezvous between neighboring elliptic orbits. J. Optim. Theory Appl. **4**(4), 260–276 (1969)

Alfriend, K. T., Schaub, H., Gim, D.-W.: Gravitational perturbations, nonlinearity and circular orbit assumption effects on formation flying control strategies. Adv. Astronaut. Sci. **104**, 139–158 (2000), also Paper AAS-00-012 of the AAS Guidance and Control Conference

Alfriend, K. T., Yan, H., Vadali, S. R.: Nonlinear considerations in satellite formation flying. In: AIAA/AAS Astrodynamics Specialist Conference, AIAA-2002-4741, Monterey, CA (2002)

Anthony, M. L., Sasaki, F. T.: Rendezvous problem for nearly circular orbits. AIAA J. **3**(9), 1666–1673 (1965)

Battin, R. H.: An Introduction to the Mathematics and Methods of Astrodynamics. AIAA Education Series, American Institute of Aeronautics and Astronautics, Inc., Reston, VA, revised edition (1999)

Billik, B. H.: Some optimal low-acceleration rendezvous maneuvers. AIAA J. **2**(3), 510–516 (1964)

Bond, V. R.: A new solution for the rendezvous problem. Adv. Astronaut. Sci. **102**(2), 1115–1143 (1999), also Paper AAS 99-178 of the AAS/AIAA Space Flight Mechanics Meeting

Born, G. H., Goldstein, D. B., Thompson, B.: An analytical theory for orbit determination. J. Astronaut. Sci. **49**(2), 345–361 (2001)

Broucke, R. A.: Solution of the elliptic rendezvous problem with the time as independent variable. J. Guid. Control Dynam. **26**(4), 615–621 (2003)

Broucke, R. A., Cefola, P. J.: On the equinoctial orbit elements. Celest. Mech. **5**, 303–310 (1972)

Brouwer, D.: Solution of the problem of artificial satellite theory without drag. Astron. J. **64**, 378–397 (1959)

Carpenter, J. R., Alfriend, K. T.: Navigation accuracy guidelines for orbital formation flying. J. Astronaut Sci. **53**(2), 207–219 (2005)

Carpenter, J. R., Leitner, J. A., Folta, D. C., Burns, R. D.: Benchmark problems for spacecraft formation flight missions. In: AIAA Guidance, Navigation, and Control Conference and Exhibit, AIAA-2003-5364, AIAA, Austin, TX (2003)

Carter, T. E.: New form for the optimal rendezvous equations near a Keplerian orbit. J. Guid. Control Dynam. **13**(1), 183–186 (1990)

Carter, T. E.: Optimal power-limited rendezvous for linearized equations of motion. J. Guid. Control Dynam. **17**(5), 1082–1086 (1994)

Carter, T. E.: State transition matrices for terminal rendezvous studies: Brief survey and new examples. J. Guid. Control Dynam. **21**(1), 148–155 (1998)

Carter, T. E., Brient, J.: Fuel-optimal rendezvous for linearized equations of motion. J. Guid. Control Dynam. **15**(6), 1411–1416 (1992)

Carter, T. E., Humi, M.: Fuel-optimal rendezvous near a point in general Keplerian orbit. J. Guid. Control Dynam. **10**(6), 567–573 (1987)

Carter, T. E., Humi, M.: Clohessy-Wiltshire equations modified to include quadratic drag. J. Guid. Control Dynam. **25**(6), 1058–1063 (2002)

Clohessy, W. H., Wiltshire, R. S.: Terminal guidance system for satellite rendezvous. J. Aerosp. Sci. **27**, 653–658, 674 (1960)

Coffey, S. L., Déprit, A.: Third-order solution to the main problem of satellite theory. J. Guid. Control Dynam. **5**(4), 366–371 (1982)

Colwell, P.: Solving Kepler's Equation Over Three Centuries. Willmann-Bell, Inc., Richmond, VA (1993)

Curtis, S. A.: The Magnetosphere Multiscale Mission... resolving fundamental processes in space plasmas. Technical Report NASA TM-2000-209883, NASA Science and Technology Definition Team for the MMS Mission (1999)

Déprit, A., Rom, A.: The main problem of artificial satellite theory for small and moderate eccentricities. Celest. Mech. **2**(2), 166–206 (1970)

Edelbaum, T. N.: Optimum low-thrust rendezvous and stationkeeping. AIAA J. **2**(7), 1196–1201 (1964)

Euler, E. A.: Optimal low-thrust rendezvous control. AIAA J. **7**(6), 1140–1144 (1969)

Euler, E. A., Shulman, Y.: Second-order solution to the elliptic rendezvous problem. AIAA J. **5**(5), 1033–1035 (1967)

Feagin, T., Gottlieb, R. G.: Generalization of Lagrange's implicit function theorem to n-dimensions. Celest. Mech. **3**, 227–231 (1971)

Garrison, J. L., Gardner, T. G., Axelrad, P.: Relative motion in highly elliptical orbits. Adv. Astronaut. Sci. **89**(2), 1359–1376 (1995), also Paper AAS 95-194 of the AAS/AIAA Space Flight Mechanics Meeting

Gim, D.-W., Alfriend, K. T.: State transition matrix of relative motion for the perturbed noncircular reference. J. Guid. Control Dynam. **26**(6), 956–971 (2003)

Gim, D.-W., Alfriend, K. T.: Satellite relative motion using differential equinoctial elements. Celest. Mech. Dynam. Astron. **92**(4), 295–336 (2005)

Gobetz, F. W.: Linear theory of optimum low-thrust rendezvous trajectories. J. Astronaut. Sci. **12**(3), 69–76 (1965)

Goldstein, H.: Classical Mechanics. Series in Advanced Physics, Addison-Wesley Publishing Company, Inc., Reading, MA (1965)

Guelman, M., Aleshin, M.: Optimal bounded low-thrust rendezvous with fixed terminal-approach direction. J. Guid. Control Dynam. **24**(2), 378–385 (2001)

Gurfil, P.: Euler parameters as nonsingular orbital elements in near-equatorial orbits. J. Guid. Control Dynam. **28**(5), 1079–1083 (2005a)

Gurfil, P.: Relative motion between elliptic orbits: generalized boundedness conditions and optimal formationkeeping. J. Guid. Control Dynam. **28**(4), 761–767 (2005b)

Gurfil, P., Kasdin, N. J.: Nonlinear modeling of spacecraft relative motion in the configuration space. J. Guid. Control Dynam. **27**(1), 154–157 (2004)

Gurfil, P., Kholshevnikov, K. V.: Manifolds and metrics in the relative spacecraft motion problem. J. Guid. Control Dynam. **29**(4), 1004–1010 (2006)

Hill, G. W.: Researches in the lunar theory. Am. J. Math. **1**(1), 5–26 (1878)

Hoots, F. R.: Reformulation of the Brouwer geopotential theory for improved computational efficiency. Celest. Mech. **24**(4), 367–375 (1981a)

Hoots, F. R.: Theory of motion of an artificial earth satellite. Celest. Mech. **23**(4), 307–363 (1981b)

How, J. P., Twiggs, R. J., Weidow, D. A., Hartman, K. R., Bauer, F. H.: Orion - a low-cost demonstration of formation flying in space using GPS. In: AIAA/AAS Astrodynamics Specialist Conference and Exhibit, AIAA-1998-4398, Boston, MA (1998)

Humi, M.: Fuel-optimal rendezvous in a general central gravity field. J. Guid. Control Dynam. **16**(1), 215–217 (1993)

Humi, M., Carter, T. E.: Rendezvous equations in a central force field with linear drag. J. Guid. Control Dynam. **25**(1), 74–79 (2002)

Inalhan, G., Tillerson, M., How, J. P.: Relative dynamics and control of spacecraft formations in eccentric orbits. J. Guid. Control Dynam. **25**(1), 48–59 (2002)

Jezewski, D. J., Stoolz, J. M.: A closed-form solution for minimum-fuel, constant-thrust trajectories. AIAA J. **8**(7), 1229–1234 (1970)

Junkins, J. L., Turner, J. D.: On the analogy between orbital dynamics and rigid body dynamics. J. Astronaut. Sci. **27**(4), 345–358 (1979)

Junkins, J. L., Turner, J. D.: Optimal Spacecraft Rotational Maneuvers, Studies in Astronautics, volume 3. Elsevier Science Publishers B. V., The Netherlands (1986)

Karlgaard, C. D., Lutze, F. H.: Second-order relative motion equations. J. Guid. Control Dynam. **26**(1), 41–49 (2003)

Karlgaard, C. D., Lutze, F. H.: Second-order equations for rendezvous in a circular orbit. J. Guid. Control Dynam. **27**(3), 499–501 (2004)

Kasdin, N. J., Gurfil, P., Kolemen, E.: Canonical modelling of relative spacecraft motion via epicyclic orbital elements. Celest. Mech. Dynam. Astron. **92**(4), 337–370 (2005)

Kaula, W. M.: Theory of Satellite Geodesy. Dover Publications, Inc., Mineola, NY (2000)

Kechichian, J. A.: Motion in general elliptic orbit with respect to a dragging and precessing coordinate frame. J. Astronaut. Sci. **46**(1), 25–46 (1998)

Ketema, Y.: An analytical solution for relative motion with an elliptic reference orbit. J. Astronaut. Sci. **53**(4), 373–389 (2005)

Knollman, G. C., Pyron, B. O.: Relative trajectories of objects ejected from a near satellite. AIAA J. **1**(2), 424–429 (1963)

Kozai, Y.: The motion of a close earth satellite. Astron. J. **64**, 367–377 (1959)

Lane, C. M., Axelrad, P.: Formation design in eccentric orbits using linearized equations of relative motion. J. Guid. Control Dynam. **29**(1), 146–160 (2006)

Laser Interferometer Space Antenna homepage. `http://lisa.jpl.nasa.gov/` (Cited September 27, 2006)

Lawden, D. F.: Optimal Trajectories for Space Navigation. Butterworths, London, UK, 2nd edition (1963)

Lewis, F. L., Syrmos, V. L.: Optimal Control. John Wiley & Sons, Inc., New York, NY, 2nd edition (1995)

London, H. S.: Second approximation to the solution of rendezvous equations. AIAA J. **1**(7), 1691–1693 (1963)

Lyddane, R. H.: Small eccentricities or inclinations in the Brouwer theory of the artificial satellite. Astron. J. **68**(8), 555–558 (1963)

Marec, J.-P.: Optimal Spacecraft Trajectories, Studies in Astronautics, volume 1. Elsevier Scientific Publishing Company, The Netherlands (1979)

Martin, M., Stallard, M. J.: Distributed satellite missions and technologies - the TechSat 21 program. In: AIAA Space Technology Conference and Exposition, AIAA-1999-4479, AIAA, Albuquerque, NM (1999)

Melton, R. G.: Time explicit representation of relative motion between elliptical orbits. J. Guid. Control Dynam. **23**(4), 604–610 (2000)

Mishne, D.: Formation control of satellites subject to drag variations and J_2 perturbations. J. Guid. Control Dynam. **27**(4), 685–692 (2004)

Nayfeh, A. H.: Perturbation Methods. John Wiley & Sons, Inc., New York City, NY (1973)

Palmer, P. L.: Optimal relocation of satellites flying in near-circular-orbit formations. J. Guid. Control Dynam. **29**(3), 519–526 (2006)

Richardson, D. L., Mitchell, J. W.: A third-order analytical solution for relative motion with a circular reference orbit. J. Astronaut. Sci. **51**(1), 1–12 (2003)

Sabol, C. A., McLaughlin, C. A., Luu, K. K.: Meet the cluster orbits with perturbations of Keplerian elements (COWPOKE) equations. Adv. Astronaut. Sci. **114**(3), 573–594 (2003), also Paper AAS 03-138 of the AAS/AIAA Space Flight Mechanics Meeting

Schaub, H.: Relative orbit geometry through classical orbit element differences. J. Guid. Control Dynam. **27**(5), 839–848 (2004)

Schaub, H., Alfriend, K. T.: Impulse feedback control to establish specific mean orbit elements of spacecraft formations. J. Guid. Control Dynam. **24**(4), 739–745 (2001)

Schweigart, S. A., Sedwick, R. J.: High-fidelity linearized J_2 model for satellite formation flight. J. Guid. Control Dynam. **25**(6), 1073–1080 (2002)

Sengupta, P., Sharma, R., Vadali, S. R.: Periodic relative motion near a general Keplerian orbit with nonlinear differential gravity. J. Guid. Control Dynam. **29**(5), 1110–1121 (2006)

Sengupta, P., Vadali, S. R.: Satellite orbital transfer and formation reconfiguration via an attitude control analogy. J. Guid. Control Dynam. **28**(6), 1200–1209 (2005)

Sengupta, P., Vadali, S. R., Alfriend, K. T.: Modeling and control of satellite formations in high eccentricity orbits. J. Astronaut. Sci. **52**(1-2), 149–168 (2004)

Smith, O. K.: Computation of coordinates from Brouwer's solution of the artificial satellite problem. Astron. J. **66**(7), 359–360 (1961)

Tschauner, J. F. A., Hempel, P. R.: Rendezvous zu einemin elliptischer bahn umlaufenden ziel. Astronaut. Acta **11**(2), 104–109 (1965)

Turner, J. D.: Automated generation of high-order partial derivate models. AIAA J. **41**(8), 1590–1598 (2003)

Vadali, S. R.: An analytical solution for relative motion of satellites. In: 5th Dynamics and Control of Systems and Structures in Space Conference, Cranfield University, Cranfield, UK (2002)

Vadali, S. R., Vaddi, S. S., Alfriend, K. T.: A new concept for controlling formation flying satellite constellations. Adv. Astronaut. Sci. **108**(2), 1631–1648 (2001), also Paper AAS 01-218 of the AAS/AIAA Space Flight Mechanics Meeting

Vadali, S. R., Vaddi, S. S., Alfriend, K. T.: An intelligent control concept for formation flying satellites. Int. J. Robust Nonlinear Control **12**, 97–115 (2002)

Vaddi, S. S., Alfriend, K. T., Vadali, S. R., Sengupta, P.: Formation establishment and reconfiguration using impulsive control. J. Guid. Control Dynam. **28**(2), 262–268 (2005)

Vaddi, S. S., Vadali, S. R., Alfriend, K. T.: Formation flying: Accommodating nonlinearity and eccentricity perturbations. J. Guid. Control Dynam. **26**(2), 214–223 (2003)

de Vries, J. P.: Elliptic elements in terms of small increments of position and velocity components. AIAA J. **1**(11), 2626–2629 (1963)

Wnuk, E., Golebiewska, J.: The relative motion of earth orbiting satellites. Celest. Mech. Dynam. Astron. **91**(3-4), 373–389 (2005)

Wnuk, E., Golebiewska, J.: Differential perturbations and semimajor axis estimation for satellite formation orbits. In: AIAA/AAS Astrodynamics Specialist Conference and Exhibit, AIAA-2006-6018, Keystone, CO (2006)

Wolfsberger, W., Weiß, J., Rangnitt, D.: Strategies and schemes for rendezvous on geostationary transfer orbit. Acta Astronaut. **10**(8), 527–538 (1983)

Yamanaka, K., Ankersen, F.: New state transition matrix for relative motion on an arbitrary elliptical orbit. J. Guid. Control Dynam. **25**(1), 60–66 (2002)

Yan, H.: Dynamics and Real-Time Optimal Control of Aerospace Systems. Ph. D. Dissertation, Texas A&M University, College Station, TX (2006)

Yan, H., Sengupta, P., Vadali, S. R., Alfriend, K. T.: Development of a state transition matrix for relative motion using the unit sphere approach. Adv. Astronaut. Sci. **119**(1), 935–946 (2004), also Paper AAS 04-163 of the AAS/AIAA Space Flight Mechanics Meeting

Zanon, D. J., Campbell, M. E.: Fuel optimal maneuvers with spacecraft attitude constraints. In: AIAA Guidance, Navigation, and Control Conference and Exhibit, AIAA-2006-6588, Keystone, CO (2006a)

Zanon, D. J., Campbell, M. E.: Optimal planner for spacecraft formations in elliptical orbits. J. Guid. Control Dynam. **29**(1), 161–171 (2006b)

APPENDIX A

MATRICES $\mathbf{W}^{(0\ldots3)}$ FOR RENDEZVOUS

By denoting $1/R_i = r_i$, the non-zero components of $\mathbf{W}^{(0\ldots3)}(f)$ are:

$$W_{44}^{(3)} = \frac{3}{2}\frac{e^2 r_1}{\eta^{15}} + 3\frac{r_2}{\eta^{13}}, \quad W_{24}^{(3)} = eW_{44}^{(3)}, \quad W_{22}^{(3)} = e^2 W_{44}^{(3)} \tag{A.1}$$

$$W_{44}^{(2)} = -\frac{3}{4}\frac{e^2 r_1}{\eta^{12}}\frac{\sin f\,(5e + 6\cos f + e\cos 2f)}{(1+e\cos f)^3} \tag{A.2a}$$

$$W_{34}^{(2)} = \frac{3}{2\eta^8}\left(\frac{e^2}{2\eta^2}r_1 + r_2\right) \tag{A.2b}$$

$$W_{14}^{(2)} = -\frac{3}{4}\frac{e}{\eta^{12}}\left(r_1 - 5r_2\right) \tag{A.2c}$$

$$W_{24}^{(2)} = eW_{44}^{(2)}, \quad W_{12}^{(2)} = eW_{14}^{(2)}, \quad W_{22}^{(2)} = eW_{24}^{(2)}, \quad W_{32}^{(2)} = eW_{34}^{(2)} \tag{A.2d}$$

$$W_{66}^{(1)} = \frac{1}{8}\frac{\left(4 + 41\,e^2 + 18\,e^4\right) r_3}{\eta^{11}}, \quad W_{55}^{(1)} = \frac{1}{8}\frac{\left(4 + 3\,e^2\right) r_3}{\eta^9} \tag{A.3a}$$

$$\begin{aligned} W_{44}^{(1)} = {} & \frac{r_1}{16\eta^{15}(1+e\cos f)^4} \times \\ & \Bigg[e^3\left(32\,e^8 - 260\,e^6 + 273\,e^4 + 876\,e^2 + 80\right)\left(\frac{e}{8}\cos 4f + \cos 3f\right) \\ & + \frac{e^2}{2}\left(32\,e^{10} - 20\,e^8 - 1503\,e^6 + 2874\,e^4 + 5072\,e^2 + 552\right)\cos 2f \\ & + e\left(96\,e^{10} - 588\,e^8 - 541\,e^6 + 4296\,e^4 + 3296\,e^2 + 448\right)\cos f \\ & + \left(12\,e^{12} + \frac{45}{2}\,e^{10} - \frac{6477}{8}\,e^8 + \frac{2503}{2}\,e^6 + 2583\,e^4 + 1256\,e^2 + 64\right)\Bigg] \\ & + \frac{r_2}{8\eta^{13}(1+e\cos f)^3}\Bigg[\frac{e^2}{2}\left(2\,e^6 - 41\,e^4 + 76\,e^2 + 40\right)\left(\frac{e}{2}\cos 3f + 3\cos 2f\right) \end{aligned}$$

$$+\frac{3e}{4}\left(2\,e^8-e^6-184\,e^4+440\,e^2+128\right)\cos f$$
$$+\frac{e^2}{2}\left(6\,e^6-39\,e^4-94\,e^2+512\right)\Bigg] \tag{A.3b}$$

$$W_{34}^{(1)}=\frac{\eta^5}{3}W_{44}^{(2)},\quad W_{33}^{(1)}=\frac{2\eta^5}{3}W_{34}^{(2)} \tag{A.3c}$$

$$W_{24}^{(1)}=-\frac{er_1}{16\eta^{15}(1+e\cos f)^4}\times$$
$$\Bigg[e\left(70\,e^8-113\,e^6-746\,e^4-220\,e^2+8\right)\left(\frac{e}{8}\cos 4f+\cos 3f\right)$$
$$+\frac{1}{2}\left(46\,e^{10}+403\,e^8-1544\,e^6-4672\,e^4-1264\,e^2+24\right)\cos 2f$$
$$+e\left(178\,e^8+101\,e^6-2946\,e^4-3516\,e^2-824\right)\cos f$$
$$+\frac{1}{8}\left(114\,e^{10}+2237\,e^8-6662\,e^6-17004\,e^4-12504\,e^2-1216\right)\Bigg]$$
$$+\frac{r_2}{8\eta^{13}(1+e\cos f)^3}\Bigg[-\frac{e}{2}\left(13e^6-4e^4-66e^2-20\right)\left(\frac{e}{2}\cos 3f+3\cos 2f\right)$$
$$+\left(\frac{9}{4}\,e^8-60\,e^6+\frac{123}{2}\,e^4+237\,e^2+48\right)\cos f$$
$$+\frac{e}{2}\left(e^6-94\,e^4+206\,e^2+272\right)\Bigg] \tag{A.3d}$$

$$W_{23}^{(1)}=\frac{e\eta^5}{3}W_{44}^{(2)} \tag{A.3e}$$

$$W_{22}^{(1)}=-\frac{r_1}{16\eta^{15}(1+e\cos f)^4}\times$$
$$\Bigg[e^3\left(113e^6+536e^4+360e^2-8\right)\left(\frac{e}{8}\cos 4f+\cos 3f\right)$$
$$+\frac{e^4}{2}\left(137\,e^6+1094\,e^4+3792\,e^2+1984\right)\cos 2f$$
$$+e\left(339\,e^8+1996\,e^6+3416\,e^4+1224\,e^2+32\right)\cos f$$
$$+\left(-\frac{141}{8}\,e^{10}+744\,e^8+1588\,e^6+1793\,e^4+264\,e^2+8\right)\Bigg]$$
$$+\frac{r_2}{8\eta^{13}(1+e\cos f)^3}\Bigg[-\frac{7e^2}{2}\left(4e^4-7e^2-8\right)\left(\frac{e}{2}\cos 3f+3\cos 2f\right)$$

$$+\frac{3e}{4}\left(4\,e^6-159\,e^4+348\,e^2+192\right)\cos f+$$
$$\left(-2\,e^6-\frac{149}{2}\,e^4+253\,e^2+16\right)\Bigg] \qquad (A.3f)$$

$$W_{14}^{(1)}=\frac{\sin f}{2\eta^9(1+e\cos f)^3}\times$$
$$\left[3e\,(r_1-5r_2)\cos f+\frac{e^2}{2}\,(r_1-5r_2)\cos 2f+\frac{e^2}{2}\,(5r_1-r_2)-12\,r_2\right] \qquad (A.3g)$$

$$W_{11}^{(1)}=\frac{1}{2}\,\frac{r_1}{\eta^9}+\frac{1}{8}\,\frac{(47\,e^2+16)\,r_2}{\eta^{11}},\quad W_{13}^{(1)}=\frac{2\eta^5}{3}W_{14}^{(2)},\quad W_{12}^{(1)}=eW_{14}^{(1)} \qquad (A.3h)$$

$$W_{66}^{(0)}=-\frac{r_3\sin f}{120\eta^8(1+e\cos f)^5}\Bigg[\frac{e^2}{4}\left(190e^4+131e^2-6\right)\left(\frac{e}{2}\cos 4f+5\cos 3f\right)$$
$$+\frac{e}{2}\left(150\,e^6+1789\,e^4+1271\,e^2-60\right)\cos 2f$$
$$+\left(\frac{1385}{2}\,e^6+\frac{6365}{4}\,e^4+\frac{2325}{2}\,e^2-60\right)\cos f$$
$$+\frac{e}{8}\left(410e^6+6993e^4+7282e^2+2640\right)\Bigg] \qquad (A.4a)$$

$$W_{55}^{(0)}=-\frac{r_3\sin f}{120\eta^6(1+e\cos f)^5}\Bigg[\frac{e^2}{4}\left(29e^2+6\right)\left(\frac{e}{2}\cos 4f+5\cos 3f\right)$$
$$+\frac{e}{2}\left(21\,e^4+269\,e^2+60\right)\cos 2f+\left(\frac{395}{4}\,e^4+\frac{435}{2}\,e^2+60\right)\cos f$$
$$+\frac{e}{8}\left(247e^4+478e^2+1200\right)\Bigg] \qquad (A.4b)$$

$$W_{56}^{(0)}=-\frac{(5e^2-1)}{80\eta^{10}}\frac{(\cos f+e)r_3}{(1+e\cos f)^5}\Bigg[\frac{e^3}{2}\cos 4f-e^2\left(e^2-5\right)\cos 3f$$
$$+2e\,\left(e^4-4\,e^2+10\right)\cos 2f+\left(-4\,e^6+17\,e^4-25\,e^2+40\right)\cos f$$
$$+\frac{e\,(12\,e^6-49\,e^4+137\,e^2+40)}{2(5\,e^2-1)} \qquad (A.4c)$$

$$W_{44}^{(0)}=-\frac{r_1 e\sin f}{240\eta^{12}\,(1+e\cos f)^5}\times$$
$$\Bigg[\frac{e^3}{4}\left(240\,e^6-2460\,e^4+5047\,e^2+2178\right)\left(\frac{e}{2}\cos 4f+5\cos 3f\right)$$

$$
\begin{aligned}
&+\frac{e^2}{2}\left(21300+46687\,e^2-18357\,e^4+180\,e^6+240\,e^8\right)\cos 2f\\
&+\frac{5e}{4}\left(-5556\,e^6+720\,e^8+31098\,e^2+893\,e^4+15888\right)\cos f\\
&+\left(7680+\frac{80197}{4}\,e^4-\frac{76939}{8}\,e^6+\frac{795}{2}\,e^8+90\,e^{10}-15810\,e^2\right)\Bigg]\\
&+\frac{r_2 e\sin f}{120\eta^{10}\left(1+e\cos f\right)^5}\Bigg[\frac{e^3}{4}\left(10\,e^4+211\,e^2-606\right)\left(\frac{e}{2}\cos 4f+5\cos 3f\right)\\
&-\frac{e^2}{2}\left(30\,e^6-289\,e^4-1591\,e^2+5700\right)\cos 2f\\
&-\frac{5e}{4}\left(82\,e^6-761\,e^4+198\,e^2+3792\right)\cos f\\
&-\left(\frac{65}{4}\,e^8+\frac{47}{8}\,e^6+2250\,e^2-\frac{4261}{4}\,e^4+1440\right)\Bigg]
\end{aligned}
\tag{A.4d}
$$

$$
W_{33}^{(0)}=\frac{\eta^{10}}{9}W_{44}^{(2)}
\tag{A.4e}
$$

$$
\begin{aligned}
W_{34}^{(0)}=&-\frac{r_1 e}{12\eta^{10}(1+e\cos f)^4}\Bigg[e^2\left(9\,e^4-20\,e^2-2\right)\left(\frac{e}{8}\cos 4f+\cos 3f\right)\\
&-\frac{e}{2}\left(6\,e^8-36\,e^6+11\,e^4+89\,e^2+21\right)\cos 2f\\
&+\left(-8\,e^8+67\,e^6-96\,e^4-30\,e^2-24\right)\cos f\\
&-\frac{e}{8}\left(24\,e^8-191\,e^6+208\,e^4+66\,e^2+348\right)\Bigg]\\
&-\frac{r_2 e}{6\eta^8(1+e\cos f)^3}\Bigg[\frac{e}{2}\left(12\,e^2-5\right)\left(\frac{e}{2}\cos 3f+3\cos 2f\right)\\
&+\left(18\,e^4+\frac{93}{4}\,e^2-3\,e^6-12\right)\cos f-\frac{e}{2}\left(10\,e^4-66\,e^2+21\right)\Bigg]
\end{aligned}
\tag{A.4f}
$$

$$
\begin{aligned}
W_{22}^{(0)}=&-\frac{r_1\sin f}{240\eta^{12}\left(1+e\cos f\right)^5}\times\\
&\Bigg[\frac{e^2}{4}\left(1247\,e^6+3318\,e^4+480\,e^2-40\right)\left(\frac{e}{2}\cos 4f+5\cos 3f\right)\\
&+\frac{e}{2}\left(1143\,e^8+12947\,e^6+31920\,e^4+4320\,e^2-280\right)\cos 2f\\
&+\left(\frac{19865}{4}\,e^8+\frac{34695}{2}\,e^6+27960\,e^4+3650\,e^2-120\right)\cos f
\end{aligned}
$$

$$+\frac{e}{8}\left(61\,e^8+61414\,e^6+119520\,e^4+84520\,e^2+9760\right)\Bigg]$$

$$+\frac{r_2\sin f}{120\eta^{10}\left(1+e\cos f\right)^5}\Bigg[\frac{e^2}{4}\left(220\,e^4-559\,e^2-46\right)\left(\frac{e}{2}\cos 4f+5\cos 3f\right)$$

$$+\frac{e}{2}\left(60\,e^6+1909\,e^4-5419\,e^2-400\right)\cos 2f$$

$$+\left(385\,e^6+\frac{2855}{4}\,e^4-\frac{9995}{2}\,e^2-240\right)\cos f$$

$$\frac{e}{8}\left(20\,e^6+5763\,e^4-11278\,e^2-15680\right)\Bigg] \qquad (A.4g)$$

$$W_{23}^{(0)}=-\frac{r_1 e}{12\eta^{10}(1+e\cos f)^4}\Bigg[e\left(3e^6-6\,e^4-12\,e^2+2\right)\left(\frac{e}{8}\cos 4f+\cos 3f\right)$$

$$+\left(\frac{27}{2}\,e^6-\frac{75}{2}\,e^4-\frac{49}{2}\,e^2+3\right)\cos 2f+e\left(9\,e^6+2\,e^4-84\,e^2-18\right)\cos f$$

$$\left(\frac{69}{8}\,e^8-\frac{75}{4}\,e^6+14\,e^4-\frac{255}{4}\,e^2+3\right)\Bigg]$$

$$-\frac{r_2}{6\eta^8(1+e\cos f)^3}\Bigg[\frac{e}{2}\left(9e^4+3e^2-5\right)\left(\frac{e}{2}\cos 3f+3\cos 2f\right)$$

$$+\left(\frac{15}{4}\,e^6+\frac{153}{4}\,e^4-\frac{15}{4}\,e^2-12\right)\cos f+\frac{e}{2}\left(17\,e^4+57\,e^2-39\right)\Bigg] \qquad (A.4h)$$

$$W_{24}^{(0)}=\frac{r_1\sin f}{240\eta^{12}\left(1+e\cos f\right)^5}\times \qquad (A.4i)$$

$$\Bigg[\frac{e^3}{4}\left(730\,e^6-2347\,e^4-3348\,e^2-40\right)\left(\frac{e}{2}\cos 4f+5\cos 3f\right)$$

$$+\frac{e^2}{2}\left(450\,e^8+5107\,e^6-23617\,e^4-31410\,e^2-580\right)\cos 2f$$

$$+\frac{5e}{4}\left(1886\,e^8-2513\,e^6-20448\,e^4-21248\,e^2-720\right)\cos f$$

$$+\left(\frac{535}{4}\,e^{10}+\frac{25239}{8}\,e^8-11488\,e^6-16600\,e^4-9130\,e^2-480\right)\Bigg]$$

$$+\frac{r_2\sin f}{120\eta^{10}\left(1+e\cos f\right)^5}\Bigg[\frac{e^3}{4}\left(115\,e^4-174\,e^2-326\right)\left(\frac{e}{2}\cos 4f+5\cos 3f\right)$$

$$+\frac{e^2}{2}\left(15\,e^6+1099\,e^4-1914\,e^2-3050\right)\cos 2f$$

$$+\frac{5e}{4}\left(113\,e^6+666\,e^4-2098\,e^2-1992\right)\cos f$$
$$\left(-\frac{55}{8}\,e^8+\frac{1429}{4}\,e^6-\frac{689}{4}\,e^4-2105\,e^2-720\right)\Bigg] \qquad (A.4j)$$

$$W_{11}^{(0)}=-\frac{r_1\sin f}{12\eta^6(1+e\cos f)^3}\left(5\,e+6\,\cos f+e\cos 2f\right)$$
$$-\frac{r_2\sin f}{120\eta^8\,(1+e\cos f)^5}\Bigg[\frac{e^2}{4}\left(361\,e^2-46\right)\left(\frac{e}{2}\cos 4f+5\cos 3f\right)$$
$$+\frac{e}{2}\left(249\,e^4+3301\,e^2-400\right)\cos 2f+\left(\frac{4735}{4}\,e^4+\frac{4885}{2}\,e^2-240\right)\cos f$$
$$+\frac{e}{8}\left(443\,e^4+13362\,e^2+3520\right)\Bigg] \qquad (A.4k)$$

$$W_{12}^{(0)}=\frac{r_1}{12\eta^{12}(1+e\cos f)^4}\Bigg[e\left(3\,e^6-6\,e^4-12\,e^2+2\right)\left(\frac{e}{8}\cos 4f+\cos 3f\right)$$
$$+\frac{1}{2}\left(27\,e^6-75\,e^4-49\,e^2+6\right)\cos 2f+e\left(9\,e^6+2\,e^4-84\,e^2-18\right)\cos f$$
$$+\left(\frac{69}{8}\,e^8-\frac{75}{4}\,e^6+14\,e^4-\frac{255}{4}\,e^2+3\right)\Bigg]$$
$$-\frac{r_2}{60\eta^{12}(1+e\cos f)^5}\times$$
$$\Bigg[\frac{e^2}{8}\left(75\,e^6+450\,e^4+75\,e^2+23\right)\left(\frac{e}{2}\cos 5f+5\cos 4f\right)$$
$$+\frac{5e}{16}\left(111\,e^8+966\,e^6+3711\,e^4+659\,e^2+160\right)\cos 3f$$
$$+\left(270\,e^8+\frac{2615}{2}\,e^6+2520\,e^4+515\,e^2+60\right)\cos 2f$$
$$+\frac{5e}{8}\left(81\,e^8+1752\,e^6+5017\,e^4+5225\,e^2+1008\right)\cos f$$
$$+\frac{1}{8}\left(1449\,e^8+10370\,e^6+16105\,e^4+10845\,e^2+480\right)\Bigg] \qquad (A.4l)$$

$$W_{13}^{(0)}=\frac{\eta^5}{3}W_{14}^{(1)} \qquad (A.4m)$$

$$W_{14}^{(0)}=\frac{r_1}{12\eta^{12}(1+e\cos f)^4}\Bigg[e^2\left(9\,e^4-20\,e^2-2\right)\left(\frac{e}{8}\cos 4f+\cos 3f\right)$$
$$\frac{e}{2}\left(6\,e^8-36\,e^6+11\,e^4+89\,e^2+21\right)\cos 2f$$

$$
\begin{aligned}
&+\left(-8\,e^8+67\,e^6-96\,e^4-30\,e^2-24\right)\cos f\\
&-\frac{e}{8}\left(24\,e^8-191\,e^6+208\,e^4+66\,e^2+348\right)\Bigg]\\
&+\frac{r_2}{60\eta^{12}(1+e\cos f)^5}\Bigg[-\frac{e^3}{8}\left(105\,e^4+355\,e^2+163\right)\left(\frac{e}{2}\cos 5f+5\cos 4f\right)\\
&+\frac{5e^2}{16}\left(24\,e^8-261\,e^6-871\,e^4-3279\,e^2-1220\right)\cos 3f\\
&+\frac{5e}{2}\left(22\,e^8-248\,e^6-268\,e^4-1126\,e^2-249\right)\cos 2f\\
&+\frac{1}{8}\left(300\,e^{10}-1135\,e^8-11685\,e^6-14825\,e^4-35190\,e^2-2880\right)\cos f\\
&+\frac{e}{8}\left(656\,e^8-4995\,e^6-4505\,e^4-18585\,e^2-11820\right)\Bigg] \qquad (A.4n)
\end{aligned}
$$

APPENDIX B

MATRIX G AND TENSOR H FOR DIFFERENTIAL ORBITAL ELEMENT PROPAGATION

Let $g_{1...9}(\theta)$ denote the following functions:

$$g_1(\theta) = \frac{\alpha^2}{\eta^3} \tag{B.1a}$$

$$g_2(\theta) = \frac{q_2\alpha^2}{(1+\eta)\eta^3} + \frac{\sin\theta\,\alpha}{\eta^2} + \frac{q_2+\sin\theta}{\eta^2} \tag{B.1b}$$

$$g_3(\theta) = -\frac{q_1\alpha^2}{(1+\eta)\eta^3} - \frac{\cos\theta\,\alpha}{\eta^2} - \frac{q_1+\cos\theta}{\eta^2} \tag{B.1c}$$

$$g_4(\theta) = -\frac{\alpha^3\beta}{\eta^6} \tag{B.1d}$$

$$\begin{aligned} g_5(\theta) = {} & \frac{q_1q_2(3+4\eta)\alpha^2}{2\eta^5(1+\eta)^2} + \frac{\alpha}{\eta^4(1+\eta)}\left[(1+\eta)q_1\sin\theta + \eta q_2\cos\theta\right] \\ & + \frac{q_1}{\eta^4}(q_2+\sin\theta) + \frac{g_2(\theta)}{2\eta^2}\left[(\alpha+1)\cos\theta - \beta\sin\theta - \frac{2q_2\alpha\beta}{\eta(1+\eta)}\right] \\ & + \frac{1}{2\eta^2}\sin\theta\,\cos\theta \end{aligned} \tag{B.1e}$$

$$\begin{aligned} g_6(\theta) = {} & -\frac{q_1q_2(3+4\eta)\alpha^2}{2\eta^5(1+\eta)^2} - \frac{\alpha}{\eta^4(1+\eta)}\left[\eta q_1\sin\theta + (1+\eta)q_2\cos\theta\right] \\ & - \frac{q_2}{\eta^4}(q_1+\cos\theta) + \frac{g_3(\theta)}{2\eta^2}\left[(\alpha+1)\sin\theta + \beta\cos\theta + \frac{2q_1\alpha\beta}{\eta(1+\eta)}\right] \\ & \frac{1}{2\eta^2}\sin\theta\,\cos\theta \end{aligned} \tag{B.1f}$$

$$g_7(\theta) = \frac{2\alpha^3}{(1+\eta)\eta^6}\left[q_1 + (1+\eta)\cos\theta\right] - \frac{q_1\alpha^2}{(1+\eta)\eta^6}\left[2\alpha^2 + \eta(1+\eta)\right] \tag{B.1g}$$

$$g_8(\theta) = \frac{2\alpha^3}{(1+\eta)\eta^6}\left[q_2 + (1+\eta)\sin\theta\right] - \frac{q_2\alpha^2}{(1+\eta)\eta^6}\left[2\alpha^2 + \eta(1+\eta)\right] \tag{B.1h}$$

$$
\begin{aligned}
g_9(\theta) = & \frac{(q_2^2 - q_1^2)}{2\eta^5(1+\eta)^2}\left[(3+4\eta)\alpha^2 + 2\eta(1+\eta)^2\right] \\
& - \frac{(q_1\cos\theta - q_2\sin\theta)}{\eta^4(1+\eta)}\left[(1+2\eta)\alpha + 1 + \eta\right] \\
& - \frac{1}{2\eta^2}\cos 2\theta + \frac{(\alpha+1)}{2\eta^2}\left[g_2(\theta)\,\sin\theta + g_3(\theta)\,\cos\theta\right] \\
& + \frac{\beta}{2\eta^2}\left[g_2(\theta)\,\cos\theta - g_3(\theta)\,\sin\theta\right] + \frac{\alpha\beta}{\eta^3(1+\eta)}\left[q_1\,g_2(\theta) - q_2\,g_3(\theta)\right] \qquad (B.1i)
\end{aligned}
$$

Using these functions, the non-zero components of $\mathbf{G}$ are:

$$G_{11} = G_{33} = G_{44} = G_{55} = G_{66} = 1 \qquad (B.2a)$$

$$G_{21} = -\frac{3}{2}\,g_1(\theta_2)\,K(\theta_2,\theta_1) \qquad (B.2b)$$

$$G_{22} = \frac{g_1(\theta_2)}{g_1\,(\theta_1)} \qquad (B.2c)$$

$$G_{24} = -\frac{g_1(\theta_2)}{g_1(\theta_1)}\,g_2(\theta_1) + g_2(\theta_2) \qquad (B.2d)$$

$$G_{25} = -\frac{g_1(\theta_2)}{g_1(\theta_1)}\,g_3(\theta_1) + g_3(\theta_2) \qquad (B.2e)$$

The non-zero components of $\mathbf{H}$ are (with $H_{ijk} = H_{ikj}$):

$$H_{211} = \frac{9}{2}\,g_4(\theta_2)\,K^2(\theta_2,\theta_1) + \frac{15}{4}\,g_1(\theta_2)\,K(\theta_2,\theta_1) \qquad (B.3a)$$

$$H_{212} = -3\,\frac{g_4(\theta_2)}{g_1(\theta_1)}\,K(\theta_2,\theta_1) \qquad (B.3b)$$

$$H_{214} = -\frac{3}{2}\,g_7\,(\theta_2)\,K(\theta_2,\theta_1) + 3\,\frac{g_4(\theta_2)\,g_2(\theta_1)}{g_1(\theta_1)}\,K(\theta_2,\theta_1) \qquad (B.3c)$$

$$H_{215} = -\frac{3}{2}\,g_8(\theta_2)\,K(\theta_2,\theta_1) + 3\,\frac{g_4(\theta_2)\,g_3(\theta_1)}{g_1(\theta_1)}\,K(\theta_2,\theta_1) \qquad (B.3d)$$

$$H_{222} = 2\,\frac{g_4(\theta_2)}{g_1^2(\theta_1)} - 2\,\frac{g_1(\theta_2)\,g_4(\theta_1)}{g_1^3(\theta_1)} \qquad (B.3e)$$

$$H_{224} = \frac{g_7(\theta_2)}{g_1(\theta_1)} - \frac{g_7(\theta_1)\,g_1(\theta_2) + 2\,g_4(\theta_2)\,g_2(\theta_1)}{g_1^2(\theta_1)} + 2\,\frac{g_1(\theta_2)\,g_4(\theta_1)\,g_2(\theta_1)}{g_1^3(\theta_1)} \qquad (B.3f)$$

$$H_{225} = \frac{g_8(\theta_2)}{g_1(\theta_1)} - \frac{g_1(\theta_2)\,g_8(\theta_1) + 2\,g_4(\theta_2)\,g_3(\theta_1)}{g_1^2(\theta_1)} + 2\,\frac{g_1(\theta_2)\,g_4(\theta_1)\,g_3(\theta_1)}{g_1^3(\theta_1)} \qquad (B.3g)$$

$$H_{244} = 2\,g_5(\theta_2) - 2\,\frac{g_5(\theta_1)\,g_1(\theta_2) + g_7(\theta_2)\,g_2(\theta_1)}{g_1(\theta_1)}$$
$$+2\,\frac{g_2(\theta_1)\,\left[g_7(\theta_1)\,g_1(\theta_2) + g_4(\theta_2)\,g_2(\theta_1)\right]}{g_1^2(\theta_1)} - 2\,\frac{g_1(\theta_2)\,g_4(\theta_1)\,g_2^2(\theta_1)}{g_1^3(\theta_1)} \quad (B.3h)$$

$$H_{245} = g_9(\theta_2) - \frac{g_1(\theta_2)\,g_9(\theta_1) + g_7(\theta_2)\,g_3(\theta_1) + g_8(\theta_2)\,g_2(\theta_1)}{g_1(\theta_1)}$$
$$+\frac{2\,g_4(\theta_2)\,g_3(\theta_1)\,g_2(\theta_1) + g_1(\theta_2)\,g_8(\theta_1)\,g_2(\theta_1) + g_1(\theta_2)\,g_3(\theta_1)\,g_7(\theta_1)}{g_1^2(\theta_1)}$$
$$-2\,\frac{g_1(\theta_2)\,g_4(\theta_1)\,g_3(\theta_1)\,g_2(\theta_1)}{g_1^3(\theta_1)} \quad (B.3i)$$

$$H_{255} = 2\,g_6(\theta_2) - 2\,\frac{g_8(\theta_2)\,g_3(\theta_1) + g_1(\theta_2)\,g_6(\theta_1)}{g_1(\theta_1)}$$
$$+2\,\frac{g_3(\theta_1)\,\left[g_4(\theta_2)g_3(\theta_1) + g_1(\theta_2)\,g_8(\theta_1)\right]}{g_1^2(\theta_1)} - 2\,\frac{g_1(\theta_2)\,g_4(\theta_1)\,g_3^2(\theta_1)}{g_1^3(\theta_1)} \quad (B.3j)$$

APPENDIX C

MATRICES P AND $\overline{\mathbf{R}}$, AND TENSORS Q AND $\overline{\mathbf{S}}$ RELATING RELATIVE STATES TO DIFFERENTIAL ORBITAL ELEMENTS

Let $\mathcal{Q} = e\exp(\jmath\, g) = q_1 + \jmath\, q_2$, and $\Theta = \exp(\jmath\,\theta) = \cos\theta + \jmath\,\sin\theta$, where $\jmath = \sqrt{-1}$. Furthermore, let $\mathcal{Q}^*$ and Θ^* denote the complex conjugates of $\mathcal{Q}$ and Θ, respectively. The non-zero components of the matrices, $\mathbf{P}$, $\overline{\mathbf{R}}$, and tensors $\mathbf{Q}$ and $\overline{\mathbf{S}}$ (with $Q_{ijk} = Q_{ikj}$ and $\overline{S}_{ijk} = \overline{S}_{ikj}$, respectively), are listed below, by using $\mathcal{Q}$ and Θ, for conciseness:

$$P_{11} = 1 \tag{C.1a}$$

$$P_{12} = \frac{\beta}{\alpha} \tag{C.1b}$$

$$P_{14} + \jmath\, P_{15} = -\frac{\Theta}{\alpha} - \frac{2\mathcal{Q}}{\eta^2} \tag{C.1c}$$

$$P_{22} = 1 \tag{C.1d}$$

$$P_{26} = \cos i \tag{C.1e}$$

$$P_{33} + \jmath\left(\frac{P_{36}}{\sin i}\right) = -\jmath\,\Theta \tag{C.1f}$$

$$P_{41} = \frac{-3\beta}{2\alpha} \tag{C.1g}$$

$$P_{42} = 2 - \frac{3}{\alpha} + \frac{\eta^2}{\alpha^2} \tag{C.1h}$$

$$P_{44} + \jmath\, P_{45} = \frac{3\beta\,\mathcal{Q}}{\eta^2\alpha} - \jmath\,(\alpha + \jmath\,\beta)\frac{\Theta}{\alpha^2} \tag{C.1i}$$

$$P_{51} = -\frac{3}{2} \tag{C.1j}$$

$$P_{52} = -\frac{2\beta}{\alpha} \tag{C.1k}$$

$$P_{54} + \jmath\, P_{55} = \frac{2\Theta}{\alpha} + \frac{3\mathcal{Q}}{\eta^2} \tag{C.1l}$$

$$P_{63} + \jmath \left(\frac{P_{66}}{\sin i} \right) = \Theta \tag{C.1m}$$

$$\overline{R}_{11} = -2 + \frac{6\alpha}{\eta^2} \tag{C.2a}$$

$$\overline{R}_{14} + \jmath \overline{R}_{15} = \frac{2\alpha}{\eta^2}(\beta + \jmath \alpha) \tag{C.2b}$$

$$\overline{R}_{22} = 1 \tag{C.2c}$$

$$\overline{R}_{23} + \jmath \overline{R}_{26} = \cot i \, \Theta^* \tag{C.2d}$$

$$\overline{R}_{33} + \jmath \overline{R}_{36} = \jmath \Theta^* \tag{C.2e}$$

$$\overline{R}_{41} + \jmath \overline{R}_{51} = 3(\alpha - \jmath \beta) \Theta \tag{C.2f}$$

$$\overline{R}_{42} + \jmath \overline{R}_{52} = \jmath (\alpha - 1 - \jmath \beta) \Theta \tag{C.2g}$$

$$\overline{R}_{43} + \jmath \overline{R}_{53} = \jmath \, \cot i \, \cos\theta (\alpha - 1 - \jmath \beta) \tag{C.2h}$$

$$\overline{R}_{44} + \jmath \overline{R}_{54} = -\jmath \alpha \Theta \tag{C.2i}$$

$$\overline{R}_{45} + \jmath \overline{R}_{55} = (2\alpha - \jmath \beta) \Theta \tag{C.2j}$$

$$\overline{R}_{46} + \jmath \overline{R}_{56} = -\jmath \, \cot i \, \sin\theta (\alpha - 1 - \jmath \beta) \tag{C.2k}$$

$$\overline{R}_{63} + \jmath \overline{R}_{66} = -\csc i \, \Theta^* \tag{C.2l}$$

$$Q_{112} = \frac{\beta}{\alpha} \tag{C.3a}$$

$$Q_{114} + \jmath Q_{115} = -\frac{\Theta}{\alpha} - \frac{2\mathcal{Q}}{\eta^2} \tag{C.3b}$$

$$Q_{122} = -2 + \frac{3}{\alpha} - \frac{2\eta^2}{\alpha^2} \tag{C.3c}$$

$$Q_{124} + \jmath Q_{125} = -\jmath (\alpha - 2\jmath \beta) \frac{\Theta}{\alpha^2} - \frac{2\beta\mathcal{Q}}{\alpha\eta^2} \tag{C.3d}$$

$$Q_{126} = -\cos i \tag{C.3e}$$

$$Q_{133} + \jmath\left(\frac{Q_{136}}{\sin i}\right) = \jmath \sin\theta\,\Theta \tag{C.3f}$$

$$Q_{144} = -\frac{2}{\eta^2} + \frac{4q_1\cos\theta}{\eta^2\alpha} + \frac{2\cos^2\theta}{\alpha^2} \tag{C.3g}$$

$$Q_{145} = \frac{2(q_1\sin\theta + q_2\cos\theta)}{\eta^2\alpha} + \frac{2\sin\theta\,\cos\theta}{\alpha^2} \tag{C.3h}$$

$$Q_{155} = -\frac{2}{\eta^2} + \frac{4q_2\sin\theta}{\eta^2\alpha} + \frac{2\sin^2\theta}{\alpha^2} \tag{C.3i}$$

$$Q_{212} = 1 \tag{C.4a}$$

$$Q_{216} = \cos i \tag{C.4b}$$

$$Q_{222} = \frac{2\beta}{\alpha} \tag{C.4c}$$

$$Q_{224} + \jmath\,Q_{225} = -\frac{\Theta}{\alpha} - \frac{2\mathcal{Q}}{\eta^2} \tag{C.4d}$$

$$Q_{226} = \cos i\frac{\beta}{\alpha} \tag{C.4e}$$

$$Q_{233} + \jmath\left(\frac{Q_{236}}{\sin i}\right) = -\sin\theta\,\Theta \tag{C.4f}$$

$$Q_{246} + \jmath\,Q_{256} = -\cos i\left(\frac{\Theta}{\alpha} + \frac{2\mathcal{Q}}{\eta^2}\right) \tag{C.4g}$$

$$Q_{313} + \jmath\left(\frac{Q_{316}}{\sin i}\right) = -\jmath\,\Theta \tag{C.5a}$$

$$Q_{323} + \jmath\left(\frac{Q_{326}}{\sin i}\right) = (\alpha - \jmath\,\beta)\frac{\Theta}{\alpha} \tag{C.5b}$$

$$Q_{334} + \jmath\,Q_{335} = -\sin\theta\left(\frac{\Theta}{\alpha} + \frac{2\mathcal{Q}}{\eta^2}\right) \tag{C.5c}$$

$$Q_{346} + \jmath\,Q_{356} = \sin i\,\cos\theta\left(\frac{\Theta}{\alpha} + \frac{2\mathcal{Q}}{\eta^2}\right) \tag{C.5d}$$

$$Q_{411} = \frac{3}{4}\frac{\beta}{\alpha} \tag{C.6a}$$

$$Q_{412} = 2 - \frac{3}{2\alpha} + \frac{\eta^2}{\alpha^2} \tag{C.6b}$$

$$Q_{414} + \jmath\, Q_{415} = \frac{3\beta\mathcal{Q}}{2\eta^2\alpha} + \jmath\,(\alpha - 2\jmath\,\beta)\frac{\Theta}{2\alpha^2} \tag{C.6c}$$

$$Q_{416} = \frac{3}{2}\cos i \tag{C.6d}$$

$$Q_{422} = \frac{\beta}{\alpha}\left(4 - \frac{3}{\alpha} + \frac{2\eta^2}{\alpha^2}\right) \tag{C.6e}$$

$$Q_{426} = \cos i\frac{2\beta}{\alpha} \tag{C.6f}$$

$$Q_{424} + \jmath\, Q_{425} = -(3\alpha^2 - 4\alpha + 2\eta^2 - \jmath\,\alpha\beta)\frac{\Theta}{\alpha^3} - (4\alpha^2 - 3\alpha + 2\eta^2)\frac{\mathcal{Q}}{\eta^2\alpha^2} \tag{C.6g}$$

$$Q_{433} + \jmath\left(\frac{Q_{436}}{\sin i}\right) = \jmath\,\Theta^2 \tag{C.6h}$$

$$Q_{444} = -\frac{2\beta\,\cos^2\theta}{\alpha^3} - \frac{4q_1\beta\,\cos\theta}{\eta^2\alpha^2} + \frac{1}{\eta^4\alpha}\left[3(1-q_2^2)\beta + 2\eta^2 q_1\sin\theta\right] \tag{C.6i}$$

$$Q_{455} = -\frac{2\beta\,\sin^2\theta}{\alpha^3} - \frac{4q_2\beta\,\sin\theta}{\eta^2\alpha^2} + \frac{1}{\eta^4\alpha}\left[3(1-q_1^2)\beta - 2\eta^2 q_2\cos\theta\right] \tag{C.6j}$$

$$\begin{aligned} Q_{445} = &-\frac{2\beta\,\sin\theta\,\cos\theta}{\alpha^3} - \frac{2}{\eta^2\alpha^2}(q_1\sin\theta + q_2\cos\theta) \\ &+\frac{1}{\eta^4\alpha}\left[3q_1q_2\beta + \eta^2(q_2\sin\theta - q_1\cos\theta)\right] \end{aligned} \tag{C.6k}$$

$$Q_{446} + \jmath\, Q_{456} = \cos i\left(\frac{2\Theta}{\alpha} + \frac{3\mathcal{Q}}{\eta^2}\right) \tag{C.6l}$$

$$Q_{511} = \frac{3}{4} \tag{C.7a}$$

$$Q_{512} = -\frac{2\beta}{\alpha} \tag{C.7b}$$

$$Q_{514} + \jmath\, Q_{515} = \frac{\Theta}{2\alpha} + \frac{3\mathcal{Q}}{2\eta^2} \tag{C.7c}$$

$$Q_{522} = 4 - \frac{8}{\alpha} + \frac{4\eta^2}{\alpha^2} \tag{C.7d}$$

$$Q_{524} + \jmath\, Q_{525} = \jmath\,(\alpha - \jmath\, 3\beta)\frac{\Theta}{\alpha^2} + \frac{4\beta\,\mathcal{Q}}{\eta^2\alpha} \tag{C.7e}$$

$$Q_{526} = \cos i\left(2 - \frac{3}{\alpha} + \frac{\eta^2}{\alpha^2}\right) \tag{C.7f}$$

$$Q_{533} + \jmath\left(\frac{Q_{536}}{\sin i}\right) = -\Theta^2 \tag{C.7g}$$

$$Q_{544} = \frac{3}{\eta^4}(1 - q_2^2) - \frac{2\cos^2\theta}{\alpha^2} - \frac{2q_1\cos\theta}{\eta^2\alpha} \tag{C.7h}$$

$$Q_{555} = \frac{3}{\eta^4}(1 - q_1^2) - \frac{2\sin^2\theta}{\alpha^2} - \frac{2q_2\sin\theta}{\eta^2\alpha} \tag{C.7i}$$

$$Q_{545} = \frac{3q_1q_2}{\eta^4} - \frac{2\sin\theta\,\cos\theta}{\alpha^2} - \frac{1}{\eta^2\alpha}(q_1\sin\theta + q_2\cos\theta) \tag{C.7j}$$

$$Q_{546} + \jmath\, Q_{556} = \cos i\frac{3\beta\,\mathcal{Q}}{\eta^2\alpha} - \jmath\,\cos i\,(\alpha + \jmath\,\beta)\frac{\Theta}{\alpha^2} \tag{C.7k}$$

$$Q_{613} + \jmath\left(\frac{Q_{616}}{\sin i}\right) = -(\alpha - \jmath\, 3\beta)\frac{\Theta}{2\alpha} \tag{C.8a}$$

$$Q_{623} + \jmath\left(\frac{Q_{626}}{\sin i}\right) = -\jmath\,(\alpha^2 - 3\alpha + \eta^2 - \jmath\,\alpha\beta)\frac{\Theta}{\alpha^2} \tag{C.8b}$$

$$Q_{634} + \jmath\, Q_{635} = \frac{1}{\alpha} + (\alpha\,\cos\theta + 3\beta\,\sin\theta)\frac{\mathcal{Q}}{\eta^2\alpha} + \beta\,\sin\theta\frac{\Theta}{\alpha^2} \tag{C.8c}$$

$$Q_{646} + \jmath\, Q_{656} = \jmath\,\frac{\sin i}{\alpha} + \sin i\,(\alpha\,\sin\theta - 3\beta\,\cos\theta)\frac{\mathcal{Q}}{\eta^2\alpha} - \sin i\,\beta\,\cos\theta\frac{\Theta}{\alpha^2} \tag{C.8d}$$

$$Q_{166} + \jmath\, Q_{266} = \jmath\,\sin^2 i\,\sin\theta\,\Theta^* - 1 \tag{C.9a}$$

$$Q_{466} + \jmath\, Q_{566} = -\jmath\,\sin^2 i\,\Theta^2 \tag{C.9b}$$

$$Q_{366} + \jmath\, Q_{666} = \jmath\,\sin i\,\cos i\,\Theta^* \tag{C.9c}$$

$$\overline{S}_{111} = \frac{6}{\eta^4}(\eta^2 - 2\alpha)(\eta^2 - 6\alpha) \tag{C.10a}$$

$$\overline{S}_{114} = -\frac{6\alpha\beta}{\eta^4}(\eta^2 - 4\alpha) \tag{C.10b}$$

$$\overline{S}_{115} = -\frac{6\alpha^2}{\eta^4}(\eta^2 - 4\alpha) \tag{C.10c}$$

$$\overline{S}_{122} = -\frac{2}{\eta^2}(\eta^2 - 3\alpha) \tag{C.10d}$$

$$\overline{S}_{124} = -\frac{2\alpha^2}{\eta^2} \tag{C.10e}$$

$$\overline{S}_{125} = \frac{2\alpha\beta}{\eta^2} \tag{C.10f}$$

$$\overline{S}_{133} = -\frac{2}{\eta^2}(\eta^2 - 3\alpha + \alpha^2) \tag{C.10g}$$

$$\overline{S}_{136} = \frac{2\alpha\beta}{\eta^2} \tag{C.10h}$$

$$\overline{S}_{144} = -\frac{2\alpha^2}{\eta^2}(3\eta^2 - 8\alpha + 4\alpha^2) \tag{C.10i}$$

$$\overline{S}_{145} = \frac{8\alpha^3\beta}{\eta^4} \tag{C.10j}$$

$$\overline{S}_{155} = \frac{2\alpha^2}{\eta^4}(\eta^2 + 4\alpha^2) \tag{C.10k}$$

$$\overline{S}_{166} = \frac{2\alpha^2}{\eta^2} \tag{C.10l}$$

$$\overline{S}_{212} = -1 \tag{C.11a}$$

$$\overline{S}_{213} + \jmath\,\overline{S}_{216} = -\cot i\,\Theta^* \tag{C.11b}$$

$$\overline{S}_{223} + \jmath\,\overline{S}_{226} = -\jmath\,\cot i\,\Theta^* \tag{C.11c}$$

$$\overline{S}_{233} = -(\cot^2 i + \csc^2 i)\,\sin\theta\,\cos\theta \tag{C.11d}$$

$$\overline{S}_{234} = \cot i\,\sin\theta \tag{C.11e}$$

$$\overline{S}_{236} = -\cot^2 i\,\cos^2\theta + \csc^2 i\,\sin^2\theta \tag{C.11f}$$

$$\overline{S}_{256} = \cot i\,\sin\theta \tag{C.11g}$$

$$\overline{S}_{266} = (\cot^2 i + \csc^2 i)\,\sin\theta\,\cos\theta \tag{C.11h}$$

$$\overline{S}_{313} + \jmath\,\overline{S}_{316} = -\jmath\,\Theta^* \tag{C.12a}$$

$$\overline{S}_{323} + \jmath\overline{S}_{326} = \Theta^* \tag{C.12b}$$

$$\overline{S}_{333} + \jmath\,\overline{S}_{336} = \cot i\,\cos\theta\,\Theta^* \tag{C.12c}$$

$$\overline{S}_{356} = -\cos\theta \tag{C.12d}$$

$$\overline{S}_{366} = \cot i\,\sin^2\theta \tag{C.12e}$$

$$\overline{S}_{411} + \jmath\,\overline{S}_{511} = 6(\Theta + \mathcal{Q}) \tag{C.13a}$$

$$\overline{S}_{412} + \jmath\,\overline{S}_{512} = \jmath\,(3\Theta + 2\mathcal{Q}) \tag{C.13b}$$

$$\overline{S}_{413} + \jmath\,\overline{S}_{513} = \jmath\,\cot i\,\cos\theta\,(3\Theta + 2\mathcal{Q}) \tag{C.13c}$$

$$\overline{S}_{414} + \jmath\,\overline{S}_{514} = -2\jmath\,\alpha\,\Theta \tag{C.13d}$$

$$\overline{S}_{415} + \jmath\,\overline{S}_{515} = 2(\alpha+1)\,\Theta - 2\mathcal{Q} \tag{C.13e}$$

$$\overline{S}_{416} + \jmath\,\overline{S}_{516} = -\jmath\,\cot i\,\sin\theta\,(3\Theta + 2\mathcal{Q}) \tag{C.13f}$$

$$\overline{S}_{422} + \jmath\,\overline{S}_{522} = (3\Theta + 2\mathcal{Q}) \tag{C.13g}$$

$$\overline{S}_{423} + \jmath\,\overline{S}_{523} = -\cot i\,\Theta\,\mathcal{Q} \tag{C.13h}$$

$$\overline{S}_{424} + \jmath\,\overline{S}_{524} = -(\Theta + \mathcal{Q}) \tag{C.13i}$$

$$\overline{S}_{433} + \jmath\,\overline{S}_{533} = (\Theta + 2\mathcal{Q}) - \frac{1}{2}\csc^2 i\,\mathcal{Q}\,(1+\Theta^2) + \frac{1}{2}(\mathcal{Q} - \mathcal{Q}^*)\Theta^2 - \frac{\csc^2 i}{4}\,\mathcal{Q}\,(\Theta^2 - \Theta^{*2}) \tag{C.13j}$$

$$\overline{S}_{434} + \jmath\,\overline{S}_{534} = \cot i\,\,(\alpha\,\cos\theta\,\Theta + \jmath\,\sin\theta\,\mathcal{Q}) \tag{C.13k}$$

$$\overline{S}_{435} + \jmath\,\overline{S}_{535} = \jmath\,\cot i\,\cos\theta\,[(\alpha+1)\Theta + \mathcal{Q}] \tag{C.13l}$$

$$\overline{S}_{436} + \jmath\,\overline{S}_{536} = -\jmath\,\Theta - \jmath\,\frac{1}{2}\csc^2 i\,\mathcal{Q}\,\Theta^2 + \frac{1}{2}\jmath\,(\mathcal{Q} - \mathcal{Q}^*)\Theta^2 + \jmath\frac{\csc^2 i}{4}\,\mathcal{Q}\,(\Theta^2 - \Theta^{*2}) \tag{C.13m}$$

$$\overline{S}_{425} + \jmath\,\overline{S}_{525} = \jmath\,(\Theta + \mathcal{Q}) \tag{C.13n}$$

$$\overline{S}_{426} + \jmath\,\overline{S}_{526} = -\jmath\,\cot i\,\Theta\,\mathcal{Q} \tag{C.13o}$$

$$\overline{S}_{445} + \jmath\,\overline{S}_{545} = -\jmath\,\alpha\,\Theta \tag{C.13p}$$

$$\overline{S}_{446} + \jmath\,\overline{S}_{546} = -\cot i\,\sin\theta\,\alpha\,\Theta \tag{C.13q}$$

$$\overline{S}_{455} + \jmath\,\overline{S}_{555} = 2\alpha\,\Theta \tag{C.13r}$$

$$\overline{S}_{456} + \jmath\,\overline{S}_{556} = -\jmath\,\cot i\,(\alpha + 1)\,\sin\theta\,\Theta \tag{C.13s}$$

$$\overline{S}_{466} + \jmath\,\overline{S}_{566} = 2(\Theta + \mathcal{Q}) - \frac{1}{2}\csc^2 i\,\mathcal{Q}\,(1 - \Theta^2) - \frac{1}{2}(\mathcal{Q} - \mathcal{Q}^*)\Theta^2 + \frac{\csc^2 i}{4}\,\mathcal{Q}\,(\Theta^2 - \Theta^{*2}) \tag{C.13t}$$

$$\overline{S}_{613} + \jmath\,\overline{S}_{616} = \csc i\,\Theta^* \tag{C.14a}$$

$$\overline{S}_{623} + \jmath\,\overline{S}_{626} = \jmath\,\csc i\,\Theta^* \tag{C.14b}$$

$$\overline{S}_{633} + \jmath\,\overline{S}_{636} = \jmath\,\cot i\,\csc i\,\Theta^{*2} \tag{C.14c}$$

$$\overline{S}_{656} = -\csc i\,\sin\theta \tag{C.14d}$$

$$\overline{S}_{666} = -\cot i\,\csc i\,\sin 2\theta \tag{C.14e}$$

APPENDIX D

COEFFICIENTS FOR PERIODIC RELATIVE MOTION EXPRESSIONS

Coefficients $\Lambda_0, \Lambda_{c_k}, \Lambda_{s_k}$:

$$\Lambda_0 = \frac{9e}{8}\rho_1^2 \cos 2\psi_0 + 3\rho_1\rho_2 \cos\psi_0 \tag{D.1a}$$

$$\Lambda_{c_1} = -\frac{3}{8}\,{\rho_3}^2 \cos 2\,\phi_0 - \frac{3}{4}\,{\rho_3}^2 + \frac{3}{4}\,{\rho_1}^2 \cos 2\,\psi_0 - \frac{3}{2}\,{\rho_1}^2 + \frac{3e^2}{16}\,{\rho_1}^2 + \frac{3e}{4}\,\rho_1\rho_2 \cos\psi_0 - \frac{3}{2}\,{\rho_2}^2 + \frac{e^2}{4}\,{\rho_1}^2 \cos 2\,\psi_0 \tag{D.1b}$$

$$\Lambda_{s_1} = -\frac{e^2}{16}\,{\rho_1}^2 \sin 2\,\psi_0 + \frac{3}{8}\,{\rho_3}^2 \sin 2\,\phi_0 - \frac{3}{4}\,{\rho_1}^2 \sin 2\,\psi_0 + \frac{3e}{4}\,\rho_1\rho_2 \sin\psi_0 \tag{D.1c}$$

$$\Lambda_{c_2} = \frac{e}{4}\,{\rho_1}^2 \cos 2\,\psi_0, \quad \Lambda_{s_2} = -\frac{e}{4}\,{\rho_1}^2 \sin 2\,\psi_0 \tag{D.1d}$$

$$\Lambda_{c_3} = \frac{e}{4}\,\rho_1\rho_2 \cos\psi_0 + \frac{1}{8}\,{\rho_3}^2 \cos 2\,\phi_0 - \frac{1}{4}\,{\rho_1}^2 \cos 2\,\psi_0 + \frac{e^2}{32}\,{\rho_1}^2 \cos 2\,\psi_0 + \frac{e^2}{16}\,{\rho_1}^2 \tag{D.1e}$$

$$\Lambda_{s_3} = -\frac{e^2}{32}\,{\rho_1}^2 \sin 2\,\psi_0 + \frac{1}{4}\,{\rho_1}^2 \sin 2\,\psi_0 - \frac{e}{4}\,\rho_1\rho_2 \sin\psi_0 - \frac{1}{8}\,{\rho_3}^2 \sin 2\,\phi_0 \tag{D.1f}$$

$$\Lambda_{c_4} = -\frac{e}{8}\,{\rho_1}^2 \cos 2\,\psi_0, \quad \Lambda_{s_4} = \frac{e}{8}\,{\rho_1}^2 \sin 2\,\psi_0 \tag{D.1g}$$

$$\Lambda_{c_5} = -\frac{e^2}{32}\,{\rho_1}^2 \cos 2\,\psi_0, \quad \Lambda_{s_5} = \frac{e^2}{32}\,{\rho_1}^2 \sin 2\,\psi_0 \tag{D.1h}$$

Evaluating $\int \Lambda / \sin^2 f \; df$:

$$\int \frac{1}{\sin^2 f}\; df = -\cot f \tag{D.2a}$$

$$\int \frac{\sin f}{\sin^2 f}\; df = \ln\frac{(1-\cos f)}{\sin f}, \quad \int \frac{\cos f}{\sin^2 f}\; df = -\mathrm{cosec} f \tag{D.2b}$$

$$\int \frac{\sin 2f}{\sin^2 f}\; df = 2\ln\sin f, \quad \int \frac{\cos 2f}{\sin^2 f}\; df = -\cot f - 2f \tag{D.2c}$$

$$\int \frac{\sin 3f}{\sin^2 f}\, df = 4\cos f + 3\ln\frac{(1-\cos f)}{\sin f},$$
$$\int \frac{\cos 3f}{\sin^2 f}\, df = -3\ \mathrm{cosec} f + 2\frac{\cos 2f}{\sin f} \qquad (D.2d)$$
$$\int \frac{\sin 4f}{\sin^2 f}\, df = 2\cos 2f + 2 + 4\ln\sin f,$$
$$\int \frac{\cos 4f}{\sin^2 f}\, df = -2\cot f + \frac{\cos 3f}{\sin f} - 4f \qquad (D.2e)$$
$$\int \frac{\sin 5f}{\sin^2 f}\, df = \frac{4}{3}\cos 3f + 8\cos f + 5\ln\frac{(1-\cos f)}{\sin f},$$
$$\int \frac{\cos 5f}{\sin^2 f}\, df = -5\ \mathrm{cosec} f + \frac{2}{3}\frac{\cos 4f}{\sin f} + \frac{10}{3}\frac{\cos 2f}{\sin f} \qquad (D.2f)$$

Evaluating $\int \Lambda/\phi^2\ df$:

$$\int \frac{1}{\phi^2}\, df = 2e\, J(f) - \frac{1}{\phi^2}\frac{\sin 2f}{2} \qquad (D.3a)$$
$$\int \frac{\cos f}{\phi^2}\, df = -\frac{2}{3}(2+e^2)\, J(f) + \frac{1}{\phi^2}\left[\frac{e}{6}\sin 2f - \frac{1}{3}\sin 3f - \frac{e}{12}\sin 4f\right] \qquad (D.3b)$$
$$\int \frac{\cos 2f}{\phi^2}\, df = \frac{2}{3e}(2+e^2)\, J(f) + \frac{1}{\phi^2}\left[-\frac{1}{e}\sin f - \frac{2}{3}\sin 2f + \frac{1}{3e}\sin 3f + \frac{1}{12}\sin 4f\right] \qquad (D.3c)$$
$$\int \frac{\cos 3f}{\phi^2}\, df = -2(2-e^2)\, J(f) + \frac{1}{\phi^2}\left[-\sin f - \frac{e}{2}\sin 2f + \frac{e}{4}\sin 4f\right] \qquad (D.3d)$$
$$\int \frac{\cos 4f}{\phi^2}\, df = -\frac{2}{3e^3}(8 - 24e^2 + 13e^4)\, J(f) - \frac{8}{e^2}f + \frac{1}{\phi^2}\left[\frac{4}{e^3}(1+e^2)\sin f + \frac{1}{6e^2}(4+13e^2)\sin 2f - \frac{4}{3e^3}(1+e^2)\sin 3f - \frac{1}{3e^2}(1+4e^2)\sin 4f\right] \qquad (D.3e)$$

$$\int \frac{\cos 5f}{\phi^2}\, df = -\frac{2}{3e^4}(-32+80e^2-50e^4+5e^6)\, J(f) + \frac{32}{e^3} f \qquad (D.3f)$$

$$+\frac{1}{\phi^2}\left[. - \frac{1}{e^4}(16+24e^2+e^4)\sin f \right.$$
$$-\frac{1}{6e^3}(16+96e^2-5e^4)\sin 2f$$
$$+\frac{1}{3e^4}(16+24e^2-5e^4)\sin 3f$$
$$\left.+\frac{1}{12e^3}(16+96e^2-5e^4)\sin 4f + \sin 5f\right] \qquad (D.3g)$$

$$\eta^4 \int \frac{\sin f}{\phi^2}\, df = \frac{1}{2}(1-e)^2 \ln(1-\cos f) - \frac{1}{2}(1+e)^2 \ln(1+\cos f)$$
$$+2e\ln(1+e\cos f) - \frac{e\eta^2}{1+e\cos f} \qquad (D.3h)$$

$$\eta^4 \int \frac{\sin 2f}{\phi^2}\, df = (1-e)^2 \ln(1-\cos f) + (1+e)^2 \ln(1+\cos f)$$
$$-2(1+e^2)\ln(1+e\cos f) + \frac{2\eta^2}{1+e\cos f} \qquad (D.3i)$$

$$\eta^4 \int \frac{\sin 3f}{\phi^2}\, df = \frac{3}{2}(1-e)^2 \ln(1-\cos f) - \frac{3}{2}(1+e)^2 \ln(1+\cos f)$$
$$+6e\ln(1+e\cos f) - \frac{(4-e^2)}{e}\frac{\eta^2}{1+e\cos f} \qquad (D.3j)$$

$$\eta^4 \int \frac{\sin 4f}{\phi^2}\, df = 2(1-e)^2 \ln(1-\cos f) + 2(1+e)^2 \ln(1+\cos f)$$
$$+\frac{4}{e^2}(2-5e^2+e^4)\ln(1+e\cos f)$$
$$+\frac{4(2-e^2)}{e^2}\frac{\eta^2}{1+e\cos f} \qquad (D.3k)$$

$$\eta^4 \int \frac{\sin 5f}{\phi^2}\, df = \frac{5}{2}(1-e)^2 \ln(1-\cos f) - \frac{5}{2}(1+e)^2 \ln(1+\cos f)$$
$$+\frac{16}{e^2}\eta^4\cos f - \frac{2}{e^3}(16-32e^2+11e^4)\ln(1+e\cos f)$$
$$-\frac{(16-12e^2+e^4)}{e^3}\frac{\eta^2}{1+e\cos f} \qquad (D.3l)$$

Coefficients $Q_k, \overline{Q}_k, E_k, F_k, G_k, H_k$:

$$Q_1 = \frac{e}{4}\rho_1^2\cos 2\psi_0 + 2\rho_1\rho_2\cos\psi_0 + \frac{e}{2}\rho_1^2 - \frac{1}{e}\left(2\rho_1^2+2\rho_2^2+\rho_3^2\right) \qquad (D.4a)$$

$$Q_2 = \frac{1}{2}\rho_1^2 \cos 2\psi_0 - \frac{1}{4}\rho_3^2 \cos 2\phi_0 - \frac{1}{4}\left(2\rho_1^2 + 2\rho_2^2 + \rho_3^2\right) \tag{D.4b}$$

$$Q_3 = \frac{e}{12}\rho_1^2 \cos 2\psi_0 \tag{D.4c}$$

$$\overline{Q}_0 = \rho_1^2 \left(\frac{1}{4} - \frac{1}{2e^2}\right) \sin 2\psi_0 + \frac{1}{2e^2}\rho_3^2 \sin 2\phi_0 + \frac{1}{e}\rho_1\rho_2 \sin \psi_0 \tag{D.4d}$$

$$\overline{Q}_1 = \rho_1^2 \left(\frac{e}{4} - \frac{1}{e}\right) \sin 2\psi_0 + \frac{1}{e}\rho_3^2 \sin 2\phi_0 + 2\rho_1\rho_2 \sin \psi_0 \tag{D.4e}$$

$$\overline{Q}_2 = \frac{1}{4}\rho_1^2 \sin 2\psi_0 \tag{D.4f}$$

$$\overline{Q}_3 = \frac{e}{12}\rho_1^2 \sin 2\psi_0 \tag{D.4g}$$

$$E_1 = -\frac{3e}{4}\rho_1^2 \cos 2\psi_0 - 3\rho_1\rho_2 \cos \psi_0,$$

$$F_1 = -\frac{3e}{4}\rho_1^2 \sin 2\psi_0 - 3\rho_1\rho_2 \sin \psi_0 \tag{D.4h}$$

$$E_2 = -\frac{3}{4}\rho_1^2 \cos 2\psi_0, \quad F_2 = -\frac{3}{4}\rho_1^2 \sin 2\psi_0 \tag{D.4i}$$

$$E_3 = -\frac{e}{12}\rho_1^2 \cos 2\psi_0, \quad F_3 = -\frac{e}{12}\rho_1^2 \sin 2\psi_0 \tag{D.4j}$$

$$G_1 = \overline{Q}_1/2, \quad G_2 = \overline{Q}_2, \quad G_3 = 3\overline{Q}_3/2 \tag{D.4k}$$

$$H_0 = -\frac{e^2}{16}\rho_1^2 \cos 2\psi_0 - \frac{e}{2}\rho_1\rho_2 \cos \psi_0 + \left(\frac{1}{2} - \frac{e^2}{8}\right)\rho_1^2 + \frac{1}{2}\rho_2^2 + \frac{1}{4}\rho_3^2 \tag{D.4l}$$

$$H_1 = -\frac{7e}{8}\rho_1^2 \cos 2\psi_0 - 3\rho_1\rho_2 \cos \psi_0 - \frac{e}{8}\rho_3^2 \cos 2\phi_0$$
$$-\frac{e}{8}\left(2\rho_1^2 + 2\rho_2^2 + \rho_3^2\right) \tag{D.4m}$$

$$H_2 = -\frac{1}{8}(4 + e^2)\rho_1^2 \cos 2\psi_0 - \frac{e}{2}\rho_1\rho_2 \cos \psi_0 + \frac{1}{4}\rho_3^2 \cos 2\phi_0$$
$$+\left(1 - \frac{e^2}{8}\right)\rho_1^2 + \rho_2^2 + \frac{1}{2}\rho_3^2 \tag{D.4n}$$

$$H_3 = -\frac{3e}{8}\rho_1^2 \cos 2\psi_0 + \frac{e}{8}\rho_3^2 \cos 2\phi_0 + \frac{e}{8}\left(2\rho_1^2 + 2\rho_2^2 + \rho_3^2\right) \tag{D.4o}$$

$$H_4 = -\frac{e^2}{16}\rho_1^2 \cos 2\psi_0 \tag{D.4p}$$

APPENDIX E

COEFFICIENTS FOR AVERAGE RELATIVE MOTION

The components of $\mathbf{P}_0$ and $\mathbf{P}_J$ are as follows:

$$P_{011} = \frac{\bar{\eta}^2}{\bar{\alpha}} \tag{E.1a}$$

$$P_{012} = \frac{\bar{\beta}}{\bar{\eta}} \tag{E.1b}$$

$$P_{013} = 0 \tag{E.1c}$$

$$P_{014} = \frac{\bar{q}_1\bar{q}_2 \sin\bar{\theta}}{\bar{\eta}(1+\bar{\eta})} - \frac{(1+\bar{\eta}-\bar{q}_1{}^2)\cos\bar{\theta}}{\bar{\eta}(1+\bar{\eta})} \tag{E.1d}$$

$$P_{015} = \frac{\bar{q}_1\bar{q}_2 \cos\bar{\theta}}{\bar{\eta}(1+\bar{\eta})} - \frac{(1+\bar{\eta}-\bar{q}_2{}^2)\sin\bar{\theta}}{\bar{\eta}(1+\bar{\eta})} \tag{E.1e}$$

$$P_{016} = 0 \tag{E.1f}$$

$$P_{021} = 0 \tag{E.2a}$$

$$P_{022} = \frac{\bar{\alpha}}{\bar{\eta}} \tag{E.2b}$$

$$P_{023} = 0 \tag{E.2c}$$

$$P_{024} = \frac{\bar{q}_2\bar{\alpha}}{(1+\bar{\eta})\bar{\eta}} + \sin\bar{\theta} + \frac{\bar{q}_2 + \sin\bar{\theta}}{\bar{\alpha}} \tag{E.2d}$$

$$P_{025} = -\frac{\bar{q}_1\bar{\alpha}}{(1+\bar{\eta})\bar{\eta}} - \cos\bar{\theta} - \frac{\bar{q}_1 + \cos\bar{\theta}}{\bar{\alpha}} \tag{E.2e}$$

$$P_{026} = \frac{\bar{\eta}^2}{\bar{\alpha}}\cos\bar{i} \tag{E.2f}$$

$$P_{031} = 0 \tag{E.3a}$$

$$P_{032} = 0 \tag{E.3b}$$

$$P_{033} = \frac{\bar{\eta}^2}{\bar{\alpha}} \sin\bar{\theta} \tag{E.3c}$$

$$P_{034} = 0 \tag{E.3d}$$

$$P_{035} = 0 \tag{E.3e}$$

$$P_{036} = -\frac{\bar{\eta}^2}{\bar{\alpha}} \cos\bar{\theta}\, \sin\bar{i} \tag{E.3f}$$

$$P_{041} = -\frac{\bar{\beta}}{2\eta} \tag{E.4a}$$

$$P_{042} = \frac{\bar{\alpha}^2}{\bar{\eta}^4}(\bar{\alpha} - 1) \tag{E.4b}$$

$$P_{043} = 0 \tag{E.4c}$$

$$P_{044} = \frac{\bar{\alpha}^2}{\bar{\eta}^4(1+\bar{\eta})} \left[\bar{q}_2(\bar{\alpha} - 1) + \bar{\eta}(1+\bar{\eta}) \sin\bar{\theta}\right] \tag{E.4d}$$

$$P_{045} = \frac{\bar{\alpha}^2}{\bar{\eta}^4(1+\bar{\eta})} \left[\bar{q}_2\bar{\beta} + (1+\bar{\eta}) \cos\bar{\theta}\right] \tag{E.4e}$$

$$P_{046} = 0 \tag{E.4f}$$

$$P_{051} = -\frac{3\bar{\alpha}}{2\eta} \tag{E.5a}$$

$$P_{052} = -\frac{\bar{\alpha}^2\bar{\beta}}{\bar{\eta}^4} \tag{E.5b}$$

$$P_{053} = 0 \tag{E.5c}$$

$$P_{054} = \frac{3\bar{q}_1}{\bar{\eta}^3}\bar{\alpha} + \frac{2}{\bar{\eta}} \cos\bar{\theta} - \frac{\bar{\beta}}{\bar{\eta}^3}\left[\frac{\bar{q}_2}{\bar{\eta}(1+\bar{\eta})}\bar{\alpha}^2 + (\bar{\alpha}+1)\, \sin\bar{\theta} + \bar{q}_2\right] \tag{E.5d}$$

$$P_{055} = \frac{3\bar{q}_2}{\bar{\eta}^3}\bar{\alpha} + \frac{2}{\bar{\eta}} \sin\bar{\theta} + \frac{\bar{\beta}}{\bar{\eta}^3}\left[\frac{\bar{q}_1}{\bar{\eta}(1+\bar{\eta})}\bar{\alpha}^2 + (\bar{\alpha}+1)\, \cos\bar{\theta} + \bar{q}_1\right] \tag{E.5e}$$

$$P_{056} = \frac{\bar{\beta}}{\bar{\eta}} \cos\bar{i} \tag{E.5f}$$

$$P_{061} = 0 \tag{E.6a}$$

$$P_{062} = 0 \tag{E.6b}$$

$$P_{063} = \frac{1}{\bar{\eta}}(\bar{q}_1 + \cos\bar{\theta}) \tag{E.6c}$$

$$P_{064} = 0 \tag{E.6d}$$

$$P_{065} = 0 \tag{E.6e}$$

$$P_{066} = \frac{1}{\bar{\eta}}(\bar{q}_2 + \sin\bar{\theta})\sin\bar{i} \tag{E.6f}$$

$$P_{J11} = -\frac{3}{4}\bar{\eta}(1 - 3\cos^2\bar{i}) - \frac{\bar{\eta}^2}{4}\frac{(1+2\bar{\eta})}{(1+\bar{\eta})^2}({\bar{q}_1}^2 - {\bar{q}_2}^2)\sin^2\bar{i} \tag{E.7a}$$

$$P_{J12} = 0 \tag{E.7b}$$

$$P_{J13} = \frac{9}{2}\bar{\eta}\sin\bar{i}\,\cos\bar{i} + \frac{\bar{\eta}^2}{2}\frac{(1+2\bar{\eta})}{(1+\bar{\eta})^2}({\bar{q}_1}^2 - {\bar{q}_2}^2)\sin\bar{i}\,\cos\bar{i} \tag{E.7c}$$

$$\begin{aligned} P_{J14} = {} & \frac{9\bar{q}_1}{4\bar{\eta}}(1 - 3\cos^2\bar{i}) \\ & + \frac{\bar{q}_1\sin^2\bar{i}}{(1+\bar{\eta})^2}\left[\frac{1+3\bar{\eta}+3\bar{\eta}^2}{(1+\bar{\eta})}{\bar{q}_1}^2 - \frac{1}{2}(1+2\eta-\bar{\eta}^2-5\bar{\eta}^3)\right] \end{aligned} \tag{E.7d}$$

$$\begin{aligned} P_{J15} = {} & \frac{9\bar{q}_2}{4\bar{\eta}}(1 - 3\cos^2\bar{i}) \\ & - \frac{\bar{q}_2\sin^2\bar{i}}{(1+\bar{\eta})^2}\left[\frac{1+3\bar{\eta}+3\bar{\eta}^2}{(1+\bar{\eta})}{\bar{q}_2}^2 - \frac{1}{2}(1+2\eta-\bar{\eta}^2-5\bar{\eta}^3)\right] \end{aligned} \tag{E.7e}$$

$$P_{J16} = 0 \tag{E.7f}$$

$$P_{J21} = \frac{9}{4}\bar{q}_1\bar{q}_2\sin^2\bar{i} \tag{E.8a}$$

$$P_{J22} = \frac{3}{8}\left(3 - \bar{\eta}^2\right)(1 - 3\cos^2\bar{i}) - \frac{\bar{\eta}}{4}\frac{(1+2\bar{\eta})}{(1+\bar{\eta})^2}({\bar{q}_1}^2 - {\bar{q}_2}^2)\sin^2\bar{i} \tag{E.8b}$$

$$P_{J23} = -\frac{\bar{q}_1\bar{q}_2}{(1+\bar{\eta})^2}(3+6\bar{\eta}+2\bar{\eta}^2-2\bar{\eta}^3)\sin\bar{i}\,\cos\bar{i} \tag{E.8c}$$

$$P_{J24} = \frac{3\bar{q}_2}{8}\frac{(3+\bar{\eta})}{(1+\bar{\eta})}(1-3\cos\bar{i}^2) - \frac{\bar{q}_2}{8}\frac{(9+7\bar{\eta}-4\bar{\eta}^2)}{(1+\bar{\eta})}\sin^2\bar{i} - \frac{\bar{q}_1{}^2\bar{q}_2}{4\bar{\eta}^2(1+\bar{\eta})^3}(18+54\bar{\eta}+51\bar{\eta}^2+11\bar{\eta}^3-6\bar{\eta}^4)\sin^2 i \tag{E.8d}$$

$$P_{J25} = -\frac{3\bar{q}_1}{8}\frac{(3+\bar{\eta})}{(1+\bar{\eta})}(1-3\cos\bar{i}^2) - \frac{\bar{q}_1}{8}\frac{(9+7\bar{\eta}-4\bar{\eta}^2)}{(1+\bar{\eta})}\sin^2\bar{i} - \frac{\bar{q}_2{}^2\bar{q}_1}{4\bar{\eta}^2(1+\bar{\eta})^3}(18+54\bar{\eta}+51\bar{\eta}^2+11\bar{\eta}^3-6\bar{\eta}^4)\sin^2\bar{i} \tag{E.8e}$$

$$P_{J26} = \frac{3\bar{\eta}}{4}(1-3\cos^2\bar{i})\cos\bar{i} + \frac{(\bar{q}_1{}^2-\bar{q}_2{}^2)}{8(1+\bar{\eta})^2}(3+6\bar{\eta}+\bar{\eta}^2-4\bar{\eta}^3)\sin 2\bar{i}\,\cos\bar{i} \tag{E.8f}$$

$$P_{J31} = \frac{3\bar{q}_2}{4}\sin\bar{i}\,\cos\bar{i} \tag{E.9a}$$

$$P_{J32} = \frac{3\eta^3\bar{q}_1}{(1+\bar{\eta})^3(3-\bar{\eta}^2)}(1+\bar{\eta}-2\bar{q}_2{}^2)\sin\bar{i}\,\cos\bar{i} + \frac{9\bar{q}_1}{4}\sin\bar{i}\,\cos\bar{i} \tag{E.9b}$$

$$P_{J33} = -\frac{3\bar{q}_2}{8(1+\bar{\eta})}(1-3\bar{\eta}+2\bar{\eta}^2) + \frac{3\bar{q}_2}{8(1+\bar{\eta})^2}\sin^2\bar{i}\left[\frac{(3+9\bar{\eta}+8\bar{\eta}^2)}{(1+\bar{\eta})}\bar{q}_1{}^2 + (2-2\bar{\eta}-6\bar{\eta}^2-\bar{\eta}^3)\right] \tag{E.9c}$$

$$P_{J34} = -\frac{3}{2\bar{\eta}^2}(1-\bar{\eta}^2)\bar{q}_1\bar{q}_2\sin\bar{i}\,\cos\bar{i} \tag{E.9d}$$

$$P_{J35} = -\frac{3}{2\bar{\eta}^2}\left[\bar{q}_2{}^2(1-\bar{\eta}^2)+\bar{\eta}^2(2-\bar{\eta}^2)\right]\sin\bar{i}\,\cos\bar{i} \tag{E.9e}$$

$$P_{J36} = \frac{3\bar{\eta}\bar{q}_1}{8(1+\bar{\eta})}\left[(3+2\bar{\eta})(\bar{\eta}-2)\cos^2\bar{i}+(2+\bar{\eta})\right]\sin\bar{i} - \frac{3\bar{q}_1}{8}(1-2\bar{\eta}^2)\sin\bar{i} + \frac{3\bar{q}_1}{8(1+\bar{\eta})^2}\sin^3\bar{i}\left[\frac{(3+9\eta+8\eta^2)}{(1+\bar{\eta})}\bar{q}_2{}^2 + (1+2\eta-2\eta^3-2\eta^4)\right] \tag{E.9f}$$

$$P_{J41} = P_{J42} = P_{J43} = P_{J44} = P_{J45} = P_{J46} = 0 \tag{E.10}$$

$$P_{J51} = -\frac{3\bar{\eta}}{4}(4-\bar{\eta}) - \left[\frac{3\eta}{4}\frac{(1+2\bar{\eta})}{(1+\bar{\eta})^2}{\bar{q}_2}^2 - \frac{3\bar{\eta}}{8(1+\bar{\eta})}(13+10\bar{\eta}-5\bar{\eta}^2)\right]\sin^2\bar{i} \quad (E.11a)$$

$$P_{J52} = 0 \quad (E.11b)$$

$$P_{J53} = -3\bar{\eta}(2+\bar{\eta})\sin\bar{i}\,\cos\bar{i} - \frac{3}{4}(3-\bar{\eta}^2)\sin\bar{i}\,\cos\bar{i} \quad (E.11c)$$

$$P_{J54} = -\frac{\bar{q}_1}{4\bar{\eta}(1+\bar{\eta})}(12+17\bar{\eta}+7\bar{\eta}^2)(1-3\cos^2\bar{i}) \quad (E.11d)$$

$$P_{J55} = -\frac{\bar{q}_2}{4\bar{\eta}(1+\bar{\eta})}(12+17\bar{\eta}+7\bar{\eta}^2)(1-3\cos^2\bar{i}) \quad (E.11e)$$

$$P_{J56} = 0 \quad (E.11f)$$

$$P_{J61} = \frac{3\bar{\eta}\bar{q}_1}{(1+\bar{\eta})}\sin\bar{i}\,\cos\bar{i} \quad (E.12a)$$

$$P_{J62} = -\frac{3\bar{q}_2}{\bar{\eta}(1+\bar{\eta})}(2+2\bar{\eta}+\bar{\eta}^2)\sin\bar{i}\,\cos\bar{i} \quad (E.12b)$$

$$P_{J63} = \frac{3\bar{\eta}\bar{q}_1}{4(1+\bar{\eta})}(3-7\cos^2\bar{i}) \quad (E.12c)$$

$$P_{J64} = -\frac{3}{\bar{\eta}(1+\bar{\eta})}(1+\bar{\eta}+{\bar{q}_1}^2)\sin\bar{i}\,\cos\bar{i} + \frac{3}{2}\sin\bar{i}\,\cos\bar{i} \quad (E.12d)$$

$$P_{J65} = -\frac{3}{\bar{\eta}(1+\bar{\eta})}\bar{q}_1\bar{q}_2\sin\bar{i}\,\cos\bar{i} \quad (E.12e)$$

$$P_{J66} = \frac{3\bar{\eta}\bar{q}_2}{4(1+\bar{\eta})}(1-5\cos^2\bar{i})\sin\bar{i} - \frac{3\bar{q}_2}{2}\cos^2\bar{i}\,\sin\bar{i} \quad (E.12f)$$

VITA

Prasenjit Sengupta was born on November 30, 1979, in New Delhi, India. He received the degree of Bachelor of Technology (with Honors) in aerospace engineering from the Indian Institute of Technology, Kharagpur, in 2001, and that of Master of Science in aerospace engineering from Texas A&M University, in 2003. In 2006 he received the American Astronautical Society Breakwell Student Travel Award for the AAS/AIAA Space Flight Mechanics Meeting in Tampa, FL.

He can be reached via Dr. Srinivas R. Vadali, Department of Aerospace Engineering, TAMU 3141, Texas A&M University, College Station, TX 77843, or by email at prasenjits@gmail.com.

This document was typeset using LaTeX by Prasenjit Sengupta.